Groundwater Hydrology

Edited by Muhammad Salik Javaid

Groundwater Hydrology

Edited by Muhammad Salik Javaid

IntechOpen

Supporting open minds since 2005

Notice
Statements and opinions expressed in the chapters are these of the individual contributors and not necessarily those of the editors or publisher. No responsibility is accepted for the accuracy of information contained in the published chapters. The publisher assumes no responsibility for any damage or injury to persons or property arising out of the use of any materials, instructions, methods or ideas contained in the book.

We are IntechOpen,
the world's leading publisher of Open Access books
Built by scientists, for scientists

4,600+
Open access books available

120,000+
International authors and editors

135M+
Downloads

151
Countries delivered to

Our authors are among the
Top 1%
most cited scientists

12.2%
Contributors from top 500 universities

Interested in publishing with us?
Contact book.department@intechopen.com

Numbers displayed above are based on latest data collected.
For more information visit www.intechopen.com

Meet the editor

Dr. Muhammad Salik Javaid has a long meritorious career interacting with hydrology, hydraulics, and water resources as an engineering student, registered professional engineer, researcher, and university teaching professor. For over three decades he has worked as a hydraulics engineer, a disaster risk consultant, and a water resources expert in Pakistan and abroad in the Corps of Engineers, Earthquake Reconstruction and Rehabilitation Authority, Frontier Works Organization, and Design & Consultancy Department. His undergraduate engineering education is from the Military College of Engineering. He is a graduate of Georgia Tech, Atlanta, USA, where he earned his Master's and Doctoral degrees in Civil Engineering. He has been on the faculty of the National University of Sciences and Technology, University of Lahore, and Abasyn University Islamabad, teaching undergraduate and graduate level courses related to hydrology and hydraulics.

Contents

Preface

Geohydrology is an important branch of the hydrology that focuses on the subsurface geologic aspects of water and rock structure. The movement, transportation, geobiochemical actions and reactions, and physical behavior of water and other fluids inside the ground are most fascinating for engineers, researchers, hydrologists, agriculturists, industrialists, and general consumers. Aquifer maintenance and management, aquifer conservation, and aquifer resource balance between discharge and recharge are the areas for study to avoid and mitigate conflicts among the transboundary stakeholders. The positive contribution by engineers and scientists not only adds to the development of water and hydrocarbon resources, but also helps in the just and equitable utilization of these by everybody.

On the one hand, the rapid development of built-up areas, residential and industrial complexes, and communication infrastructure has grossly reduced the infiltration, percolation, and groundwater recharge, while on the other hand, extraction has increased manifold. There is thus a dire need to check the depletion rate and work for conservation and enhancement of precious liquid resources lying under the ground. These aspects can form the goals for future research and investment by all nations of the world. Numerical and computer modeling of groundwater movement and contaminant transport may help identify the gray areas and also suggest solutions in concrete terms.

This book contains six chapters that broadly deal with two major aspects of geohydrology: (1) the physical structure of the aquifer itself, and (2) fluid content, water, and their characteristics. The first chapter by Bon Andres provides an insight into the hydrogeological context of shallow hard rock aquifers by compiling and analyzing field and laboratory studies to obtain hydrometric and piezometric characteristics data. Chapter 2 by Ziadi Amira describes the economic, agricultural, and social problems arising from anthropogenic contamination and excessive water consumption that endanger overexploitation of groundwater, leading to mineralization in coastal aquifers. Several geological tools and hydrogeological data used in combination with geochemical and geophysical methods are also discussed. The third chapter coauthored by myself, Laila Khalid, and Zeshan Sameja presents an analytical study of environmental impacts and discusses their effects on groundwater hydrology. Chapter 4 by Dehban Avan appraises hydrogeological attributes of karst aquifers in Iran. Use of geochemical software and rockware software to analyze chemical compounds in karst aquifers is also explored. Water composition of springs and karstification of recharge areas are also discussed. Chapter 5 by Goncalves Manuel Vitor investigates the relationship between consumption of water with natural fluoride levels and the prevalence of dental fluorosis in parts of Brazil. The last chapter by Moharir Kanak evaluates analytical methods to determine aquifer characteristics.

This book has a broad-based scope due to elaborate coverage on many aspects of geology, hydrology, and subsurface water. The book aims to serve the needs of academia and field professionals in groundwater engineering, hydrogeology, water resource management, environmental sciences, and geotechnical engineering.

The consistent efforts of all persons who contributed directly or indirectly towards the completion of this book project are thankfully acknowledged. It would not have been possible to complete this book without the professional contributions of the eminent authors whose names appear with each chapter title, as well as the groundwater scientists and engineers the world over. The guidance, advice, and blessings of my professional colleagues and friends and unwavering support of my family members (wife Sultana, daughters Humaira and Sumayyah, and son Hammaad) are fully acknowledged. Therefore, I dedicate this book to my family and colleagues working in the field of hydrology. Abasyn University, Islamabad, needs a mention for providing me with a working atmosphere, space, time, and resources at university's cost. Last but not least I would like to thank Ms. Dolores Kuzelj, the author service manager, whose patience, guidance, and relentless efforts made us all follow and obey the laid-out timelines.

It is hoped that this book will be well received and found useful by both hydrogeologists and geohydrologists in academia as well as professional practice.

<div align="right">

Dr. Muhammad Salik Javaid
Abasyn University,
Islamabad, Pakistan

</div>

Chapter 1

Hydrogeological Characteristics of Shallow Hard Rock Aquifers in Yaounde (Cameroon, Central Africa)

*Jules Rémy Ndam Ngoupayou, André Firmin Bon,
Guillaume Ewodo Mboudou, Nasser Ngouh Abdou
and Georges Emmanuel Ekodeck*

Abstract

The groundwater contained in the alterites is one of the main sources of water supply for many households in the city of Yaounde and its surroundings. Information from the field and laboratory studies was compiled and analyzed in order to understand the hydrogeological context of this superficial aquifer. Preliminary results show a staged morphology of the alteration mantle (regolith) of Yaounde migmatitic representative of the polyphase character of alteration processes observed in all granito-gneissic formations of the world. This mantle has a multilayer system whose soil sets could have a different hydrodynamic functioning. The values of the hydraulic conductivity have a normal distribution and vary over four orders of magnitude, attesting the variability of the hydraulic conductivity of the soft materials. The hydrometric and piezometric characteristics indicate that the aquifer has highly heterogeneous zones that would be related to the morphostructural character of the region. The $\delta^{18}O$ mean values of the rain (−2.47‰) and shallow groundwater (−2.57‰) are not significantly different. They indicate that the recharge of the shallow aquifer of Yaounde Precambrian basement is recent and is done directly by infiltration of precipitation without any notable change due to evaporation.

Keywords: hydrological context, polyphase character, hydraulic conductivity, morphostructural character, recharge, shallow aquifer, Precambrian basement, Yaounde, Cameroon

1. Introduction

Hard rocks (plutonic and metamorphic rocks) constitute the basement of the continents and outcrop over more than 40% of the entire African continent [1–3]. About 90% of the Cameroon area is occupied by Precambrian basement rocks and the rest by sedimentary formations [4]. The former were transformed in the humid tropical zone into a thick alteration mantle (>20 m) due to the infiltration of rain on the ground surface [5, 6]. The aquifers of these metamorphic formations (gneiss, migmatite, schist, etc.) are exploited through wells and boreholes for the supply of drinking water to the

populations of rural and urban areas. In Yaounde, as a little everywhere in sub-Saharan Africa's urban areas, exploitation of groundwater is an alternative to the deficit of surface water resources. It represents, with the exception of the northern part of the country, the main source of drinking water supply captured and distributed by the national body in charge of water supply, that is, Camwater. This deficit is generally due to joint action of population explosion, hydroclimatic conditions, and social progress. Beyond its alternative character, the efficient exploitation of groundwater resources, particularly those of basement areas, requires a better understanding of the characteristics of their reservoir. Thus, two research programs were initiated by the
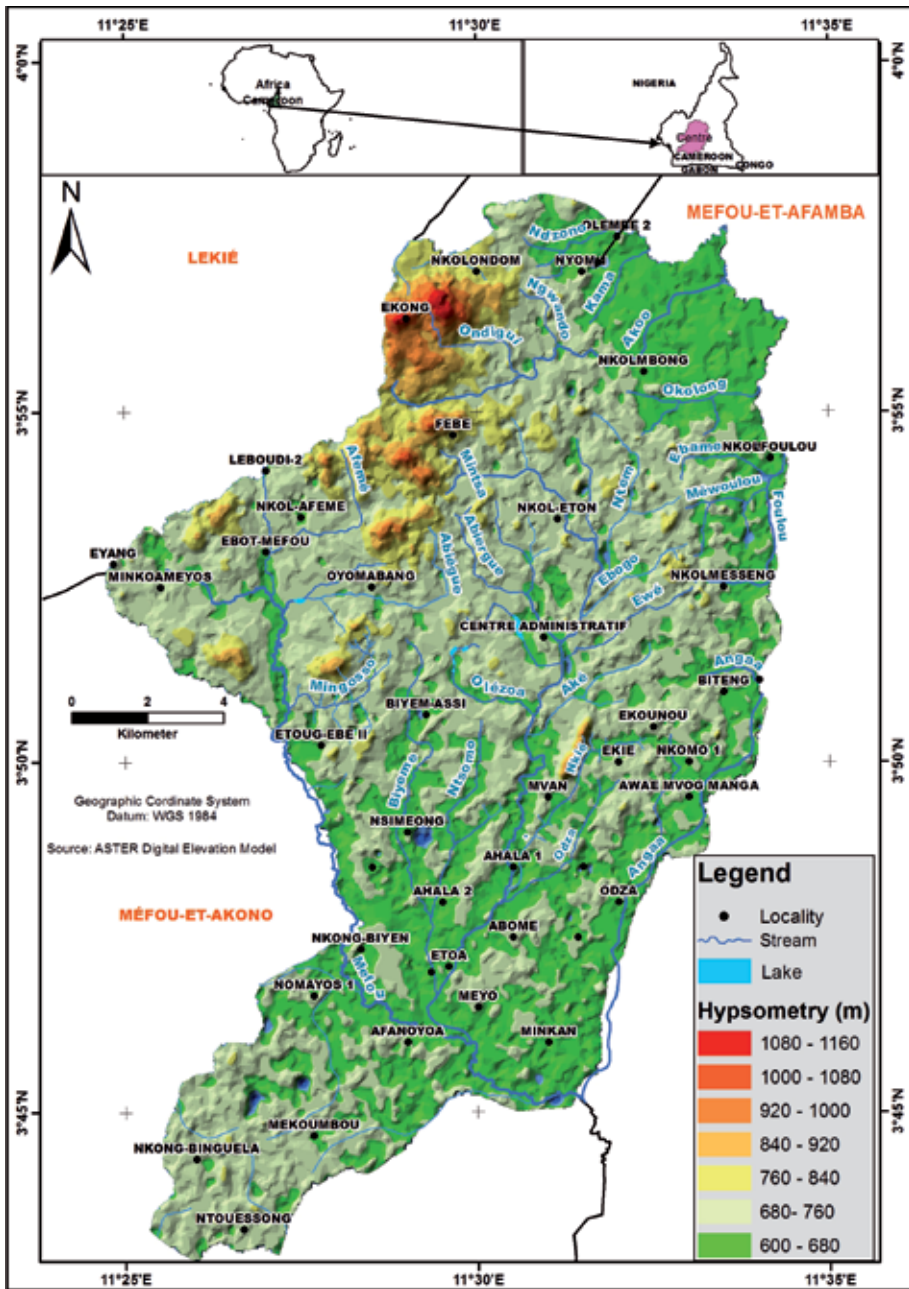
Figure 1.
Geographic location of the Yaounde region.

Laboratory of Geology of Engineering and Alterology (LAGIA) of the Department of Earth Sciences of the University of Yaounde I. These programs relate to (a) "physical, hydrodynamic, and bacteriological characterizations of groundwater resources in the sedimentary and basement areas of Cameroon" and (b) "the impact of climate change and human activities on the water resources of Cameroon." The activities carried out within the framework of these programs are more implemented in the alterites of the geological formations of the South Cameroon Plateau specifically those of the region of Yaounde and its surroundings [7–12]. In fact, because of the deficit service of the water distribution network, the groundwater of shallow unconfined aquifer constitutes, for many households in this region, one of the main sources of water supply.

This chapter is a review of the main results obtained during the research carried out in the aquifers of the Pan-African basement of the Yaounde series in Central Africa. It is a synthesis of the results of the Theses [4, 13–17], DEA, DESS, and Master [11, 18, 19] studies focusing on the hydrogeological context of the upper part of the weathered and cracked basement of the Mfoundi watershed, which includes 11 sub-basins, Anga'a and Mingosso in Mefou (**Figure 1**). This compilation makes it possible to fill the gaps and/or to improve the knowledge of the aquifers of the weathered mantle in humid tropical zone, particularly in this part of South Cameroon facing the problems of drinking water supply.

2. Geographical and geological setting

The Yaounde region is located between latitudes 3°45′ and 4°00′ N and longitudes 11°20′ and 11°40′E (**Figure 1**). It has a humid tropical climate marked by two rainy seasons (mid-March to mid-June, mid-September to mid-November) alternating with two dry seasons (mid-November to mid-March, mid-June to mid-September) unevenly distributed. This region is located in the South Cameroonian Plateau (average altitude 750 m) and dominated by smooth rocky hills (>800 m) with large
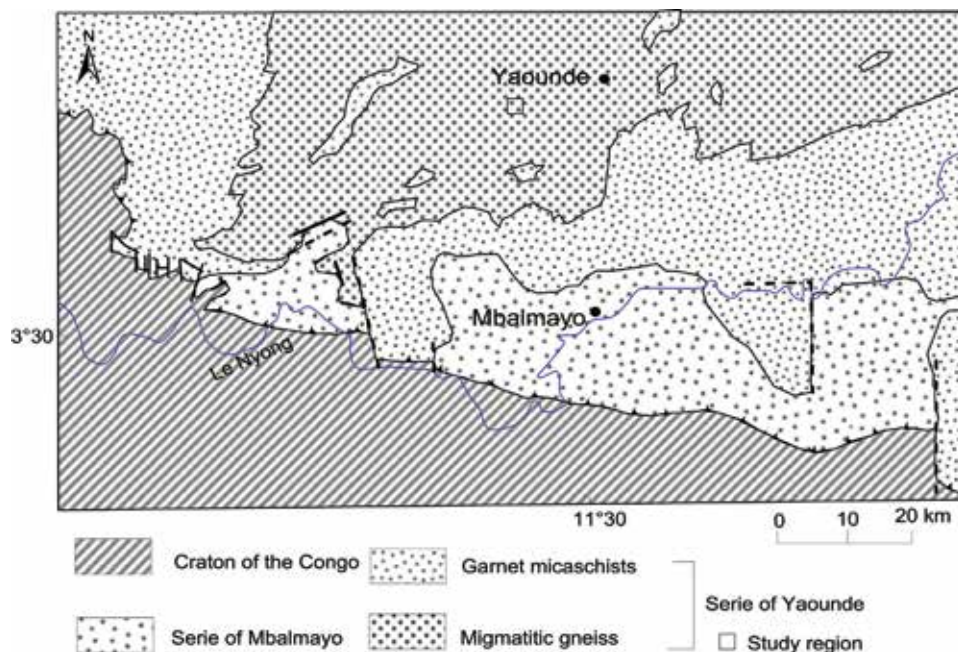
Figure 2.
Geological units of the southern domain of the North-Equatorial Pan-African Chain (modified after [22]).

convex slopes relayed by large swampy valleys (<700 m) of different widths (ranging from 50 to 150 m) [5]. The vegetation corresponds to a semi-deciduous forest [19] that has been degraded and replaced by traditional plants in urban areas.

The region of Yaounde by its rapid extension is drained to the north by the Foulou tributary of the Sanaga river and to the south by the Mefou, tributary of the Nyong river. The Mefou drains the urban part of Yaounde and has for tributary Anga'a to the southeast and Mfoundi in the center of the city (**Figure 1**). The latter flows along an oriented fracture N30 at N40 in downstream and N0 at N10 in upstream [13]. The Yaounde group constitutes a part of the Central African Mobile Zone (CAMZ) and is Pan-African in age [20, 21]. It is limited in its southern part by the Congo Craton and includes the series of Mbalmayo-Bengbis-Ayos and Yaounde (**Figure 2**) [22]. Metaplutonites and metasediments constitute the migmatitic sets of the Yaounde series [23] metamorphosed between 911 and 1127 Ma [24]. On these rocks, two geomorphologically controlled systems developed: (i) a lateritic system on the hillside and (ii) a hydromorphic swamp system [25].

3. Structure of the alteration mantle (shallow aquifer)

Basement environments have local variations in thickness of weathered materials (alterites). Their formation depends on the geological facies, the rainfall, the geomorphology, and the latitude [1]. Several authors [3, 26–29] have realized descriptions of alteration profiles in various regions of the world. These authors agree that the geological environment of the basement aquifers comprises two main stratiform horizons parallel to the paleo-surface contemporaneous with the weathering processes. From the bottom up, there is a fissured/fractured compartment above the fresh rock and an altered compartment or regolith. In the humid tropical zone, rock alteration leads to the formation of lateritic profiles [6, 30, 31]. The distinct horizons developed within it depend on short- or long-term alteration processes [5, 6]. The generic model of the weathering mantle of the Yaounde geological formations belongs to the lateralization regime and is identical to whatever the lithology is [5, 25, 32]. It is composed of the base toward the top, of a (**Figure 3**):

- Weathering set (5 m and more) constituted, from bottom to top, of:

  ○ Isalterite or coarse saprolite (2 m and over) with preserved parent rock structure and overlying fresh gneiss at the base; the alteration front is surmounted by a laminated part; there are relics of the original rock (quartz, rutile, and disthene) and the development of a fissured system parallel to the original orientation; and the fissures are millimeter and filled with alteration products composed of kaolinite and oxyhydroxides of iron and alumina.

  ○ Alloterite or fine saprolite (1–2 m), consisting of goethite and hematite and with ghosts of original minerals; this horizon has, in places, small depressions or alveoli which are dry at the edge of the nodular horizon above or present a water circulation when they seem to mark the transition with the soft level; these cells are comparable to karst forms described by [33]. They are, respectively, characterized by the rarity or the absence of alteration products at the level of these pseudo karts, and the presence of a water circulation can explain the departure of the finest materials.

- Glebular set of iron oxyhydroxide accumulation and kaolinitic clay, set of iron redistribution and deferrugation; he understands, from bottom to top:
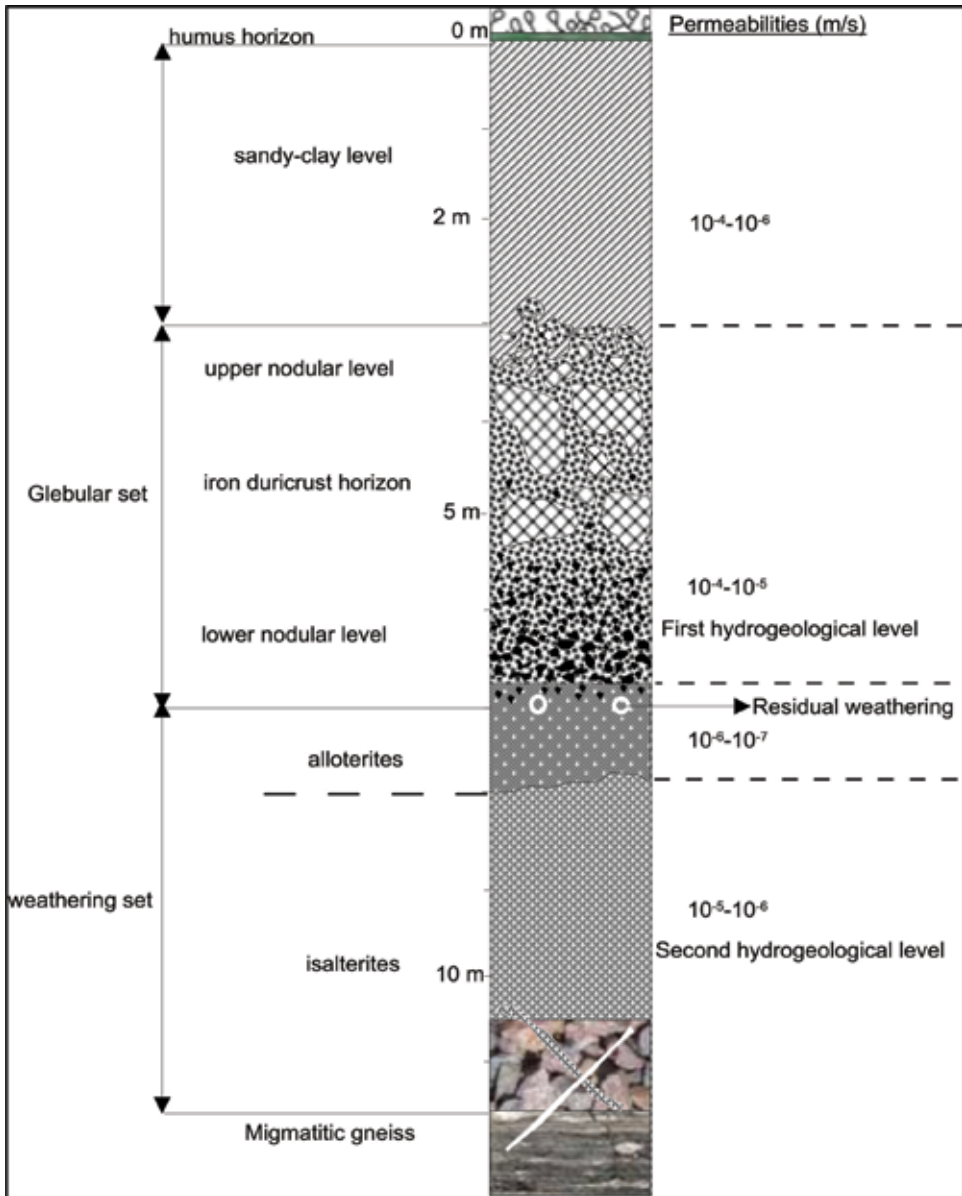
Figure 3.
Graphic illustrating the macroscopic organization of the alteration profile.

- ○ A lower nodular material (ferruginous nodule litho-relictual dominant, irregularly shaped platelet)

- ○ The iron duricrust blocks with facies varying according to the sites

- ○ A heterogeneous upper nodular material

- • Loose superficial level of variable thickness depending on the site (1–6 m); it is sandy-clay (predominantly kaolinite, hematite, and goethite) and red in color, red-brown to red-yellow. It may be absent where the glebular set is developed or outcrop.

The iron crust hillocks appear between 700 and 800 m of altitude [25]. These hillocks correspond, at the level of each sub-basin of the Mfoundi, to areas of high

altitudes (760–800 m) and moderate altitude ridges on the slopes (740–760 m). The sandy clay-sandy layer has a thickness between 2 and 47 m. Soil profiles are generally thicker (>20 m) in areas where these topographic shelves are observed and less thick (<5 m) in areas with high topography (>850 m) where the fissured/fractured compartment is by places observed. These different regional shelves are the result of successions of alteration and erosion phases (biostasis and rhexistasia) [5, 6]. These mounds are separated by flat valleys including the Mfoundi Valley. The distribution of the shelves with respect to the Mfoundi watercourse shows a predominance of the highest mounds on the right bank (770–800 m) and the lowest ones on the left bank (see **Figure 1**).

4. Hydrodynamic properties of shallow unconfined aquifer

Various techniques, as reported in the literature, are used to determine the hydrodynamic properties of aquifers in basement areas in general and its superficial part in particular. They include but are not limited to field methods (pumping test, slug test and tracer test, Porchet test) [12, 22, 34]; laboratory and mathematical methods [35], empirical formulas [36], and regional methods [37, 38]. Even though accurate estimation of hydrodynamic proprieties (effective porosity, permeability, and transmissivity) may be conducted in the field environment, poor knowledge of aquifer geometry sometimes limits their potential application [39]. The general characteristics of the altered compartment of the hard rock show that the alterites are of sandy-clay nature and have a generally low hydraulic conductivity but significant water retention capacities [29, 37]. These alterites show a heterogeneity marked by a range of variation in hydraulic conductivity between 10^{-8} and 10^{-5} m/s [28, 35, 40, 41], depending on the clay content which is low in the laminate level (base of saprolite). The variation of this hydraulic conductivity is related to topography and a weathering processes [43]; [12, 30] and presents elsewhere a decrease with the depth of the soil. This decay obeys, depending on the case, a power law or an exponential function [31, 44–47]. Transmissivity is a function of the thickness of the saturated zone and varies between 10^{-6} and 10^{-2} m²/s [1, 31]. The altered compartment (alterite) ensures, when saturated, a capacitive function, and its porosity is considered an "interstice" type [34]. The effective porosity depends on the geology and structure of the alteration profile and varies between 3 and 10% [27, 28, 38, 41].

The work leading to the determination of the hydraulic conductivity (based on the Porchet tests) in the Yaounde weathering formations is in majority carried out at depths between 0 and 100 cm. In "classical" soil profiles (with low rhexistasia), these depths generally correspond to bioturbated soils where the permeabilities are, in general, higher. In the case of this study, the morphopedological data of the studied area indicate that the processes of alteration or erosion make appear, in places, the glebular set or alteration set in surface [5, 11]. The hydraulic conductivities corresponding to these depths are therefore representative of the whole subsurface aquifer. In addition, depth investigation data (beyond 8 m), based on pumping tests or slug tests, indicating the level/horizon actually investigated, were also taken into account in the hydraulic description of this aquifer. Hydraulic conductivity values from infiltration tests range from 10^{-7} to 10^{-3} m/s [12, 36]. The normal distribution (**Figure 4**) of the hydraulic conductivity values is unimodal and varies over four orders of magnitude, attesting the variability of this propriety of the loose materials. At the scale of the soil profile (**Figure 3**), the hydraulic conductivity varies between 10^{-6} and 10^{-4} m/s in the loose superficial level, 10^{-5} and 10^{-4} m/s in the glebular set, 10^{-7} and 10^{-6} m/s in alloterite, and 10^{-6} and 10^{-5} m/s in isalterite horizon [11, 17]. At the well scale (slug test), these values vary from 5.13×10^{-6} m/s
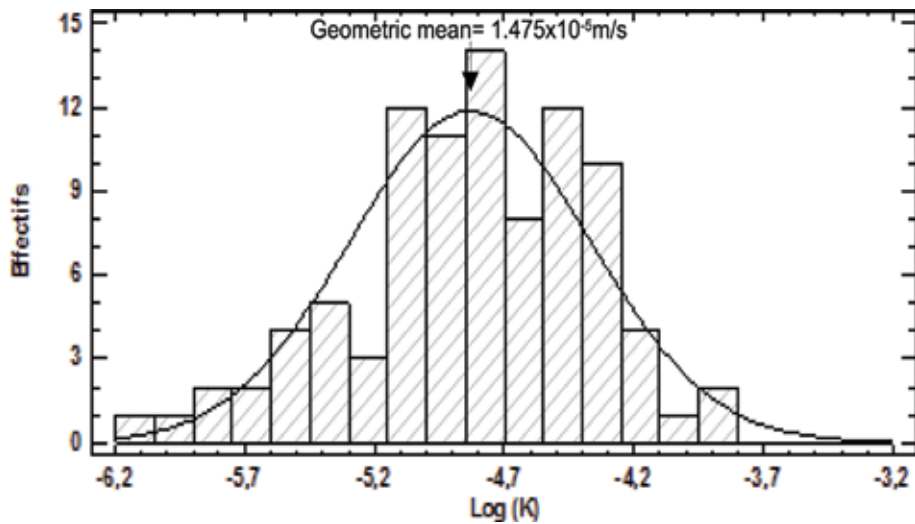
Figure 4.
Histogram of hydraulic conductivity distribution determined by Porchet hydraulic tests (constant head).

in the glebular set [36] to 5.8 × 10^{-5} m/s in saprolite [17] for a transmissivity of 2.3 ± 1.5.10^{-4} m^2/s [8]. The effective porosity determined at the sample scale is 7.4% [47]. These properties are important for the movement of shallow groundwater, both in the altered compartment (regolith) and in the underlying bedrock [30, 48].

5. Hydrodynamic of the weathering mantle

5.1 Hydrogeological levels

The hydrodynamics of the alteration mantle in the tropical zones present, globally, two hydrogeological levels illustrated in **Figure 3**. These distinctions are based on the hydraulic characteristics of confining layers.

5.1.1 Perched aquifer of iron crust

The iron crust has alveolar permeability due to its structure and fracture permeability due to its dismantling [48]. It promotes rapid infiltration into areas where it is preserved from subsequent erosion. The voids present below the indurated level (**Figure 3**) can create a strong permeability contrast with the altered level (alloterite), giving rise to a locally perched aquifer with a few sources that exhibit an epikarst-type function [3]. In the case of heavy precipitation, the temporary water table in this aquifer can be loaded under the iron crust and give rise locally to artesian sources [48].

5.1.2 Aquifer of alterite

Its hydrodynamic properties (high porosity and low permeability) give it the capacitive function of the aquifer system [3, 17]. Seepage areas may be locally observed on outcrops of laterites during high water events [48]. Its lower part (coarse saprolite), composed of very weathered rock and relatively healthy blocks, facilitates the circulation of water. This gives it a transmissive function, thus feeding the main resurgences of the slopes and the streams base flow. The rates obtained

in the aquifer of alterites are of the order of 1 m^3 h [49]. The distinction between different types of aquifers is often difficult. It is necessary to have data about sub-surface lithology, water levels, and hydraulic parameters of aquifer and confining layers for identifying a particular type of aquifer.

5.2 Hydrometry and piezometry

The common groundwater structures used to study the hydrodynamic operation of aquifers are wells, springs, and boreholes. Wells are generally dug to the base of loose alterite as the springs emerge either between the alloterite and the overlying horizon or between the isalterite (coarse saprolite) and the upper fissured horizon (saprock). Boreholes most often pick up the basement or basement-alterite system whose behavior is sometimes comparable to that of a shallow unconfined aquifer [41]. The data presented in this work relate only to springs and wells. The discharges of springs vary between 0.04 and 6.2 m^3/h against 0.06 and 0.5 m^3/h in the wells. The recession coefficients of springs vary between 0.001 and 0.016/d against 0.06 and 0.39 m/month at wells [11]. Springs emerging on the coarse saprolite-saprock continuum generally have the highest flow rates [11]. This observation is consistent with that of the other authors [26, 35, 38] which indicates that it is at fissured horizon that the hard rock aquifers owe their productivity. At the lithological scale, the order of magnitude of productivity of the springs is between 0.03 and 3.2 m^3/h and between 0.03 and 6.2 m^3/h, respectively, in metaplutonites and metasediments. This difference of a factor of 2 is not significant with the depths of groundwater which vary between 0.0 and 17.7 m, with an average of 5.7 ± 6.2 m in the whole of the area. In the Mfoundi watershed, these depths differ by about 4 m between the two banks either between 0.0 and 13.5 m on the right bank or 0.1 and 17.7 m on the left bank. Its hydrodynamic characteristics indicate that the aquifer has, in places, highly heterogeneous areas. The ancient tectonic structuring E-W at NW-SE (592 Ma at 658 Ma [24]) controls the orientation of the hydrographic network. Thus, the landscape form, which is shaped by the hydrographic network, is at the origin of the upstream-downstream underground flows conforming to the outline of the topography, namely, NNE, NS, EW, and ESE to SE [11]. The average piezometric amplitudes corresponding to this altitudinal distribution range between 1.3 and 3.1 m in the summit zones, between 0.7 and 1.1 m in the mid-slope zones, and between 0.3 and 0.6 m in the valleys where the watercourse is generally the imposed potential [11]. The seasonal dynamics of the Yaounde shallow unconfined aquifer (alterite) are, in general, similar to those observed in the basement zone, in humid tropical climates [11, 49–51]. The piezometric increases are observed during the great rainy season and vice versa during the dry season (**Figure 5**). The discharge of the aquifer evolves according to an exponential law characteristic of environments with high inertia. This inertia and/or the continuous/discontinuous nature of the aquifer reservoir may be at the origin of piezometric anomalies (**Figure 6**) characterized by a piezometric increase in the dry season and a decrease in the rainy season [52]. According to [42], these piezometric anomalies indicate areas of high transmissivity. The relationship between well and springs behavior and rainfall has a lag of about 1 month (**Figures 5** and **6**) that can be attributed to morphopedological processes. Some authors attribute this lagging to delayed drainage between recharge and drainage areas [50] and the evapotranspiration of one part of the rain, so the degree of soil moisture during the periods proceeding rainy phases [51]. Some wells have a rapid response to precipitation (**Figure 6**). This rapid response of the water table to rainfall depends on the geological units [53] or the water-level position [54]. This position classifies the water table at local, regional, and continental
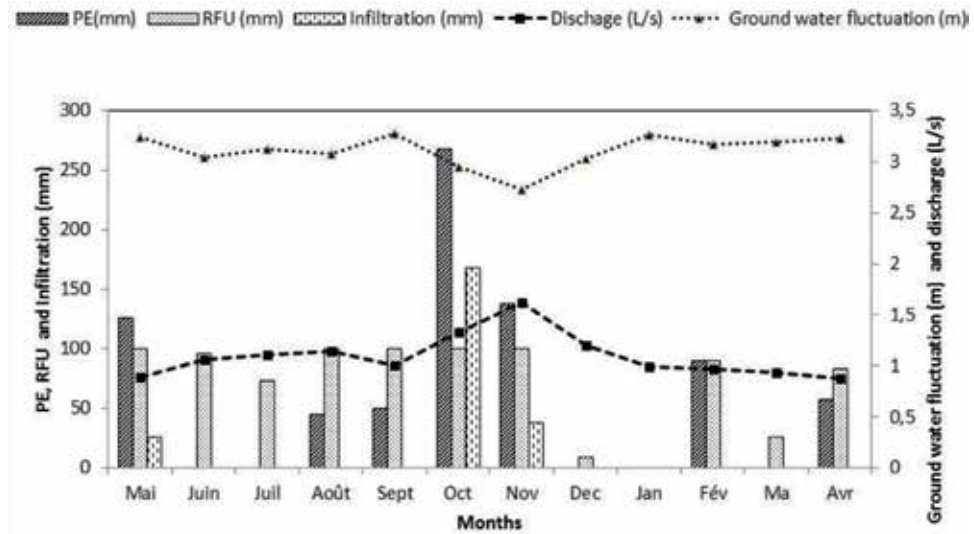
Figure 5.
Graphic illustrating the evolution of the average values of the flow of the sources and the fluctuations of the piezometric levels in the Olezoa watershed (2010–2011). PE = effective precipitation, RFU = available water content of the soil.
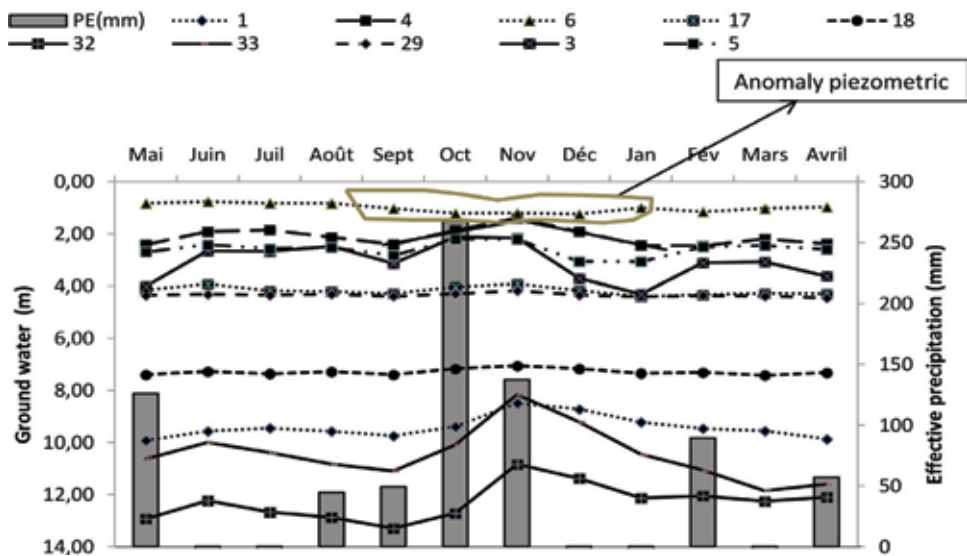
Figure 6.
Graphic illustrating the evolution of the groundwater depths of some dug wells showing the piezometric anomaly in the Olezoa watershed (2010–2011).

scales. Indeed, the character of the water table is fundamental to conceptualize the groundwater flow systems and to examine the connections between groundwater, surface water, and climate [55]. Unfortunately, studies on the classification of groundwater at various scales are limited throughout the Mfoundi basin and surrounding areas.

However, ongoing work in the Olezoa watershed has identified two topographic scales highlighting the concept of hierarchical groundwater flow systems [56]. Beyond this hierarchy, the two scales nevertheless suggest that the piezometric surface is much more controlled by the topography than by the recharge. In the first

case, water table generally coincides with the topographic surface, and the depths of water table are small. In the second case, the depths are high, and the water table is totally disconnected from the topography [54].

5.3 Estimation of aquifer recharge

In the humid tropical zones, the fluctuation of groundwater levels in weathered layer (alterites) is controlled to varying degrees by effective rainfall [51], the streams, topography [11, 57], the thickness of the saturated portion of the saprolite [58], and pumping extracting [57]. Fluctuations in groundwater levels are dynamic responses of the system to recharge (input water) and discharge (loos water) [57]. The evolution of the discharge according to an exponential law (**Figures 5** and **6**) is characteristic of a water table fed mainly by vertical contributions [59]. Several approaches are used to evaluate these input water (recharge/infiltration) including empirical methods, base flow measurement methods, water-table fluctuation (WTF) method, chloride balance method, soil moisture method, isotope method, or mathematical methods [49, 57]; [60]. The application of some of these methods in the Yaounde area indicates that the recharge of shallow aquifer of Yaounde migmatitic basement is recent and is done directly by infiltration of precipitation without any notable change due to evaporation [61]. The average isotope contents of ^{18}O of rain and shallow groundwater are, respectively, -2.47 and -2.57‰ Vs-SMOW [61] with annual and monthly isotope signature differences in precipitation values [62]. Groundwater recharge appears to occur in May, October, and November (**Figures 5** and **6**) and increase from 30 mm/yr in the lowland to 40 mm/yr in the highland [60]. The infiltration coefficient varies between 5.7 and 7.5% according to the chlorine balance method [60, 61], 6% with the WTF [17], and between 5 and 23% according to the Thornthwaite method with an available water content of the soil (RFUmax) of 100 mm [14, 15, 17].

6. Hydrogeological model of the weathered mantle of Yaounde migmatitic basement

This model is based on the following observations:

- A thick weathered mantle with two hydrogeological levels within it.

- The iron crust hillocks appearing between 740 and 760, between 760 and 780, and between 780 and 800 m.

- An altimetric phase shift of the topographic shelves between the two banks of the Mfoundi watercourse, showing a Miocene flattening surface [63].

- A variation of the piezometric surface related to this altimetric phase shift, but the piezometric level is close to the ground surface.

- Recharge to groundwater is by direct infiltration of rain into the altered aquifer to the fractured aquifer. This is more important on the high points where the piezometric fluctuations are high.

All these observations are summarized in **Figure 7**.
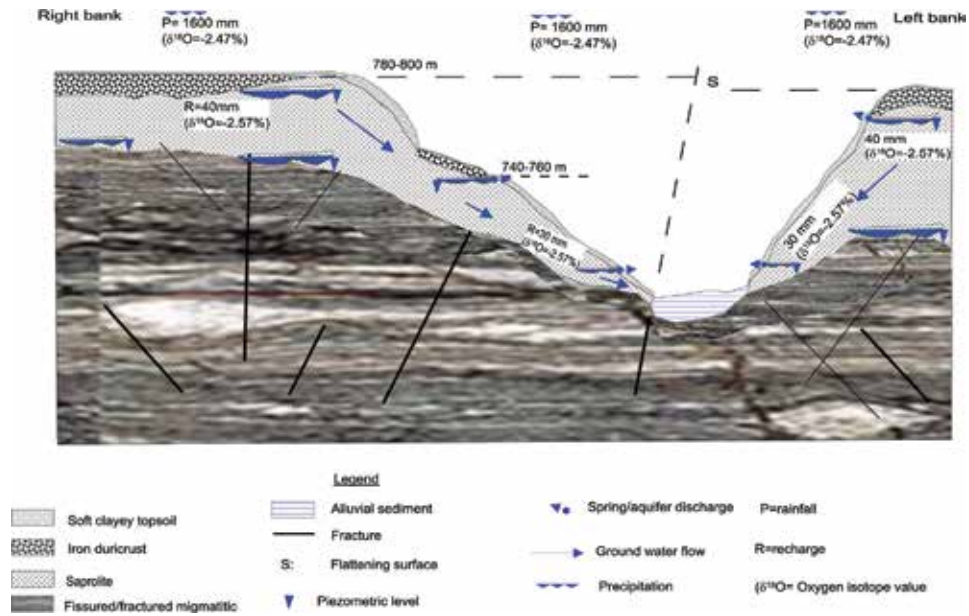
Figure 7.
Conceptual hydrogeological model of the weathered mantle of Yaounde migmatitic basement.

7. Conclusion

Hydrogeological studies in the city of Yaounde and its environs are conducted in a context where the extension of public drinking water supply does not follow unregulated urbanization, fueled by population growth, and internal migration. The compilation and analysis of the information acquired during these studies allowed to propose an image of the hydrogeological characteristics of the alteration formations of this city. The weathered mantle of migmatitics of the Pan-African series of Yaounde presents the characteristics of a hard rock aquifer in a humid tropical environment. A perched aquifer is identified, overlying the alterite aquifer and a hydraulic conductivity decreasing with the depth of the soil. The upper part of the weathered mantle (regolith) is sometimes assimilated to a homogeneous aquitard under which the saprock aquifer develops. This mantle shows an old alteration resulting from the dismantling of old lateritic systems on the one hand and, on the other hand, a polyphase alteration model, with relatively recent alterites developed on a morphology presenting a significant relief. If this structure is similar to those of the granito-gneissic formations of the world (India, France, other African countries), there are nevertheless specificities that can be related to the local scale to those of limestone environments. Indeed, the solubility of silicates in a humid tropical environment allows the formation of voids or microreliefs of weathering. These microreliefs can have a local influence on the hydrodynamism of the shallow aquifer (regolith). Hydrodynamic characteristics indicate a recent recharge by direct infiltration of precipitation without any notable change due to evaporation. These highlight the effect of several forms of heterogeneities that are related to the relief model and to the physical and hydraulic properties of the terrain.

Acknowledgements

Conflict of interest

No conflict of interest.

Author details

Jules Rémy Ndam Ngoupayou[3], André Firmin Bon[1,2,3*],
Guillaume Ewodo Mboudou[2,3], Nasser Ngouh Abdou[3]
and Georges Emmanuel Ekodeck[3]

1 Department of Meteorology, Climatology, Hydrology and Soil Science, National Advanced School of Engineering, University of Maroua, Maroua, Cameroon

2 Department of Hydraulics and Water Control, National Advanced School of Engineering, University of Maroua, Maroua, Cameroon

3 Department of Earth Sciences, Faculty of Science, University of Yaounde I, Yaounde, Cameroon

*Address all correspondence to: bon_andr@yahoo.com

IntechOpen

References

[1] Taylor RG, Howard KWF. A tectono-geomorphic model of the hydrogeology of deeply weathered crystalline rock: Evidence from Uganda. Hydrogeology Journal. 2002;**8**:79-294

[2] MacDonald M, Bonsor HC, Dochartaigh BEO, Taylor RG. Quantitative maps of groundwater resources in Africa. Environmental Research Letters. 2012;**7**. stacks.iop.org/ERL/7/024009

[3] Lachassagne P, Wyns R, Dewandel B. The fracture permeability of Hard Rock Aquifers is due neither to tectonics, nor to unloading, but to weathering processes. Terra Nova. 2011;**10**:1365-3121

[4] Mvondo Ondoa J. Caractérisation des évènements tectoniques dans le domaine Sud de la Chaine Panafricaine au Cameroun: Styles tectoniques et géochronologie des séries de Yaounde et de Bafia [Doct/Ph.D. thesis]. University of Yaounde I; 2009

[5] Bitom D, Volkoff B, Beauvais A, Seyler F, Ndjigui P-D. Rôle des héritages et du niveau des nappes dans l'évolution des modelés et des sols en zone intertropicale forestière humide. Comptes Rendus Geoscience. 2004;**336**:1161-1170

[6] Braun J-J, Ndam Ngoupayou JR, Viers J, Dupre B, Bedimo Bedimo J-P, Boeglin J-L, et al. Present weathering rates in a humid tropical watershed: Nsimi, South Cameroon. Geochimica et Cosmochimica Acta. 2005;**69**:357-387

[7] Kuitcha D, Fouépé Takounjou A, Ndjama J, Takem Eneke G, Tita Awah M, Kamgang Kabeyene B. Chemical and isotopic signal of precipitation in Yaounde-Cameroon. Archives of Applied Science Research. 2012;**4**(6):2591-2597

[8] Ewodo Mboudou G, Ombolo A, Fouepe Takounjou A, Bon AF, Ekodeck GE. Etude des Paramètres hydrauliques des aquifères de sub-surface du bassin versant de la Mingosso, région de Yaounde. Revue du CAMES-Série A. 2012;**13**:123-127

[9] Ewodo Mboudou G, Ombolo A, Bon AF, Ntep F, Bineli E. Apport des méthodes paramétriques DRASTIC, GOD et SI à l'évaluation de la vulnérabilité intrinsèque dans les aquifères du bassin versant de l'Abiergué (région de Yaounde). Revue du CAMES-Série A. 2016;**4**(2)

[10] Kringel R, Rechenburg A, Kuitcha D, Fouépé A, Bellenberg S, Kengne IM, et al. Mass balance of nitrogen and potassium in urban groundwater in Central Africa, Yaounde/Cameroon. Science of the Total Environment. 2016;**547**:382-395. DOI: 10.1016/j.scitotenv.2015.12.090

[11] Bon AF, Ndam Ngoupayou JR, Ewodo Mboudou G, Ekodeck GE. Caractérisation hydrogéologique des aquifères de socle altéré et fissuré du bassin versant de l'Olézoa à Yaounde, Cameroun. Revue des Sciences de l'Eau. 2016;**29**(2):149-166

[12] Bon AF, Ombolo A, Ewodo Mboudou G, Ndam Ngoupayou JR, Ekodeck GE. Estimation of hydraulic conductivity of soils at a watershed-scale using Porchet's method: Application in the Olezoa watershed, Yaounde, Cameroon. IJG. 2016;**7**:397-408. DOI: 10.4236/ijg.2016.73031

[13] Mpesse JE. Contribution à l'étude pétrostructurale des formations métamorphiques de la région de Yaounde et de la formation de la géométrie de sa tectonique tangentielle. Th. Doct. 3e cycle, University of Yaounde I. 1999

[14] Ewodo Mboudou G. Caractérisation et fonctionnement des aquifères de sub-surface en zone de socle cristallin et de climat intertropical humide: Cas des bassins versants de la Mingosso et de l'Abiérgué (Région de Yaounde—Cameroun) [Doct/Ph.D. thesis]. University of Yaounde I. 2012

[15] Tabue Yombi JG. Vulnérabilité de la nappe superficielle en zone de socle cristallin urbanisée. Cas du bassin versant de la Mingoa à Yaounde au Cameroun. [Doct/Ph.D. thesis]. University of Yaounde I. 2013

[16] Kuitcha D. Bactériologie et Hydrochimie des ressources en eau du bassin versant amont du Mfoundi à Yaounde (Centre-Cameroun). [Doct/Ph.D. thesis]. University of Yaounde I. 2013

[17] Bon AF. Modélisation de la structure et du fonctionnement des aquifères du socle fracturé et altéré dans le bassin versant de l'Olézoa, Yaounde – Cameroun. [Doct/ Ph.D. thesis]. University of Yaounde I. 2017

[18] Kalla MF. Caractérisation physique et hydrodynamique de l'aquifère à nappe libre du bassin versant de Ntem à Yaoundé-Cameroun [DEA]. University of Yaounde I; 2007

[19] Bon AF. Hydrodynamique d'un bassin versant en zone de socle cristallin fracturé et alteré: Cas du bassin versant de l'Olezoa au Sud – Ouest de la ville de Yaounde – Cameroun. Mém. DEA. University of Yaounde I, Fac Sci. Dpt Sciences de la Terre. 2008

[20] Letouzey R. Notice explicative de la carte phytogéographique du Cameroun à l'échelle de 1/500 000. Toulouse: Institut de la Carte Internationale de la Végétation; 1985

[21] Toteu SF, Yongue Fouateu R, Penaye J, Tchakounté J, Seme Mouangue AC, Van Schmus WR, et al. U-Pb dating of plutonic rocks involved in the nappe tectonic in southern Cameroon: Consequence for the Pan-African orogenic evolution of central African fold belt. Journal of African Earth Sciences. 2006;**44**:479-493

[22] Nzenti JP, Njanko T, Njiosseu ELT, Tchoua FM. Les domaines granulitiques de la chaîne panafricaine Nord-Equatoriale au Cameroun Géologie et environnement au Cameroun. Vicat et Bilong, editors. Collect. GEOCAM 1998;**1**:255-264

[23] Mvondo H, Owona S, Mvondo Ondoa J, Essono J. Tectonic evolution of the Yaounde segment of the Neoproterozoic Central Orogenic Belt in southern Cameroun. Canadian Journal of Earth Sciences. 2007;**44**:433-444

[24] Ngnotué T, Ganno S, Nzenti JP, Schulz B, Tchaptchet Tchato D, Suh Cheo E. Geochemistry and geochronology of Peraluminous High-K granitic leucosomes of Yaounde series (Cameroon): Evidence for a unique Pan-African magmatism and melting event in North Equatorial Fold Belt. IJG. 2012;**3**:525-548

[25] Ngon Ngon GF, Yongue-Fouateu R, Bitom DL, Bilong P. A geological study of clayey laterite and clayey hydromorphic material of the region of Yaounde (Cameroon): A prerequisite for local material promotion. Journal of African Earth Sciences. 2009;**55**:69-78

[26] Cho M, Ha KM, Choi YS, Kee WS, Lachassagne P, Wyns R. Relationships between the permeability of hard rock aquifers and their weathering cover based on geological and hydrogeological observations in South Korea. In: IAH. Conference on Groundwater in Fractured Rocks. 15-19 September 2003; Prague

[27] Wyns R, Baltassat JM, Lachassagne P, Legchenko A, Vairon J, Mathieu F. Application of SNMR soundings for

groundwater reserves mapping in weathered basement rocks (Brittany, France). Bulletin de la Société Géologique. 2004;**175**:21-34

[28] Dewandel B, Lachassagne P, Wyns R, Marechal JC, Krishnamurthy NS. A generalized 3-D geological and hydrogeological conceptual model of granite aquifers controlled by single or multiphase weathering. Journal of Hydrology. 2004;**330**:260-284

[29] Courtois N, Lachassagne P, Wyns R, Blanchin R, Bougaïre FD, Some S, et al. Large-scale mapping of hard-rock aquifer properties applied to Burkina Faso. Ground Water. 2010;**48**(2):269-283

[30] Taylor R, Tindimugaya C, Barker J, Macdonald D, Kulabako R. Convergent radial tracing of viral and solute transport in gneiss saprolite. Ground Water. 2010;**48**(2):284-294

[31] Bonsor HC, MacDonald AM, Davies J. Evidence for extreme variations in the permeability of laterite from a detailed analysis of well behaviour in Nigeria. Hydrological Processes. 2014;**28**:3563-3573

[32] Ndjigui P-D, Badinane MFB, Nyeck B, Nandjip HPK, Bilong P. Mineralogical and geochemical features of the coarse saprolite developed on orthogneiss in the SW of Yaounde, South Cameroon. Journal of African Earth Sciences. 2013;**79**:125-142

[33] Vicat JP, Mvondo H, Willems L, Pouclet A. Phénomènes karstiques fossiles et actuels au sein des formations métamorphiques silico-alumineuses de la nappe pan-africaine de Yaounde (Sud-Cameroun). Comptes Rendus Geoscience. 2002;**334**:545-550

[34] Marechal JC, Wyns R, Lachassagne P, Subrahmanyam K, Touchard F. Anisotropie verticale de la perméabilité de l'horizon fissuré

des aquifères de socle: Concordance avec la structure géologique des profils d'altération. Comptes Rendus Geoscience. 2003;**335**:451-460

[35] Angulo-Jaramillo R, Bagarello V, Massimo I, Lassabatere L. Infiltration Measurements for Soil Hydraulic Characterization. Springer International Publishing; 2016. DOI: 10.1007/978-3-319-31788-5

[36] Jaunat J, Dupuy A, Huneau F, Celle-Jeanton H, Le Coustumer P. Groundwater flow dynamics of weathered hard-rock aquifers under climate-change conditions: An illustrative example of numerical modeling through the equivalent porous media approach in the north-western Pyrenees (France). Hydrogeology Journal. 2016. DOI: 10.1007/s10040-016-1408-9

[37] Fouépé TA, Fantong W, Ndam Ngoupayou JR, Sigha NL. Comparative analysis for estimating hydraulic conductivity values to improve the estimation of groundwater recharge in Yaounde-Cameroon. British Journal of Environment and Climate Change. 2012;**2**(4):391-409

[38] Dewandel B, Maréchal JC, Bour O, Ladouche B, Ahmed S, Chandra S, et al. Upscaling and regionalizing hydraulic conductivity and effective porosity at watershed scale in deeply weathered crystalline aquifers. Journal of Hydrology. 2012;**416-417**:83-97. DOI: 10.1016/j.jhydrol.2011.11.038

[39] Dewandel B, Caballero Y, Perrin J, Boisson A, Dazin F, Ferrant S, et al. A methodology for regionalizing 3-D effective porosity at watershed scale in crystalline aquifers. Hydrological Processes. 2017:1-19. DOI: 10.1002/hyp.11187

[40] Uma KO, Egboka BCE, Onuoha KM. New statistical grain-size method for evaluating the hydraulic conductivity

of sandy aquifers. Journal of Hydrology. 1989;**108**:367-386

[41] Chilton PJ, Foster SSD. Hydrogeological characteristics and water-supply potential of basement aquifers in Tropical Africa. Hydrogeology Journal. 1995;**3**:3-49

[42] Compaore G, Lachassagne P, Pointet T, Travi Y. Evaluation du stock d'eau des altérites. Expérimentation sur le site granitique de Sanon (Burkina-Faso). In: Rabat IASH Conference, IASH. 1997;**241**:37-46

[43] Adelinet M, Fortin J, Ozouville N, Violette S. The relationship between hydrodynamic properties and weathering of soils derived from volcanic rocks, Galapagos Islands (Ecuador). Environmental Geology. 2007;**56**:45-58. DOI: 10.1007/s00254-007-1138-3

[44] Molénat J, Gascuel-Odoux C, Davy P, Durand P. How to model shallow water-table depth variations: The case of the Kervidy-Naizin catchment, France. Hydrological Processes. 2005;**19**:901-920

[45] Jiang XW, Wan L, Wang X-S, Ge S, Liu J. Effect of exponential decay in hydraulic conductivity with depth on regional groundwater flow. Geophysical Research Letters. 2009;**36**:L24402. DOI: 10.1029/2009GL041251

[46] Cardenas MB, Jiang X-W. Groundwater flow, transport, and residence times through topography-driven basins with exponentially decreasing permeability and porosity. Water Resources Research. 2010;**46**:W11538. DOI: 10.1029/2010WR009370

[47] Ameli AA, McDonnell JJ, Bishop K. The exponential decline in saturated hydraulic conductivity with depth: A novel method for exploring its effect on water flow paths and transit time

distribution. Hydrological Processes. 2016;**30**(14):2438-2450. DOI: 10.1002/hyp.10777

[48] Join JL, Robineau B, Ambrosi JP, Costis C, Colin F. Système hydrogéologique d'un massif minier ultrabasique de Nouvelle-Calédonie. Comptes Rendus Geoscience. 2005;**337**:9

[49] Chilton PJ, Smith-Carington AK. Characteristics of the weathered basement aquifer in Malawi in relation to rural water supplies. In: Challenges in African Hydrology and Water Resources (Proc. Harare Symp. Juillet 1984). IAHS Publication; 1984. p. 144

[50] Mayo AL, Morris TH, Peltier S, Petersen EC, Payne K, Holman LS, et al. Active and inactive groundwater flow systems: Evidence from a stratified, mountainous terrain. GSA Bulletin. 2003;**115**:1456-1472

[51] Owor M, Taylor RG, Tindimugaya C, Mwesigwa D. Rainfall intensity and groundwater recharge: Empirical evidence from the Upper Nile Basin. Environmental Research Letters. 2009;**4**:035009

[52] Bon AF, Ndam Ngoupayou JR, Ombolo A, Ewodo Mboudou G, Ekodeck GE. Influence de la structure de l'aquifère de socle altéré et fissuré sur son fonctionnement en zone tropicale humide du sud Cameroun. In: Actes de la Conférence «Aquifères de socle: Le point sur les concepts et les applications opérationnelles ».- 20èmes Journées techniques du Comité Français d'Hydrogéologie de l'Association Internationale des Hydrogéologues. 11-13 Juin. Vol. 2015. France: Auditorium ICES, La Roche-sur-Yon, Vendée; 2015. 8 p

[53] Cai Z, Ofterdinger U. Analysis of groundwater-level response to rainfall and estimation of annual recharge in fractured hard rock aquifers, NW Ireland. Journal of Hydrology.

2016;**535**:71-84. DOI: 10.1016/j. jhydrol.2016.01.066

[54] Gleeson T, Marklund L, Smith L, Manning AH. Classifying the water table at regional to continental scales. Geophysics Research Letter. 2011;**38**:L05401. DOI: 10.1029/2010GL046427

[55] Fan Y, Miguez-Macho G, Weaver CP, Walko R, Robock A. Incorporating water table dynamics in climate modeling: 1. Water table observations and equilibrium water table simulations. Journal of Geophysical Research. 2007;**112**:D10125. DOI: 10.1029/2006JD008111

[56] Bon et al. Discrimination of piezometric fluctuations in the Oleozoa watershed (Yaounde-Cameroon) from an exponential decay model of the hydraulic conductivity of weathered materials. Statistical Approach. In press

[57] Maréchal JC, Dewandel B, Ahmed S, Galeazzi Zaidi FK. Combined estimation of specific yield and natural recharge in semi-arid groundwater basin irrigated agriculture. Journal of Hydrology. 2006;**329**:281-293

[58] Foster SSD. Hard-rock aquifers in tropical regions: Using science to inform development and management policy. Hydrogeology Journal. 2012;**20**:659-672

[59] Tison G. Fluctuations des nappes aquifères de types divers et plus particulièrement des nappes d'alluvions, Symposia Darcy, Dijon, UGGI. Assoc. Int. d'Hydrol. Scient. 1956:210-221

[60] Fouepe TA, Ndam Ngoupayou JR, Riotte J, Takem GE, Mafany G, Marechal JC, et al. Estimation of groundwater recharge of shallow aquifer on humid environment in Yaounde, Cameroon using hybrid water-fluctuation and hydrochemistry methods. Environmental Earth Sciences. 2010. DOI: 10.1007/sl2665-010-0822-x

[61] Kuitcha D, Fouépé Takounjou AL, Ndjama J. Apport de l'hydrochimie et de l'isotope de l'environnement à la connaissance des ressources en eaux souterraines de Yaounde, Cameroun. Journal of Applied Biosciences. 2013;**67**:5194-5208

[62] Wirmvem JM, Ohba T, Kamtchueng Tchakam B, Taylor ET, Fantong WY, Ako AA. Variation in stable isotope ratios of monthly rainfall in the Douala and Yaounde cities, Cameroon: Local meteoric lines and relationship to regional precipitation cycle. Applied Water Science. 2017;**7**(5):2343-2356. DOI: 10.1007/s13201-016-0413-4

[63] Tardy Y, Roquin C. Dérive des continents—Paléoclimats et altérations tropicales. Orléans: BRGM Editions; 1998

Multivariate Pollution in the Coastal Aquifer of Lebna area, Northeastern Tunisia

Amira Ziadi, Najla Hariga Tlatli
and Jamila Tarhouni

Abstract

Anthropogenic contamination and excessive water consumption endanger an overexploitation of groundwater, which causes groundwater mineralization in coastal aquifer of Lebna area. Consequently, the salinity of groundwater reserves increases and creates big economic, agricultural, and social problems. Moreover, agricultural activities are the main source of nitrate, sulfate, and potassium ions and contribute to groundwater salinization and contamination with increasing chloride and nitrate concentrations. The objectives of this research are to determine the main source of groundwater salinization in coastal aquifer of Lebna area to not confuse between seawater intrusion and fertilizer effects and to determine the salinity effects on the ecosystem. To reach this goal, several geological tools and hydrogeological data are used in combination with geochemical and geophysical methods.

Keywords: coastal aquifer, seawater intrusion, agricultural contamination, multiple approaches, mineralization, vertical electrical soundings, stable isotopes, molar ratio, ecosystem

1. Introduction

Around the world, the coastal areas contribute most significantly to agriculture, tourist, and demographic activities. However, coastal aquifer areas are threatened by many factors such as population growth leading to increased water demand, changing climatic conditions (longer periods of drought), shoreline retreat, and tidal effect as well as overexploitation (more agricultural production) and anthropogenic activity (pollution by fertilizers, return flow of contaminated irrigation water and hydraulic barriers like dams). All these factors create seawater intrusion, which then contaminates groundwater through mineralization, depletion of groundwater storage, and salinization of soil and crops causing ecosystem changes. Saltwater intrusion is one of the major environmental problems in coastal areas due to the serious and irreversible effects on the quality of the water used for drinking and irrigation purposes.

Actually, there exist several processes and natural mechanisms that can procure the mineralization process in the coastal aquifer; the most important causes are the seawater intrusion [1, 2], the sea-level-rise effect [3, 4], the up-coming of salt groundwater from deep underground layers [5–7], the direct and indirect ion exchange [8, 9], the variable density flow effect [10, 11], and salt water irrigation return flow [12, 13].

Several authors from the world have used several approaches to study and manage the mineralization problem in coastal aquifer such as geophysical and geo-chemical techniques, conceptual and mathematical modeling, and analytical and numerical methods [1, 2, 14]. Generally, there is confusion between researchers in the determination of the principal origin of groundwater salinization in the coastal aquifer where the coastal area recognizes an intensive use of fertilizers.

In North Africa, coastal aquifers serve as major sources of freshwater supply in many countries, especially in arid and semi-arid zones.

Tunisia, located in eastern North Africa, undergoes the influence of two types of climate: the Mediterranean in the north and the Saharan in the south. Tunisia is known by a spatial and temporal variability of water resources and is menaced by relatively limited renewable water resources. In fact, Tunisia is one of the countries that are facing the problem of marine intrusion in the coastal areas where groundwater is intensively used for irrigation. Furthermore, farming consumes 80% of water resources, especially groundwater resources in the coastal areas. Numerous studies of the salinization processes in Tunisia are elaborated based on several approaches and show the phenomenon of marine invasion may extend over several kilometers inland, jeopardizing coastal groundwater supplies in these areas such as the coastal aquifer of Nabeul-Hammamet in northeastern Tunisia [15], the coastal Teboulba aquifer in the eastern Sahel of Tunisia [16], the shallow coastal aquifer of the Djeffara plain in southeastern Tunisia [17].

The study area is the coastal aquifer of Lebna plain, located in northeastern Cap-Bon, Tunisia. It is characterized by very intense agricultural activities (vegetables and spices), population growth, and a developing economy, all of which have greatly increased freshwater demand. Moreover, in recent years, the study area has seen significant changes in water and land use: some wells have been abandoned due to salty groundwater; new crops and animals have moved closer to the sea, and brackish soil and water have surrounded the river. In addition, groundwater depletion and high electrical conductivity values appeared near the coastal part of the aquifer, suggesting that seawater intrusion may occur [18, 19].

Hence, this work aims to determine the principal sources of groundwater mineralization and to identify the salinity effects to ecosystem in the Lebna area.

2. Study area

The study area, Lebna coastal plain, is part of the Lebna watershed located in northeastern Tunisia (**Figure 1**). It is near the Korba watershed, within the eastern coastal plain of Cap-Bon in northeastern Tunisia. It is surrounded by the Mediterranean Sea along the eastern border, the Djebel Sidi Abdurrahman anticline in the west, and the cities of Menzel Heur and Tafelloune in the northeast and southeast, respectively.

The study area is recognized by an important crop production than industrial production. Consequently, the irrigated areas are extended which increased the water irrigation demand. In addition, Lebna River is the main hydrology network in the Lebna plain, where in the upstream of Lebna River, a big dam was implemented in 1986 with a big water storage capacity to provide water demand. In fact, Lebna River receives water flux only during Lebna dam spill.

The area is also characterized by a semi-arid climate, an annual mean temperature of 22°C, and a highly variable annual average precipitation between 400 and 450 mm, thus resulting in the unsustainability of its water resources [20].
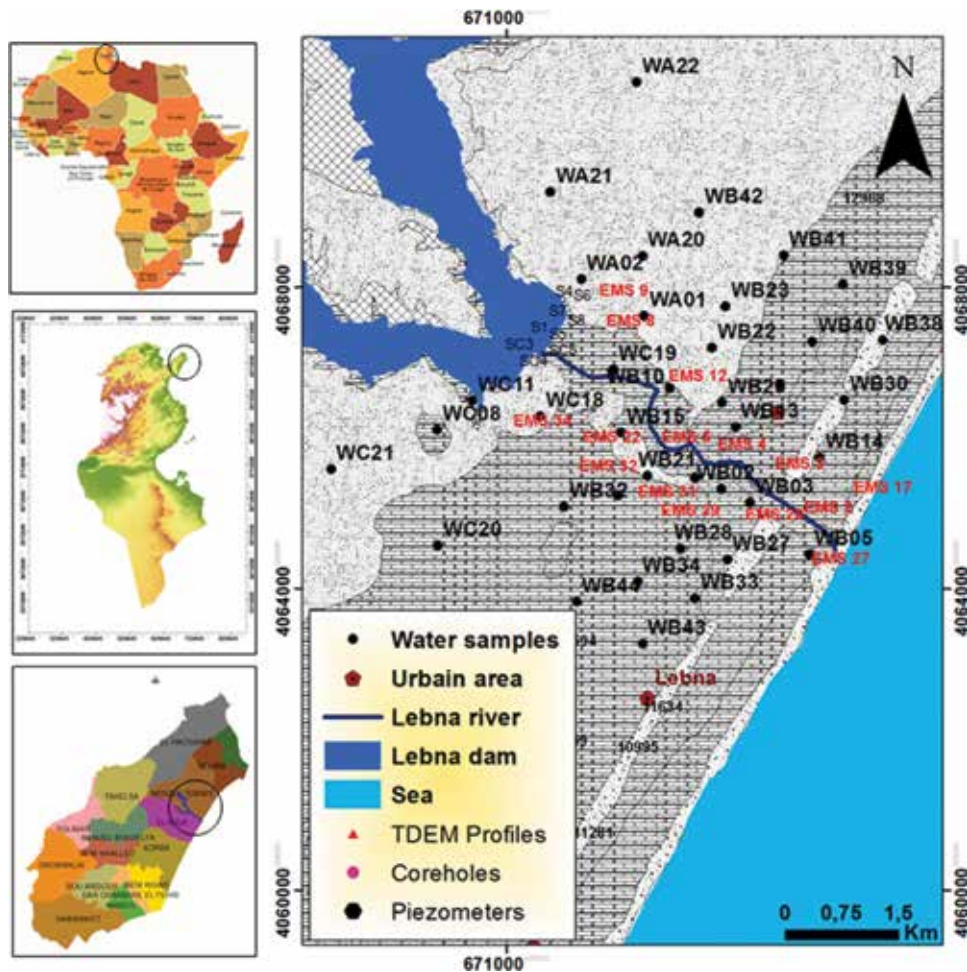
Figure 1.
Geographical location of study area.

The outcropping formations of the coastal area in the Lebna plain contain Mio-Plio-Quaternary sediments as shown in **Figure 2**. The first unit, the lower Miocene, has detrital deposits known as the Fortuna formation. The middle Miocene is composed of lenticular sandstones and marls with lignite levels called the Saouaf Formation. In the study area, the Upper Miocene is absent. The second unit, the transgressional marine Pliocene, which represents the main aquifer and has sandstone facies Astian or Porto Farina, whose outcrops are mainly composed of sandstone-sand-marl alternations topped by sandstone and sand [21]. Finally, the Quaternary deposits are generally formed by crusts, beaches, and consolidated dunes and are usually composed of two units: the lower unit of Quaternary marine facies corresponding to the Tyrrhenian outcrops along the east coast formed by the superposition of two cycles of marine sandstone limestone and sandstone dunes [22]. The upper unit is mainly composed of the Quaternary continental extending along the river which is formed of a crust of white limestone.

The coastal aquifer of Lebna area is typically unconfined aquifer consisting of Quaternary deposits whose thickness exceeds 100 meters and Pliocene sands underlying bedrock, which are composed of marl.
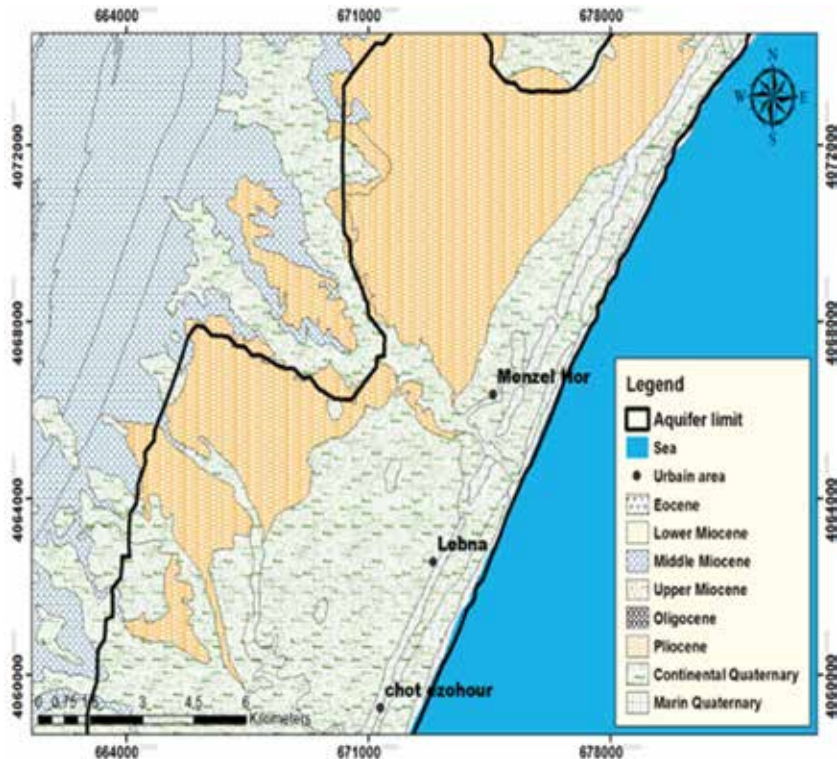
Figure 2.
Geological field of study area.

3. Materials and methods

A total of 38 water samples were collected from the Lebna aquifer as plotted in **Figure 1**. The wells were selected to be uniformly distributed throughout the study area. The groundwater samples are picked from active shallow wells where water depth ranges between 2 and 35 m (after stabilization of the physical parameters), in three similar and rinsed polyethylene bottles of 100 ml.

Then, several physical parameters are measured in situ for each groundwater sample. After that, the samples were filtered using 0.2 μm siring filters while

Parameters	Methods
pH, temperature (T °C), electrical conductivity (EC mS/cm), and oxidation-reduction potential (ORP mV)	Multiparameter probe
Nitrate (NO_3), chloride (Cl), and sulfate (SO_4)	Ion chromatograph analyzer (SHIMADZU Co. Ltd., HIC-SP/VP Super)
Bicarbonate (HCO_3)	The titration method with sulfuric acid (H_2SO_4)
Magnesium (Mg), sodium (Na), calcium (Ca), and potassium (K)	Inductively coupled plasma atomic emission spectrometer ICP-AES (Nippon Jarrel-Ash Co., Ltd. Model ICAP-757)
Stable isotope oxygen (^{18}O) and deuterium (^2H)	Mass spectrometry analyzer

Table 1.
Physicochemical analysis method of water samples.

chemical parameters are analyzed in laboratory as described in **Table 1**. Moreover, groundwater samples are kept at 4°C in an ice box with dry ice during the transmission to the Hydrology Laboratory of Tsukuba University, Japan.

During the survey, the edge (cm) and the depth of water-Table W-T (m) were determined for each well.

Quality was ensured by taking and analyzing duplicates and blank samples and by keeping ion balance errors within ±10%.

Meanwhile, geophysical characteristics were investigated in the study area using the vertical electrical sounding (VES) method by SYSCAL RII equipment based on 14 vertical electrical soundings carried out in the study area along and around Lebna River.

4. Results and discussion

4.1 Groundwater geochemistry characterization

A statistical analysis of eight ions and EC values are presented in **Table 2**. At first, we found that the maximum concentrations of the analyzed ions are decreasing in the order $Cl > Na > Ca > SO_4 > Mg > NO3 > K > HCO_3$. Consequently, the most dominant ion is chloride.

Normally, fresh groundwater is dominated by Ca^{2+}; but under specific conditions, an increase in Cl^- concentration was considered as an indicator of a salinity trend and as a possible seawater intrusion in coastal aquifer [13, 23].

Then, for all groundwater samples, the Cl concentrations exceed the WHO (World Health Organization) value for drinking water. Else, Na, Ca, SO4, Mg, NO_3, K, and HCO_3 ion concentrations in mg/l for most groundwater samples exceed the WHO value except for some well samples. As a result, the groundwater in Lebna area is not suitable for drinking and for irrigation purposes especially for piment and strawberry crops.

Meanwhile, the high NO_3, K, and SO_4 concentrations indicate the pollution of groundwater by these ions, which may be due to an increase of agricultural activities and return flow from water irrigation.

Further, the EC values of the shallow aquifer range between 1.7 and 7.01 mS/cm. They are heterogeneous and depend on their distance from the sea and the pumping rate and the depth of wells.

Parameters	Average	WHO	Max	Min
Cl^- (mg/l)	1063.4	250	1910.5	316.29
Na^+ (mg/l)	436	200	745.99	141.59
Ca^{2+} (mg/l)	332.35	52	550.57	109.07
SO_4^{2+} (mg/l)	304.63	250	544.6	86.65
Mg^{2+} (mg/l)	87.37	0.88	153.25	28.94
NO_3^- (mg/l)	260.07	50	805.30	33.2
K^+ (mg/l)	11.15	10	84.63	0.40
HCO_3 (mg/l)	4.45	20.5	9.55	1.58
CE (mS/cm)	268	—	7.01	1.70

Table 2.
Statistical analysis of the hydrochemical parameters of 38 groundwater samples from Lebna aquifer.

In conclusion, we found that for most wells, the water salinity is unsuitable for drinking and irrigation and we identify several origins of salinity and pollution in studying aquifer.

In other parts, several correlation coefficients are established to measures how several parameters can be explained by relationships between themselves and to determine the main contributing elements to groundwater mineralization as shown in **Figures 3** and **4**.

Figure 3 shows that EC has an important correlation coefficient with Na, Cl, Ca, and Mg. Hence, these ions are the main contributors to groundwater salinization, while we note a medium correlation coefficient with SO4 and EC and no significant correlation between EC and NO_3, HCO_3 and K ions.
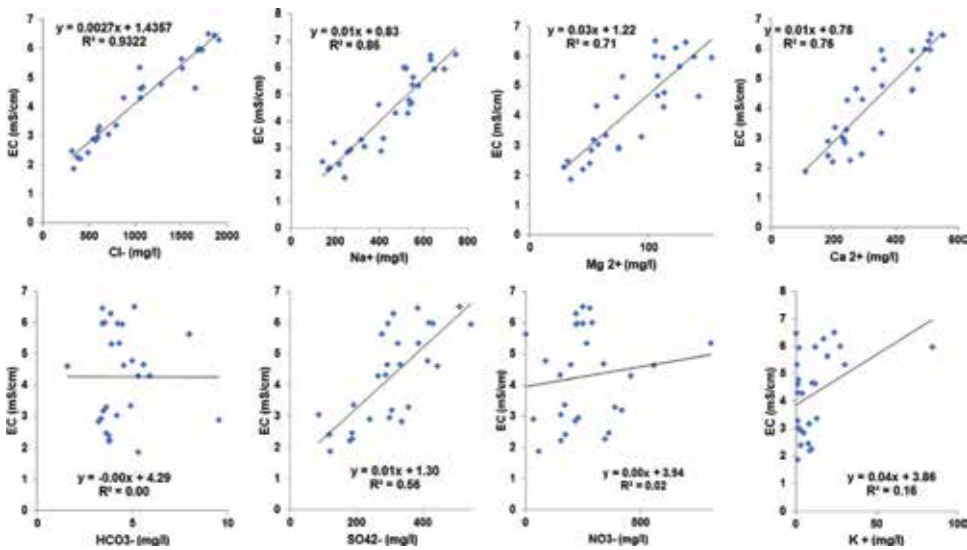
Figure 3.
Correlation between EC and eight chemical parameters.
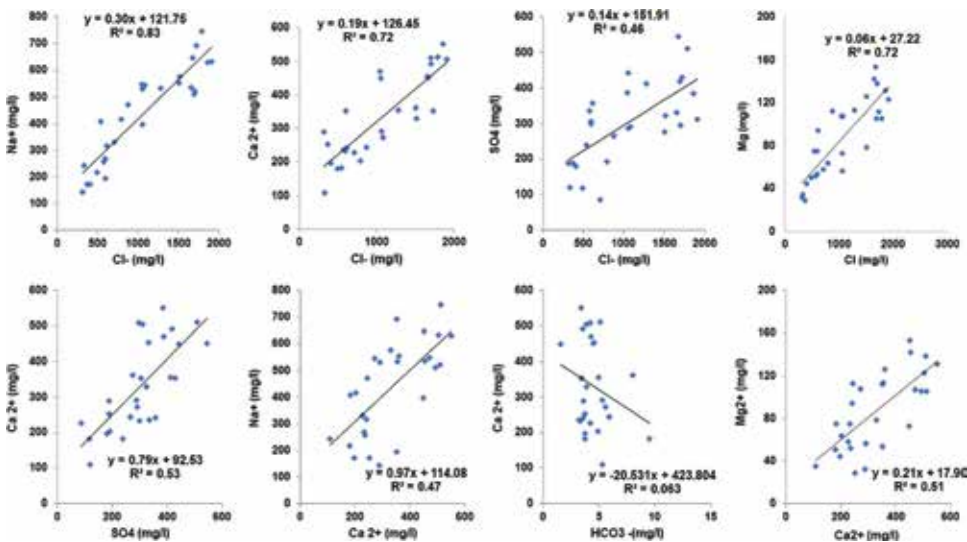
Figure 4.
Correlation between eight chemical parameters.

Further, **Figure 4** shows a high correlation coefficient between Na-Cl, Mg-Cl, and Ca-Cl, and a moderate correlation between SO_4-Ca and Mg-Ca. At this step, the result proof of the main origin of Cl, Na, Mg, and Ca is the seawater intrusion and water-rock dissolution by groundwater and/or cation exchange.

Whereas, the presence of K, SO_4, and NO_3 ions is probably related to the use of mineral fertilizers.

4.2 Groundwater mineralization processes

There exist several methods and tools to provide the groundwater mineralization processes but, in this work, we choose to use the Na/Cl molar ratio and the stable isotope analysis to determine the principal source of groundwater salinization in coastal aquifer of Lebna area.

4.2.1 Geochemistry analysis

The Na/Cl ratio and Cl concentration (mg/l) diagram is presented in **Figure 5**. From this figure, we note that no samples have Cl concentrations lower than 230 mg/l, which means that all water samples are salinized by several sources. Moreover, the water samples are divided in two groups: the first is characterized by Na-Cl water type as well as high Na/Cl ratios above the corresponding seawater dilution ratio R = 0.53 and a higher increase of Na concentrations than Ca. In the literature, these results reflect a flushing of seawater by fresh water (freshening process). This process is generated by a reverse cation exchange or/and from anthropogenic contamination sources like the irrigation by salt or brackish water [1, 24, 9, 25].

The reverse cation exchange indicates that Ca is taken up by the sediment exchanger and Na is released in the aquifer; X is the soil exchanger. The reverse cation exchange equation was explained by [9]:

$$\frac{1}{2}Ca^{2+} + NaX \rightarrow \frac{1}{2}CaX_2 + Na^+ \tag{1}$$
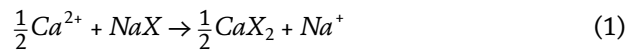
The second group G2 of water samples was located below the seawater dilution line (R = 0.53) and characterized by Na/Cl ratios lower than 0.53, the existence of
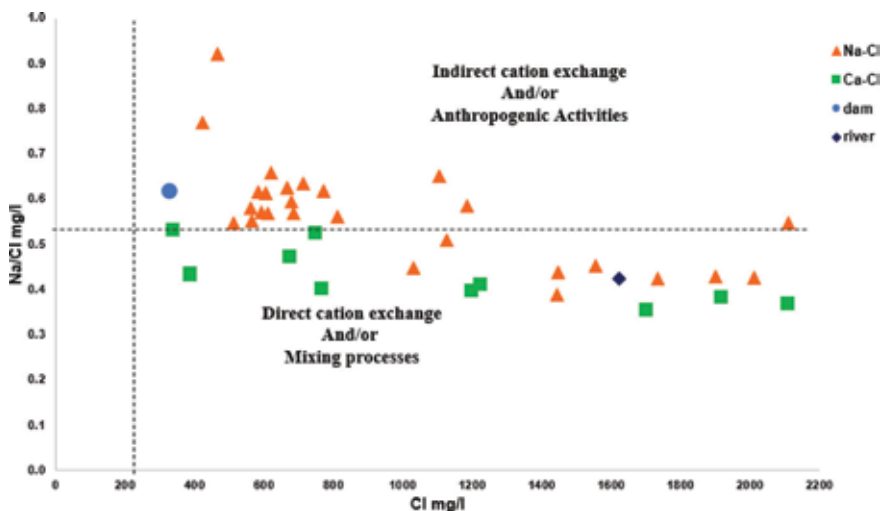
Figure 5.
Diagram plot of Na/Cl (mg/l) ratio and Cl (mg/l) concentrations for groundwater and surface water samples.

both Ca-Cl, Na-Cl water types, as well as an important increase of Cl concentrations and an increase of Ca and Mg ions. All these indicators proved that a cation exchange took place while seawater intrusion flushed fresh groundwater. In this case, sediment in contact with seawater adsorbed Na and released Ca in the aquifer [9, 26, 1]. These samples of G2 indicated that a large proportion of groundwater was affected by diluted seawater. The direct cation exchange reaction is demonstrated in the following equation [9]:

$$Na^+ + \frac{1}{2}Ca - X_2 \rightarrow Na - X + \frac{1}{2}Ca^{2+} \tag{2}$$
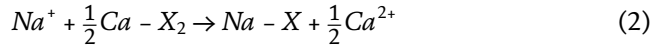
Furthermore, some groundwater samples had an Na/Cl ratio close to the seawater diluted line, which indicated a recent mixing of groundwater with seawater [13].

4.2.2 Stable isotopes

Stable isotopes of oxygen $\delta^{18}O$ and deuterium δ^2H are commonly used in the local groundwater of Lebna Plain studies to identify the sources of recharge and to describe the mixing process between saline and freshwater.

Fresh groundwater is generally depleted in both ^{18}O and ^2H (deuterium) relative to seawater [1].

The delta diagram of oxygen 18 and hydrogen isotopes ($\delta^{18}O$ and δ^2H) is plotted in **Figure 6**. The regional meteoric water line (RMWL) was calculated from the weighed annual means of precipitation in Tunis-Carthage station, the nearest global network for isotopes in precipitation (GNIP) station. RMWL follows the linear regression [27]:

$$\delta^2H = 8 * \delta^{18}O + 12.4 \tag{3}$$

The global meteoric water line (GMWL) equation is described by [28] as:

$$\delta^2H = 8 * \delta^{18}O + 10 \tag{4}$$

From **Figure 6**, we conclude that stable isotope composition of the analyzed groundwater samples from the study area revealed a large variability in the
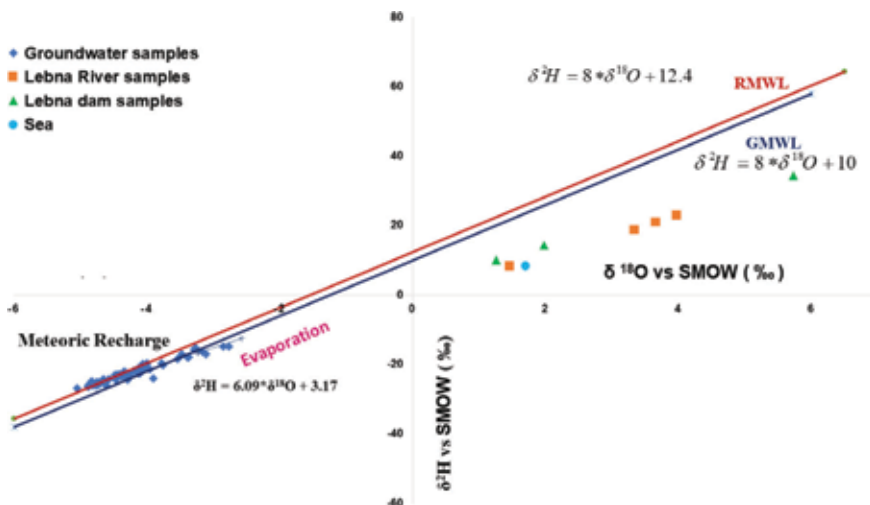
Figure 6.
Delta diagram (δ^2H vs. $\delta^{18}O$).

Plio-Quaternary aquifer, suggesting significant differences in the origin as well as in the groundwater evolution.

Further, the δ^{18}O and δ^2H contents of groundwater of the Plio-quaternary aquifer in Lebna plain vary from −5.1 to −2.6% and from −26.46 to −12.51%, respectively. This variation is controlled by local climatic parameters, including the origin of the vapor mass, the re-evaporation during rainfall and the seasonal and monthly precipitation [29–31].

In addition, the most important number of groundwater samples was falling between the regional meteoric water line (RMWL) of Tunis Carthage station and the global meteoric water line (GMWL) and were characterized by a depletion in oxygen 18 and deuterium contents. This may confirm the hypothesis of an important contribution of the meteoric water to the recharge from recent rains that would be rapidly infiltrated into the saturated zone in the study aquifer. This rapid infiltration is consistent with the relatively high hydraulic conductivity that characterizes the natural recharge zones of the aquifer [31, 32].

Moreover, the Lebna dam sea sample and the Lebna river sample were isotopically enriched in oxygen 18 and deuterium. The stable isotope contents of the Mediterranean Sea water were taken from the result published by [33], which was close to the GMWL.

Indeed, some groundwater samples were located under GMWL according to a trendline with an equation.

$$\delta^2 H = 6.09 * \delta^{18}O + 3.17 \tag{5}$$

and R^2 = 0.95. This low slope (inferior to 8) in the evaporation equation might be an indicator of evaporation processes of the infiltrated water [34]. On the other part, some groundwater samples closer to the Standard Mean Ocean Water SMOW pole (δ^{18}O SMOW = 0% and δ^2H SMOW = 0%) indicated a probable seawater intrusion. However, other groundwater samples were close to the first group, in which differentiating between the mixture with salt water and that with the evaporated water was difficult.

The plot of δ^{18}O versus Cl⁻ can be used to identify the seawater mixing with the groundwater [35]. Most of the wells that have a large isotopic composition have high levels of chloride ion concentrations [30]. Indeed, the ^{18}O isotope provides a direct means to identify and study the marine intrusion dynamics. Its relation to changes in salinity is unambiguous.

In fact, the plot of δ^{18}O versus Cl⁻ of groundwater in the Lebna plain is presented in **Figure 7**. From this figure, we distinguish four water groups in the study area:

- Samples in the left bottom with chloride concentration less than 1000 mg/l and δ^{18}O less than −4‰ were interpreted as groundwater recharged from direct meteoric water.

- Samples in the left top were characterized by an increasing level of Cl concentration in the groundwater with no significant change in δ^{18}O content (still less than −4‰). It could be attributed to the leaching of surface salt and the irrigation water return flow.

- Samples in the right bottom with chloride concentration less than 1000 mg/l and enriched in δ^{18}O more than −4‰ resulted from evaporation processes.

- Samples at the right top of the diagram with enriched contents in δ^{18}O values (more than −4‰) and high chloride content (more than 1000 mg/l) might be due to the infiltration of salt water into the wells located along the Lebna River and in the wells close to the coastal part of the seawater intrusion.
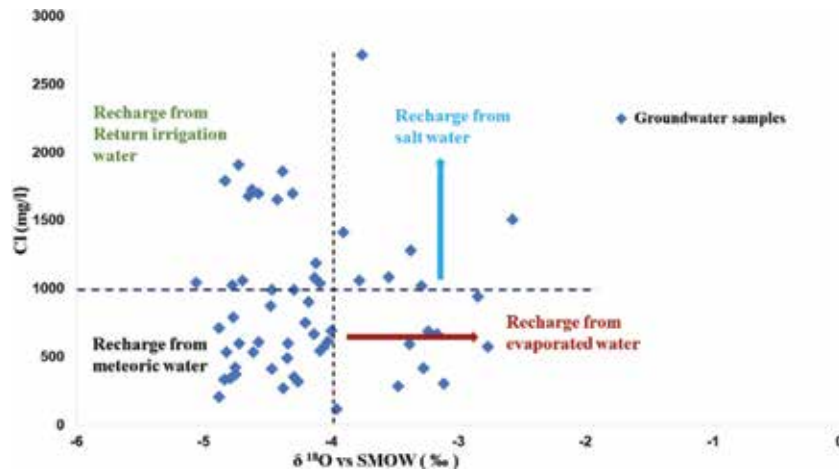
Figure 7.
The plot of $\delta^{18}O$ versus Cl^- of the groundwater in the Lebna plain.

Consequently, the groundwater in Lebna plain is recharged by seawater intrusion and surface water (direct meteoric water, evaporated water and the irrigation water return flow), which brings fertilizers during infiltration.

The seawater contribution to groundwater mineralization is determined by the end-member mixing analysis EMMA method and varies between 1 and 10% [36], while the contribution of fertilizers to groundwater mineralization is not yet determined.

4.3 The extent of seawater intrusion

The geophysical method is used in this work to determine the freshwater-saltwater interface and to prove the extent of seawater intrusion from the Mediterranean into the aquifer. This method is used by several authors from the world [37–39].

In this chapter, 14 vertical electrical soundings (VES) as shown in **Figure 8** were carried out along Lebna River and perpendicular to coastal line. The field measurements were carried out using direct current resistivity meter called SYSCAL R II,
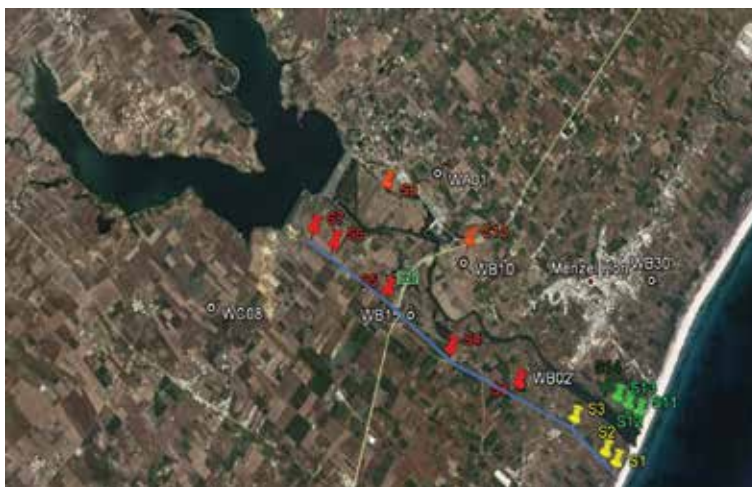
Figure 8.
Geographical location of 14 vertical electrical soundings (VES) in the Lebna area.

using Schlumberger array with AB/2 ranging from 0.5 to 400 m in successive steps. Moreover, the lithology of the existing boreholes in the study area was collected and the water table level for closer wells to electrical soundings was measured to calibrate the geophysical results.

4.3.1 Principle of VES

The principle of the vertical electrical sounding method using SYSCAL RII equipment is schematized in **Figure 9**. We conclude that the SYSCAL resistivity-meter is placed in the central part of the sounding. Then, the metallic electrodes have to be plugged into the ground as deep as possible to decrease the ground resistance, for both the transmitting electrodes A and B and the receiving electrodes M and N [40].

A current I_{AB} is transmitted between two grounded electrodes A and B, while a voltage V_{MN} is measured between the other ones: M and N electrodes. Finally, the apparent resistivity R_{AB} is computed automatically by the SYSCAL RII resistivity-meter using the following formula and we move the electrodes to the next station and start a new reading:

$$R_{AB} = K \times V_{MN}/I_{AB} \quad (6)$$

$$\text{Where } K = 2^* Pi/(1/AM - 1/AN - 1/BM + 1/BN) \quad (7)$$

The apparent resistivity values have to be plotted on a logarithmic paper sheet, to check how the new reading compares with respect to the previous ones, before moving the A, B electrodes to the next measuring point. This step is done during the survey. Then, the data are stored in the internal memory of the equipment after each reading.

The sounding starts by small values of the AB line. For some values of the AB/2, two readings for different values of MN/2 have to be taken to check the lateral variations of the resistivity of the surface. Ideally, both resistivity values are identical.

In other part, the depth of investigation varies from about 1/3 to 1/10 of the length of the AB line. The variation of the depth of investigation is obtained by increasing the length of the current line AB: small lines: shallow and long lines: deep.

The last step is the data transferred to a PC to process them, and run an inversion model using PROSYS and Winsev software to interpolate the results and get layer depths with resistivity. The resistivity values are correlated with the geological layers.
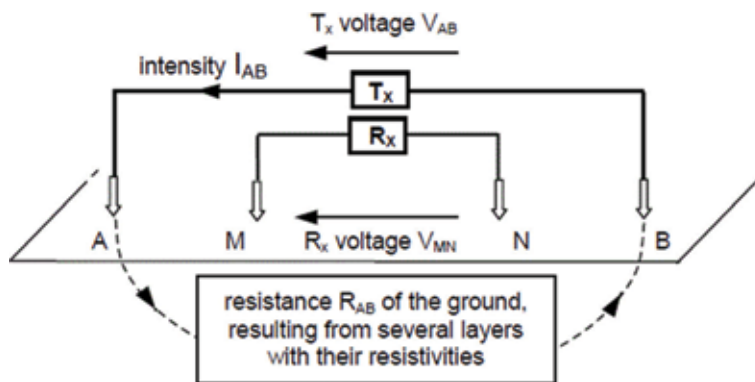
Figure 9.
The vertical electrical sounding principle for Schlumberger disposal.

4.3.2 The 2D pseudo section

The result of the inverted resistivity values from the vertical electrical soundings method is two 2D longitudinal pseudo-section of resistivity model along the Lebna River. We focus our attention on one of these profiles as shown in **Figure 10**. Further, the interpretation of resistivity profile is according to resistivity-water-rock converted table, as well as water table level and EC measurement in the nearer wells and borehole lithostratigraphic and geological fields.

The 2 D longitudinal pseudo section is based on the interpolated results from seven VES (VES1, VES2, VES 3, VES4, VES5, VES 6, and VES7) and is oriented to SE-NW from the sea to Lebna dam, perpendicular to the coastal line and parallel to Lebna River. **Figure 10** shows a heterogeneity of resistivity values along the pseudo-section, which varies from 1 to 95 Ω.m.

- We conclude that for all the VES from VES 1 to VES 7, the resistivity starts with a resistant layer (R > 25 Ω.m), which corresponds to the unsaturated zone. Moreover, the variability of values depends on geological formation. The highest resistivity values in the southeastern part correspond to the wet Tyrrhenian limestone (from marine Quaternary deposits), and in the northwestern part, they correspond to the highlighted crust and encrusting (from continental Quaternary) as well as to the wet sand (from Pliocene deposits).

- Whereas, more in depth, the resistivity value decreases (R < 15 Ω.m), and we found a very conductive layer which corresponds to the aquifer.

- The lowest resistivity values varying between 10 and 1 Ω.m are located in the VES nearer to the coast (500 m distance to the coastal line), especially for VES1, VES2, VES3, and VES 4. Else, this result is combined with high electrical conductivity values measured in the nearer wells to these electrical soundings which prove the intrusion of seawater to the aquifer.

4.4 Mineralization and nitrate pollution effect on ecosystem

The surface water level of the Lebna River decreased as a result of limited rainwater. Moreover, water quality is deteriorated due to multiple factors: water losses
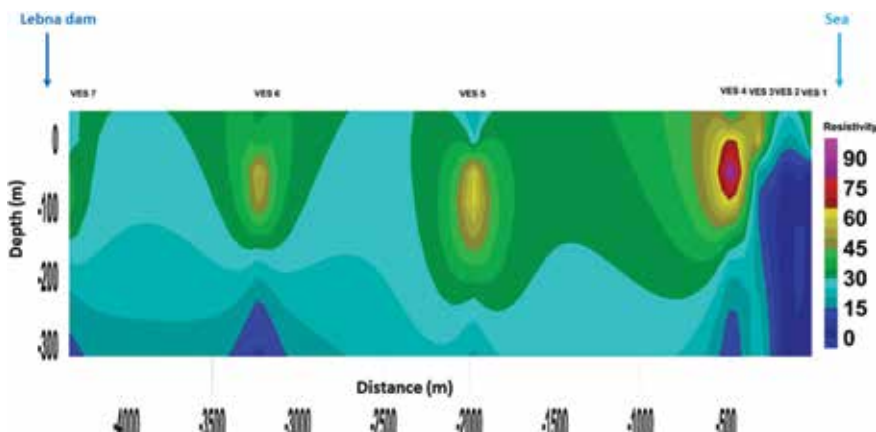
Figure 10.
Longitudinal pseudo-section along Lebna River of interpolated resistivity values from VES results.

Figure 11.
The pollution effect by the industrial discharges in the middle part of the Lebna River in winter season.

Figure 12.
The pollution effect by the industrial discharges in the middle part of the Lebna River in summer season.

from the Lebna dam, upstream of the Lebna River, and industrial discharge from two factories located in the middle part of the Lebna River, as well as tidal effects.

Figures 11 and **12** show the pollution effects on Lebna River by the industrial discharge in winter and summer seasons, respectively.

The effect of seawater intrusion to the ecosystem appeared in the downstream part of Lebna River, where the downstream measurements showed an electrical conductivity value of 45.3 mS/cm as opposed to a value of 54.1 mS/cm in the sea. Furthermore, the EC value measured in the estuarial zone in 2011 was higher than the electrical conductivity value of the sea [18]. Moreover, some halophyte crops and crabs were also depicted in the estuarial zone. Else, crustacean species from marine origins such as "Gammarus aequicaudata," "Palaemonetes varians," and "*Carcinus mediterraneus*" were observed during survey [41]. All these indicators show the salinization effect on ecosystem.

However, the fertilizer pollution effect to the ecosystem appeared also in the estuarial zone on Lebna River. Furthermore, the runoff brings nitrate, phosphate, chloride, and some pesticides which create a change in water, in soil quality, and in ecosystem behavior [42]. Moreover, some new animal species have appeared in the estuarial zone, such as "oligochaetes," "Naïs," and "Paranais" indicating the existence of nitrate pollution which comes from fertilizers.

The observations and results described above confirm the transformation of the estuarial zone to a lagoon.

5. Conclusion

The aquifer chapter is very important because it can include several kinds of aquifers from the world such as ALLUVIAL AQUIFER, karst AQUIFER, coastal

aquifer, etc. Our study is a part of Aquifer chapter, which describes some problems that can be found and threatened the coastal aquifers in the world.

The study area is a local coastal aquifer of Cap-Bon in the north-east of Tunisia. The area has witnessed an over-exploitation by the irrigation demand which created a quantitative and qualitative deterioration of the groundwater resources caused by the mixing of salt and fresh waters. Furthermore, high chloride content as well as high electrical conductivity values and low resistivity values have appeared near the coastal part of the aquifer, suggesting that a seawater intrusion may occur.

Unfortunately, we found that the groundwater in Lebna plain was unsuitable for drinking and agricultural purposes.

In this study, the use of statistical analysis and correlation between nine chemical parameters and Na/Cl molar ratio proved that a seawater intrusion as well as a reverse cation exchange between Ca, Mg, and Na and water-rock dissolution had influenced the groundwater salinity. Moreover, we showed that the agricultural activities contributed to the groundwater mineralization in the Lebna area and were the main source of NO_3, SO_4, and K ion concentrations.

In addition, the isotopic study showed that the Plio-Quaternary aquifer was recharged directly by the infiltration of the meteoric water from the Tyrrhenian consolidated dunes the sand deposits, the return of the water irrigation flow, the evaporated surface water, and the seawater intrusion from the coast.

Moreover, the existence of crustacean species of marine origins in the downstream according to the high EC value of the Lebna River confirmed the transformation of the estuarial zone to a lagoon.

Moreover, with the geophysical vertical electrical sounding (VES) method, we could note that the salinization in the coastal aquifer of the Lebna plain was due to the seawater intrusion.

Acknowledgements

Notes and thanks

Abbreviations

mg/l	milligrams per liter
Ω.m	ohm meter
R	apparent resistivity
V	voltage

I	current
SMOW	standard mean ocean water
R2	correlation coefficient
GMWL	the global meteoric water line
GNIP	global network for isotopes in precipitation
RMWL	the regional meteoric water line
R	seawater dilution ratio
X	the soil exchanger
WHO	World Health Organization
2H	deuterium
18O	stable isotope oxygen
ORP	oxidation-reduction potential
mV	milli volt
EC	electrical conductivity
mS/cm	milli siemens per centimeter
T°	temperature
VES	vertical electrical sounding
W-T	water-table
HCO_3	bicarbonate
Cl	chloride
Ca	calcium
Na	sodium
Mg	magnesium
K	potassium
SO_4	sulfate
NO_3	nitrate

Author details

Amira Ziadi[1*], Najla Hariga Tlatli[1,2] and Jamila Tarhouni[1]

1 National Institute of Agronomy of Tunis, Tunisia

2 National School of Engineering of Tunis, Tunisia

*Address all correspondence to: ziediamira@yahoo.fr

IntechOpen

References

[1] Bear J, Cheng AHD, Sorek S, Ouazar D, Herrera I. Handbook of Seawater Intrusion in Coastal Aquifer, Concepts, Methods and Practices. Dordrecht-Boston-London: Kluwer Academic Publishers; 1999. p. 26. ISBN: 0-7923-5573-3

[2] Oude Essink GHP. Mint: Saltwater intrusion in 3D large-scale aquifers: A Dutch case. Physics and Chemistry of the Earth, Part B. 2001;**26**(4):337-344

[3] Gossel W, Sefelnasr A, Mint WP. Modelling of paleo-saltwater intrusion in the northern part of the Nubian aquifer system, Northeast Africa. Hydrogeology Journal. 2010;**18**:1447-1463. DOI: 10.1007/s10040-010-0597-x

[4] Yechieli Y, Shalev E, Wollman S, Kiro Y, Kafri U. Mint: Response of the Mediterranean and Dead Sea coastal aquifers to sea level variations. Water Resources Research. 2010;**46**:W12550. DOI: 10.1029/2009WR008708

[5] Diersch HJ, Prochnow D, Thiele M. Mint: Finite-element analysis of dispersion-affected saltwater upconing below a pumping well. Applied Mathematical Modelling. 1984:305

[6] De Louw PGB, Vandenbohede A, Werner AD, Oude Essink GHP. Mint: Natural saltwater upconing by preferential groundwater discharge through boils. Journal of Hydrology. 2013;**490**:74-87. DOI: 10.1016/j.jhydrol.2013.03.025

[7] Houben G, Post VEA. Mint: The first field-based descriptions of pumping-induced saltwater intrusion and upconing. Hydrogeology Journal. 2017;**25**:243-247. DOI: 10.1007/s10040-016-1476-x

[8] Werner AD, Bakker M, Post VEA, Vandenbohede A, Lu C, Ataie-Ashtiani B, et al. Mint: Seawater intrusion processes, investigation and management: Recent advances and future challenges. Advances in Water Resources. 2013;**51**:3-26. DOI: 10.1016/j.advwatres.2012.03.004

[9] Appelo CAJ, Postma D. In: Balkema AA, editor. Handbook of Geochemistry, Groundwater and Pollution. Rotterdam, The Netherlands: Leiden; 1996

[10] Diersch H-JG, Mint KO. Variable-density flow and transport in porous media: Approaches and challenges. Advances in Water Resources. 2002;**25**:899-944. DOI: 10.1016/S0309-1708(02)00063-5

[11] Kourgialas NN, Dokou Z, Karatzas GP, Panagopoulos G, Soupios P, Vafidis A, et al. Mint: Saltwater intrusion in an irrigated agricultural area: Combining density-dependent modelling and geophysical methods. Environmental Earth Sciences. 2016;**75**:15. DOI: 10.1007/s12665-015-4856-y

[12] Slama F, Bouhlila R, Renard P. Identification of groundwater salinization sources using experimental, multivariate statistical analysis and numerical modelling tools: Case of Korba coastal aquifer (Tunisia). In: Proceeding of the XXXVIII IAH Congress, Groundwater Quality Sustainability; Krakow; 2010. pp. 12-17

[13] Zghibi A, Zouhri L, Tarhouni J. Mint: Assessment of seawater intrusion and nitrate contamination on the groundwater quality in the Korba coastal plain of cap-bon (north-east of Tunisia). Journal of African Earth Sciences. 2013;**87**:1-12

[14] Yu X, Yang J, Graf T, Koneshloo M, Neal MAO, Mint HAM. Impact of topography on groundwater salinization due to ocean surge inundation. Water Resources Research. 2016;**52**(8):

5794-5812. DOI:
10.1002/2016WR018814

[15] Trabelsi F, Ben Mammou A, Tarhouni J, Piga C, Ranieri G. Mint: Delineation of saltwater intrusion zones using the time domain electromagnetic method: The Nabeul-Hammamet coastal aquifer case study (NE Tunisia). Hydrological Processes. 2013;**27**:2004-2020

[16] Bouri S, Ben Dhia H. Mint: A thirty-year artificial recharge experiment in a coastal aquifer in an arid zone: The Teboulba aquifer system (Tunisian Sahel). Comptes Rendus Geoscience. 2010;**342**(1):60-74

[17] Trabelsi R, Abid K, Zouari K. Mint: Geochemistry processes of the Djeffara palaeo-groundwater (south eastern Tunisia). Quaternary International. 2011;**xxx**:1-13

[18] Ziadi A, Tarhouni J, Tlatli N, Atsushi K, Mizuho T, Tsujimura M, Trabelsi E. Salinization Assessment in The Coastal Aquifer of Lebna Area (Cap-Bon, North Eastern of Tunisia) Using Geochemical, Isotopic and Geophysical Methods. In: Proceedings of the 7th International Conference on Water Resources in The Mediterranean Basin (WATMED7); 08-11 October 2014, Marrakech. Morocco: WATMED 2014; p. 11. DOI: 10.13140/RG.2.1.4028.0166

[19] Ziadi A, Tarhouni J, Tlatli N, Tsujimura M, Kawachi A. Conceptualizing of seawater intrusion in Lebna plain aquifer: Local scale of coastal aquifer of Cap Bon using geophysical methods. In: Proceeding of 2nd International Conference on Integrated Environmental Management for Sustainable Development (2nd ICIEM); 27-30 November 2016; Sousse. Tunisia: Volume 2: Water resources ISSN 1737-3638; pp. 752-754

[20] INM Institut National de la Météorologie; Tableaux climatiques mensuels. Archive INM pour la période de 1985-2005. Station Nabeul

[21] Ben Salem H. Handbook of Carte géologique de la Tunisie au 1/50 000, feuilles Kélibia-Menzel Heurr n°16 et 23, Nabeul-Hammamet n°30 et n°37. 1998

[22] Kchouk F. Handbook of Contribution à l'étude des formations dunaires de Dar Chichou (Cap Bon). Notes du service géologique no. 25, Tunis: 10. 1982

[23] An TD, Tsujimura M, Phu VL, Ha DT, Hai NV. Mint: Isotopic and hydrogeochemical signatures in evaluating groundwater quality in the coastal area of the Mekong Delta, Vietnam. In: Tien Bui D, Ngoc Do A, Bui HB, Hoang ND, editors. Advances and Applications in Geospatial Technology and Earth Resources. International Conference on Geo-Spatial Technologies and Earth Resources, GTER 2017. Cham: Springer; 2018. DOI: 10.1007/978-3-319-68240-2_18

[24] Hsissou Y, Bouchaou L, Krimissa M, Mudry J. Caractérisation de l'origine de la salinité des eaux de la nappe côtière d'Agadir (Maroc). In: Proceeding of Première Conférence Internationale sur l'Intrusion d'Eau salée et les Aquifères Côtiers, Contrôle, Modélisation et Gestion; 2001; Essaouira. Maroc, 8

[25] Vengosh A, Kloppmann W, Marei A, Livshitz Y, Gutierrez A, Banna M, et al. Mint: Sources of salinity and boron in the Gaza strip: Natural contaminant flow in the southern Mediterranean coastal aquifer. Water Resources Research. 2005;**41**:W01013. DOI: 10.1029/2004WR003344

[26] Cardona A, Carrillo-Rivera JJ, Huizar-Alvarez R, Graniel-Castro E. Mint: Salinization in coastal aquifers of arid zones: An example from Santo Domingo, Baja California Sur, Mexico. Environmental Geology. 2004;**45**:350-366

[27] Zouari K, Chkir N. Mint: La mesure du temps par le carbone 14 et par uranium- thorium. Outils d'investigation dans les sciences de l'univers et de l'environnement. Revue édité par Cité des Sciences. 2002:15

[28] Craig H. Mint: Standards' for reporting concentrations of deuterium and oxygen 18 in natural water. Science. 1961;**133**:1702-1703

[29] Jouzel J, Koster RD, Suozzo RJ, Russell GL, White JWC, Broecker WS. Mint: Simulations of the HDO and $H_2^{18}O$ atmospheric cycles using the NASA GISS general circulation model: Sensitivity experiments for present-day conditions. Journal of Geophysical Research. 1991;**96**:7495-7507. DOI: 10.1029/90JD02663

[30] Clark ID, Fritz P. Handbook of Environmental Isotopes in Hydrogeology. New York, USA: Lewis Publishers; 1997. ISBN: 1-56670-249-6

[31] Hamed Y, Dhahri F. Mint: Hydro-geochemical and isotopic composition of groundwater, with emphasis on sources of salinity, in the aquifer system in north western Tunisia. Journal of African Earth Sciences. 2013;**83**:10-12

[32] Abid K, Hadj Ammar F, Weise S, Zouari K, Chkir N, Rozanski K, et al. Geochemistry and residence time estimation of groundwater from Miocenee—Pliocene and upper cretaceous aquifers of southern Tunisia. Quaternary International. 2014;**xxx**:1-12

[33] Gat JR, Shemesh A, Tziperman E, Hecht A, Georgopoulos D, Basturk O. Mint: The stable isotope composition of waters of the eastern Mediterranean Sea. Journal of Geophysical Research. 1996;**101**(C3):6441-6451

[34] Fontes JCH. Mint: Isotopes du milieu dans les eaux naturelles. La Houille Blanche. 1976;**314**:221

[35] Kanagaraj G, Elango L, Sridhar SGD, Gowrisankar G. Mint: Hydrogeochemical processes and influence of seawater intrusion in coastal aquifers south of Chennai, Tamil Nadu, India. Environmental Science and Pollution Research. 2018;**25**:8989. DOI: 10.1007/s11356-017-0910-5

[36] Ziadi A, Hariga TN, Tarhouni J. Mint: Mineralization and pollution sources in the coastal aquifer of Lebna, cap bon, Tunisia. Journal of African Earth Sciences. 2019;**151**:391-402. DOI: 10.1016/j.jafrearsci.2019.01.004

[37] Kouzana L, Benassi R, Ben Mammoua A, Mint FMS. Geophysical and hydrochemical study of the seawater intrusion in Mediterranean semi-arid zones. Case of the Korba coastal aquifer (cap-bon, Tunisia). Journal of African Earth Sciences. 2010;**58**:242-254. DOI: 10.1016/j.jafrearsci.2010.03.005

[38] Zouhri L. Mint: Geoelectrical structure and hydrogeological investigations of the southern Rif cordillera (Morocco). Hydrological Processes. 2010;**24**:1308-1317. DOI: 10.1002/hyp.7592

[39] Ziadi A, Hariga TN, Mint TJ. Use of time-domain electromagnetic (TDEM) method to investigate seawater intrusion in the Lebna coastal aquifer of eastern cap bon, Tunisia. Arabian Journal of Geosciences. 2017;**10**:492. DOI: 10.1007/s12517-017-3265-9

[40] Available from: http://www.iris-instruments.com/Pdf_file/Syscal_r2.pdf

[41] Romdhane MS, Missaoui H. Handbook of Rapport de diagnostic des sites, Partie relative au site zones humides, Diagnostic hydrobiologique et Etude des peuplements. MedWetCoast Conservation des Zones Humides

Littorales et des Ecosystèmes côtiers du
Cap-Bon. 2001

[42] Chabbi M. Handbook of Rapport
de diagnostic des sites, Partie relative
à Population, économie locale et
utilisation de l'espace. MedWetCoast
Conservation des Zones Humides
Littorales et des Ecosystèmes côtiers du
Cap-Bon. 2001

Analytical Study of Environmental Impacts and Their Effects on Groundwater Hydrology

Muhammad Salik Javaid, Laila Khalid
and Muhammad Zeshan Khalil

Abstract

The hydrology of the groundwater is not just the science of subsurface water but also encompasses the rock strata and structure matrix in which it is contained. It also deals with the natural and man-made activities that affect the quality and quantity of subsurface water and physiology, geology, and minerology of the rock structure as well as the effects of the environment, climate, and other physical and natural forces trying to alter the subsurface water source in either way. Strategies for management and upkeep of groundwater as a resource are also discussed for sustainable and equitable usage by all stakeholders.

Keywords: hydrology, groundwater, subsurface water, aquifers, variations, fluctuations, environment, meteorology, geohydrology

1. Introduction

For thousands of years, man has survived living in arid regions of the world solely by skillfully managing that vital but scarce resource called water [1]. Out of the two, the surface water and the groundwater, the groundwater has always been more important for survival due to its intrinsic quality of natural preservation. Groundwater is a vital source of fresh water for domestic, agricultural, and industrial use. Currently contribution of groundwater is almost 34% of the total annual water supply. Water consumption is increasing day by day due to continuous development of the economy, industrialization, and changes in life patterns, which cumulatively results in shortage of usable water.

To meet the increasing water demands, reliance on groundwater has been rapidly increasing, especially in the arid and semiarid regions leading to water exhaustion and overconsumption of groundwater, causing ecological problems such as decreased water levels, water pollution, seawater intrusion, and deterioration of water quality. The recharge of groundwater occurs both naturally and artificially. The natural recharge occurs through the process of infiltration where water percolates from the surface to the bed of the aquifer. But due to rapid development and stupendous growth of population in the recent past, the areas for natural infiltration have been lessening day by day; hence the scope for natural recharge of the groundwater is also declining [2].

The combination of decreasing water availability and increasing water demand can lead to drastic water shortages. Groundwater exploration involves knowledge of hydrological properties of various geological materials such as porosity, permeability, storage coefficient, transmissivity, and specific yield or in other words holding and discharge capabilities of geological materials.

2. Groundwater variations

In the nature, water resources and water demand are unevenly distributed both spatially and temporally. It is these uneven distributions that make the groundwater hydrology more complex and dynamic in its nature and form. Ironing out of the variations and equitable juxtaposition of haves and have-nots in both demand and resource is the ultimate goal of all hydrological knowledge.

2.1 Spatial variations

These variations in the groundwater levels are with respect to physical location and space. Physical properties including type of soil, groundwater depth, porosity of vadose zone, rainfall patterns, and hydrogeology tend to vary the groundwater recharge spatially. Fluctuations in the groundwater levels are generally greater in the areas of low drainage density than those in regions of moderate to high drainage density. The factors like weathering intensity, presence of fractures, and drainage density control the quantity of groundwater. In such regions groundwater flow and quantity are not controlled by highly weathered dykes in shallow unconfined aquifers. The phenomena like fracturing, weathering, and faulting increase the permeability of rocks and the recharge which controls the fluctuations in groundwater levels. For the fluctuations in groundwater levels in terrains of hard rocks, several studies have been carried out. Fractured and weathered rocks carry the groundwater under unconfined conditions, and the major source for groundwater recharge is rainfall. Due to downward seepage of rainfall, the unconfined aquifers are recharged in the unsaturated zone [3].

2.2 Temporal variations

Variations in the phreatic levels, chemical concentration levels, biological concentration levels, and fluid properties of the groundwater may be described with respect to time as seasonal variations and secular variations.

2.2.1 Seasonal variations

Such variations are periodic. The changes in the water level due to some seasonal happenings such as rainfall, storms, and irrigation pumping are referred to as seasonal variations. Water-level fluctuation in summer and winter is also considered under the same type. The lowest variations in water levels occur in winter season, while the highest occur during late spring. At the end of the irrigation season in an irrigated area, the lowest variations in water levels normally occur where frozen ground is not a factor. **Figure 1** shows the variations in the water levels for frozen ground areas in winter are periodic [4].

2.2.2 Secular variations

Such variations are nonperiodic and show the change in the water level over several years, which cover the dry and wet seasons and the related groundwater
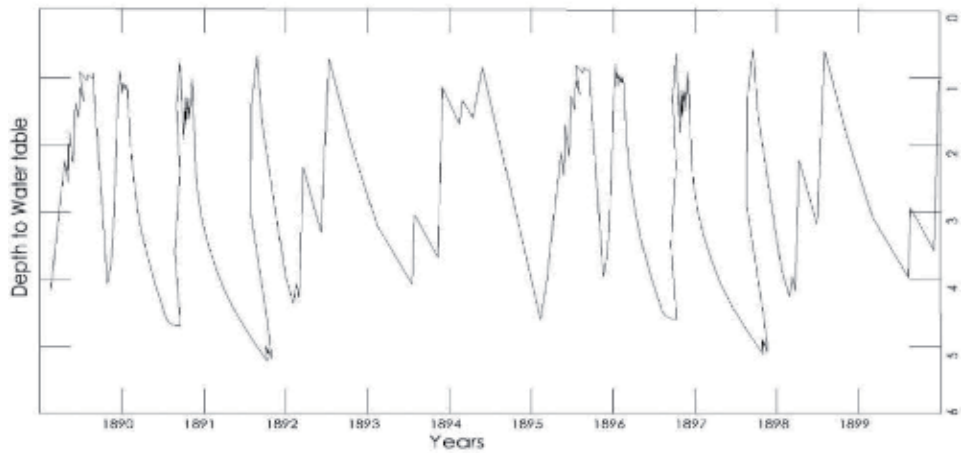
Figure 1.
Seasonal variations [4].
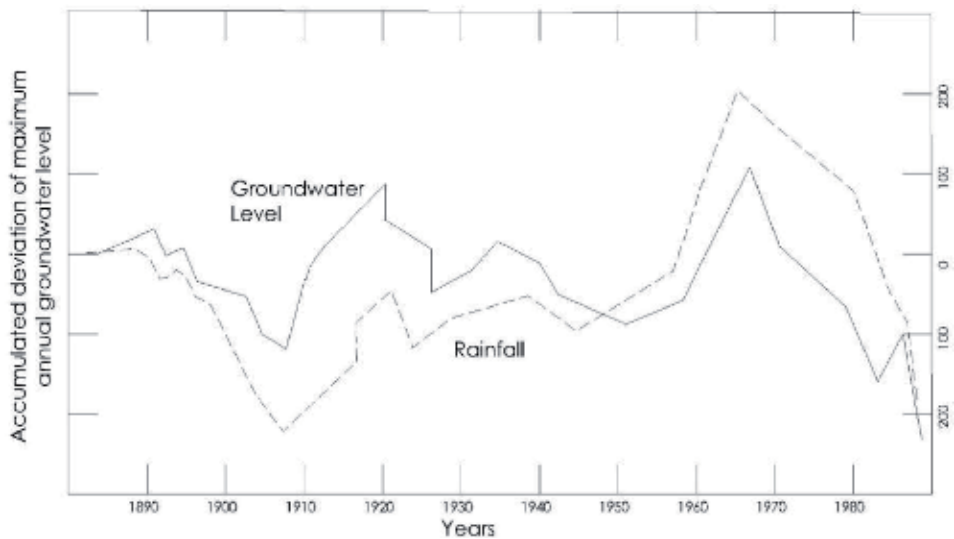
Figure 2.
Secular variations [4].

fluctuations. Long-term fluctuations in water levels are produced when rainfall is above or below the mean, during alternating a series of dry and wet years. **Figure 2** shows the long records of groundwater levels and rainfall and illustrates that rainfall is not an accurate indicator of variations in groundwater levels [4].

3. Impacts of human activities

3.1 Urbanization

Groundwater, as the world's most vital natural resource for the reliable provision of potable water supply, is affected by urbanization. Due to rapid urbanization and increasing industrial activities, the need for fresh water has increased in the past few decades. Almost 50% of the world population lives in urban areas, and

the proportion is expected to increase in the coming decades. Urbanization brings many benefits such as increased job and education opportunities, cultural activity, and economic diversification. However, unplanned urban growth is also leading to challenges such as the overexploitation of water resources. Furthermore, land-use changes and anthropogenic activities such as surface sealing due to streets and buildings, flood control, forest management, and irrigation modify the infiltration and movement of water. The authors [5] have shown that due to urbanization, built-up area increased by 271%, water bodies decreased by 46%, and bare land decreased by 129% in the study area. These modifications linked with urbanization often lead to groundwater resource deterioration [6].

There are many conditions which interrupt the subsurface water balance, and as a result groundwater levels are lowered. A few of such conditions are listed below:

a. Groundwater recharge is reduced by paving the surface areas and building the storm sewers. When the surface area is paved, it stops the surface water entry into the ground, and as a result the groundwater recharge is reduced. Also when storm sewers are built, they store the amount of surface water, stop the water entry into the ground, and result in reduction of recharge.

b. Pumping wells increase the groundwater discharge which results in lowering of groundwater table.

c. Collection of wastewater in sanitary sewers also decreases the groundwater recharge.

d. Huge reduction in groundwater recharge occurred nowadays due to excess plastic wastage.

3.2 Excessive extraction

Groundwater is our major source of water. Due to climate change, rapid urbanization, industrial activities, and intensive agricultural practices have put a tremendous pressure on groundwater. Groundwater depletion occurs when the pumping rates are excessively higher than the rate of replenishment.

The extreme use of groundwater resources can have serious concerns, such as uplifting and seismic activities, ecological environment deterioration, land subsidence, vegetation degradation, livelihoods for rural poor, and food security implications. In view of the shrinking groundwater resources, it is important to develop effective techniques and methods to study the trend of groundwater storage (increase/decrease) and its recharge-discharge relationship, which can support the mitigating measures of overpumping shallow groundwater to ensure the sustainable utilization of groundwater resources [7].

4. Environmental and natural impacts

4.1 Meteorological phenomena

Fluctuations in groundwater due to meteorological phenomena are caused by atmospheric pressure, rainfall, wind, and frost. As stated by [8], aquifers are inherently very resilient to atmospheric variations above ground, but climate adversely alters the aquifer's groundwater recharge, thus introducing uncertainties in spatial pattern definitions.

4.1.1 Atmospheric pressure

Variations in atmospheric pressure produce fluctuations in wells penetrating confined aquifers. There is an inverse relationship between atmospheric pressure and water levels. It means that increase in atmospheric pressure will decrease the water levels and vice versa. If the changes in the atmospheric pressure are expressed in terms of a column of water, then the ratio between changes in water levels and pressure is known as barometric efficiency of an aquifer. This efficiency is expressed by the following equation:

$$B = \gamma \, \Delta h / \Delta p_a \qquad\qquad (1)$$

where B = barometric efficiency of an aquifer, γ = specific weight of water [981 N/m^3 or 62.4 lb/ft^3], Δh = change in piezo-metric levels, and Δpa = change in atmospheric pressure.

Discussions related to the effect of atmospheric pressure on confined and unconfined aquifers assume that no delay occurs in the balance of pressure between the aquifer and well. But in reality, the time required for movement of a finite volume of water between the surrounding aquifers and well delays the transmission of atmospheric pressure change between the aquifer and well. This delay in time depends on the properties of aquifer (i.e., storability and transmissivity) and conditions of existing boreholes (i.e., well skin effects and well bore storage). Due to imbalance of pressure between an aquifer and a well, at the instance of pressure change, previous investigators have observed that these temporary imbalances in the pressure can be treated as individual step changes in pressure applied at the well [9]. Due to travel time for percolation and surface and subsurface losses, rainfall is not considered as an accurate indicator for groundwater recharge. The travel time for vertical percolation may vary from a few minutes for permeable formations with shallow water tables to several years for low permeable formations with deep water tables. The regions that lie between semi-humid and semiarid zones with seasonal climatic conditions observe zero recharge in the groundwater due to rainfall [4].

4.1.2 Rainfall

In arid and semiarid regions, due to heavy rainfalls, groundwater recharge tends to occur unlike those regions which are a combination of constant rate and periodic behavior. Physical properties including type of soil, groundwater depth, porosity of vadose zone, rainfall patterns, and hydrogeology tend to vary the groundwater recharge spatially [10].

4.1.3 Wind

Wind blowing over the top of wells generates minor fluctuations in water levels. It works on the principle of vacuum pump. When wind is blowing over the top of a well casing, the air pressure within the well lowers down suddenly due to which the water level rises quickly. Once the wind passes, the air pressure within the well rises and water level falls [4].

4.1.4 Frost

It has been observed in the regions of extreme frost that shallow water tables are reduced during the winter season and increased in early spring. These fluctuations are observed due to the presence of frost layer above the water table. Due to

capillary action and transfer of vapors to the frost layer, water moves upward from water table during winter. Thermal gradient and the fact that at 0°C vapor pressure over liquid water is greater than that over ice play an important role in the migration of vapors. When mean air temperature reaches 0°C in early spring, the frost layer begins thawing from the bottom due to which meltwater percolates down in the water table [4].

4.2 Tides and seawater intrusion

Groundwater is an important source of fresh water with high quality for coastal communities worldwide. These sources of fresh groundwater in the coastal communities are highly affected by intrusion of seawater caused by excessive groundwater extraction and rises in sea levels. Globally increasing population will lead to rising demands of fresh water in the coming decades and will result in a decline of groundwater sources gradually. Coastal flooding will also be increased due to rise in sea levels, which may lead to seawater intrusion and coastal erosion, and as a result it will affect the biodiversity and losses of wetland [11].

In response to the tides, sinusoidal fluctuations of groundwater levels occur in the coastal aquifers which are in contact with the ocean. If a simple harmonic motion varies the sea levels, a pattern of sinusoidal waves is propagated inland from the submarine outcrop of the aquifer. The time lag of given maximum increases, and inland amplitude of waves decreases with respect to distance [4].

In coastal regions, tidal forces acting on an adjacent groundwater are a common feature and can be important pore water phenomena in tidal and saturated zones. Near the top of the water table, the entry of saltwater and variations in the concentration of solutes can be increased due to tidal forces in shallow unconfined aquifers. Comparative studies between tidal and water-level variations show that increase in the height of tide will increase the corresponding water levels [12].

Fluctuations produced by the attraction of sun and moon on the crust of the earth are a result of earth tides. The following observations are analyzed based on well record:

a. Fluctuations occur twice in a daily cycle due to moon about 50 min later each day.

b. Retardation of cycle on average daily bases matches with that of moon's transit closely.

c. At the lower and upper peaks, the moon's transits and the troughs of water levels on daily bases are coincided.

d. Periods of full and new moon coincide with the periods of large regular fluctuations, while the periods of the first and third quarters of moon coincide with periods of small irregular fluctuations [4].

Forces of sun and moon which produce tides act in the same direction at the time of new and full moon, causing ocean tides to be greater than the average range. But at the time of the first and third quarter of moon, the forces of sun and moon which produce tides act perpendicular to each other, causing ocean tides to be smaller than the average range. At the time of coincidence of the moon's transit with time of low water, the tidal attraction will be maximum; therefore, the load on the aquifer is reduced which allows the aquifer to expand slightly [4].

4.3 Earthquakes and landslides

History reveals that there are varieties of effects of earthquakes on groundwater. Fluctuations like sudden rises and falls of water levels in wells, variations in spring discharges, formation of new springs, and venting of mud and water out of the ground are observed due to earthquake shocks. Such fluctuations produced due to earthquake shocks are known as *hydroseisms*.

Seismic waves generated by earthquakes affect the groundwater in two major ways. One is that oscillations are produced in the groundwater levels, and second is that permanent changes occur in the groundwater levels. As groundwater remains in contact with the surface water, some variations in surface water flows are also observed. Half to one year long time variations in water level have been observed due to the response of earthquakes at a great distance from the monitoring locations [13].

Response of groundwater to earthquakes is somehow complex and can be observed by different processes on varying time scales. The impact of earthquake on the groundwater is considered in three parts: before, during, and after an earthquake event. Before an earthquake, in the area of a fault zone, there will be an increase or decrease in pore pressure due to poroelastic deformation caused by variations in stresses. Increase in pore pressure will occur in compressional regime, while decrease in pore pressure will occur in extensional regime. In a confined aquifer of high permeability or in an unconfined aquifer, the variations in pore
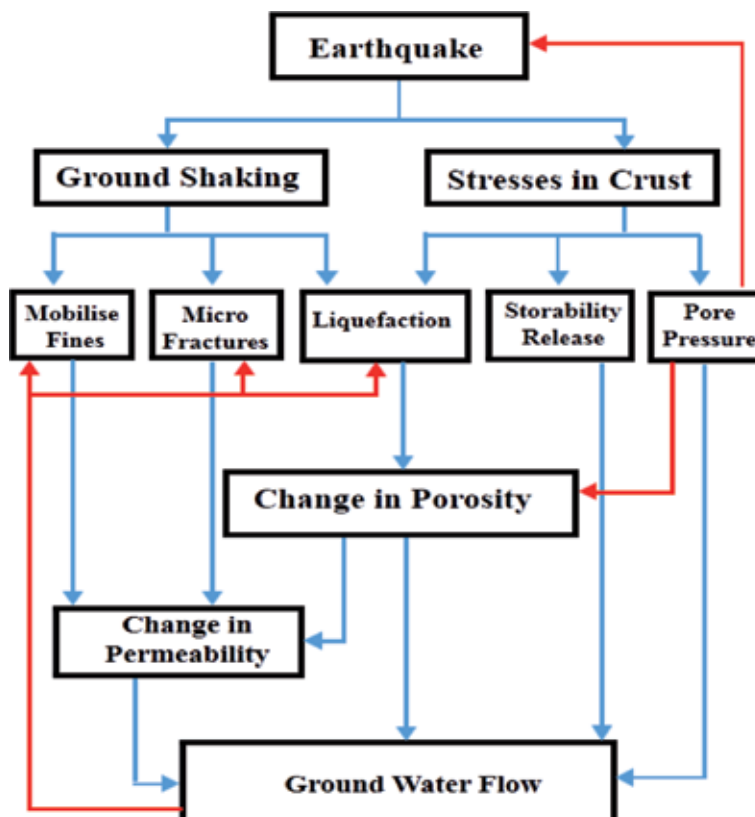

Figure 3.
Relationship between earthquake and groundwater processes.

pressure will be dissipated quickly, and no significant changes in surface water flow or groundwater will be observed. Ground deformation resulted from the passage of seismic waves during an earthquake event will change the pore pressure in an aquifer. These changes occur at different frequencies, and excess pore pressure is not allowed through groundwater flow.

The processes involved between an earthquake and groundwater are shaking of ground, stresses in the crust, mobilization of fines, microfractures, liquefaction, storability release, pore pressure, change in porosity, and change in permeability. Summary of relationships between earthquakes and groundwater processes is described in **Figure 3**.

5. Conclusion: groundwater management strategies

Groundwater resources are not managed properly in different parts of the world. For the proper management of groundwater resources, simple and effective rules and regulation must be adopted. The governing regulations may be based on knowledge and practical experiences of the local region supported by scientific and field information. The groundwater management strategies are recommended to be planned such that:

a. Groundwater withdrawal will be adjusted as per forecasted supply and demand requirements of the future.

b. The renewable character of potential aquifers must be considered with optimum aquifer pump rates, well locations, and relative priority of each sub-aquifer unit within the integrated management system of the entire aquifer field.

c. Water quality, effect of urbanization, intensive agricultural practices, economy, social impact, and local administrative strategies should also be considered.

d. Recommended groundwater management practices need to scientifically determine different hydrogeological parameters such as porosity, specific yield, and hydraulic conductivity for actual water volume calculations. It is preferable to obtain estimated parameter by field techniques like the aquifer tests and their proper interpretations.

e. For strategic planning of groundwater reservoirs that may be replenished, the groundwater quality is significant not only for management but also for controlling the excessive exploitation possibilities. Naturally existing groundwater does not have homogenous but heterogeneous properties within the same storage. Generally, the bottom layers are saline, and, therefore, during pumping operations, the up-coning must be avoided.

f. Private well owners must be convinced to allow for groundwater strategic planning by avoiding haphazard and unnecessary exploitations.

g. Implementation of artificial recharge system in order to compensate the present deficit. Increasing groundwater recharge could counteract the projected effects of climate changes on the groundwater system.

h. Construction of new management system helps in monitoring the groundwater system in terms of quantity and quality.

Author details

Muhammad Salik Javaid[1*], Laila Khalid[2] and Muhammad Zeshan Khalil[3]

1 Abasyn University, Islamabad, Pakistan

2 Capital University of Science and Technology (CUST), Islamabad, Pakistan

3 University of Engineering and Technology (UET), Taxila, Pakistan

*Address all correspondence to: msalikj@abasynisb.edu.pk

IntechOpen

References

[1] Alam R, Munna G, Chowdhury MA, Sarkar MS, Ahmed M, Rahman MT, et al. Feasibility study of rainwater harvesting system in Sylhet City. Environmental Monitoring and Assessment. 2012;**184**(1):573-580. DOI: 10.1007/s10661-011-1989-7

[2] Yadav A, Sonje A, Mathur P, Jain DA. A review on artificial groundwater recharge. International Journal of Pharma and Bio Sciences. 2012;**3**(3):304-311

[3] Rajaveni SP, Brindha K, Rajesh R, Elango L. Spatial and temporal variation of groundwater level and its relation to drainage and intrusive rocks in a part of Nalgonda District, Andhra Pradesh, India. Journal of the Indian Society of Remote Sensing. 2013;**42**(4):765-776

[4] Groundwater hydrology by David Keith Todd, Larry W. Mays. In: Handbook of Groundwater Hydrology. 3rd ed. Chichester: Wiley, Argosy Publishing; 2005 p. 279-325

[5] Shahid M, Gabriel HF, Nabi A, Javaid MS. Assessment of effect of land use change on hydrological response and sediment yield for catchment area of Simly Lake, Pakistan. In: 1st International Conference on Emerging Trends in Engineering, Management and Sciences (ICETEMS-2014); 29-30 December 2014; Islamabad, Pakistan. 2014

[6] Minnig M, Moeck C, Radny D, Schirmer M. Impact of urbanization on groundwater recharge rates in Dübendorf, Switzerland. Journal of Hydrology. 2018;**563**:1135-1146. DOI: 10.1016/j.jhydrol.2017.09.058

[7] Liu Y, Jiang X, Zhang G, Xu Y, Wang X, Qi P. Assessment of shallow groundwater recharge from extreme rainfalls in the Sanjiang plain, Northeast China. Water. 2016;**8**(10, 10):440. DOI: 10.3390/w8100440

[8] Javaid MS, Khan SA. Aquifers today and tomorrow. In: Javaid MS, Khan SA, editors. Aquifers—Matrix and Fluids. London, UK: Intech Open; 2018. pp. 3-7. DOI: 10.5772/IntechOpen/69070

[9] Spane FA. Considering barometric pressure in groundwater flow investigations. Water Resources Research. 2002;**38**(6):1078. DOI: 10.1029/2001WR000701

[10] Thomas BF, Behrangi A, James S. Famiglietti: Precipitation intensity effects on groundwater recharge in the southwestern United States. In: MDPI, Basel, Switzerland. Journal of Water. 8 March 2016;**8**(90):1-15

[11] Huizer S, Rodermacher M, de Vries S, Oude Essink GHP, Bierkens MFP. Impact of coastal forcing and groundwater recharge on the growth of a fresh groundwater lens in a mega-scale beach nourishment. Hydrology and Earth System Sciences. 2018;**22**:1065-1080

[12] Singaraja C, Chindambaram S, Jacob N. A study on the influence of tides on water table conditions of the shallow coastal aquifers. Applied Water Science. 2018;**8**:10. DOI: 10.1007/s13201-018-0654-5

[13] Digges La Touche G. Earthquakes and groundwater and surface water management at mines sites. In: Drebenstedt C, Paul M, editors. Proceedings IMWA 2016—Mining Meets Water-conflicts and Solutions; Freiberg, Germany. 2016. pp. 102-107. ISBN: 978-3-86012-533-5

The Investigation of the Dorfak Karstic Aquifer

Maryam Dehban Avan Stakhri, Mohammad Hossien Ghobadi and Ali Mirarabi

Abstract

The karstic aquifers were the best source of potable water in the northeast of Rudbar, Iran. The present study was carried out to appraise the hydrogeological attributes of karst aquifer in this area. For this objective, saturation indices (SI values) are acquired through using the geochemical PHREEQC software for a number of chemical compounds existing in the karstic aquifer. Moreover, the sources of the ions and hydrogeochemical plots were obtained by using AqQA-RockWare software packages. The water type of all springs is the Ca-HCO$_3$ type which is determined by plotting of Piper diagram and Durov diagram for spring water samples, that is confirming the calcareous effects of the region on the quality of groundwater and representing a single source for the springs. The degree of Karstification of the recharge area of the karst aquifer was determined to be 5.5 from an analysis of the hydrograph Sefidab Spring. The microbial contamination can be observed in all samples due to the intense development of karst, lack of self-purification in the karst system, and lack of an adequate cover layer on carbonate formation.

1. Introduction

Iran as a dry country with a population of 80 million has faced a water deficit in recent decades. The unorganized use of groundwater resources is created by subsidence of many plains in Iran. Guilan, a province situated in the north of Iran, has wet weather and thus is less subjected to water shortage problems compared to the southern and central provinces of Iran. The Dorfak karstic area is situated in the northeast part of the Rudbar city (**Figure 1**). The highest point of the area is a Dorfak peak with a height of 2733 m.a.s.l (meters above sea level). The karstic aquifers (excluding of the evaporating formation) are suitable groundwater resources for potable water. Dorfak karstic area is the initial well-known karstic region of Guilan province. The first study in this area was conducted by the Water Resources Management Company of Iran. In the following, we investigate the study area in terms of geology, tectonic structures, climate, and quantitative and qualitative properties of the aquifer by the analysis of water samples from springs in the region. For this purpose, information about the discharge rates of these springs and their chemical analysis was provided by the Regional Water Company of Guilan province. Information about various lithologies in the region was obtained

Figure 1.
Situation map of the study area [1].

using the 1:100,000-scale geological map published by Geological Survey of Iran. Additionally, a hydrograph analysis method was also used to estimate the degree of karstification in recharge areas.

2. Topography, climate, and vegetation

The Dorfak karst area, one of the largest karst regions of the north-east of Rudbar city, is situated in the east of the Guilan province of Iran. The region area ranges from about 1000 m elevation up to the Dorfak summit at 2733 m.a.s.l. The whole mountain range covers an area of about 429.59 km². The study area is affected by two climates: Csa and Bsk. The majority of the study area is situated in the Csa climate. The monthly average minimum and maximum temperature is 0.40°C in February and 18.5°C in August. The mean annual rainfall has been

748 mm in the last 20 years (1993–2013). The most rainfall occurs in November, December, March, and February, in the order of their appearance. The Csa Mediterranean climate can be observed in the western continents between latitude 30–45°. The rainy weather and hot and dry summers are special characteristics of this climate. The climate depends on the high-pressure semitropic system, except that coastal areas have a cooler summer because of the cold ocean flow. This cool ocean flow often creates fog and prevents rainfall. Up to an elevation of approximately 2000 m, vegetation is covered by forests with beech trees in the west and north-west parts. Above the timberline, grassy vegetation persists up to the summit, where soil coverage has not been washed out due to karstification or erosion.

3. Stratigraphy and tectonic structures

The Dorfak karst area is a part of the West Alborz that is situated on the east of the Sefidrud Valley. The trend of the mountains was east-west (EW). In the southern slope of the Dorfak summit, one can observe the outcrop of the volcanic
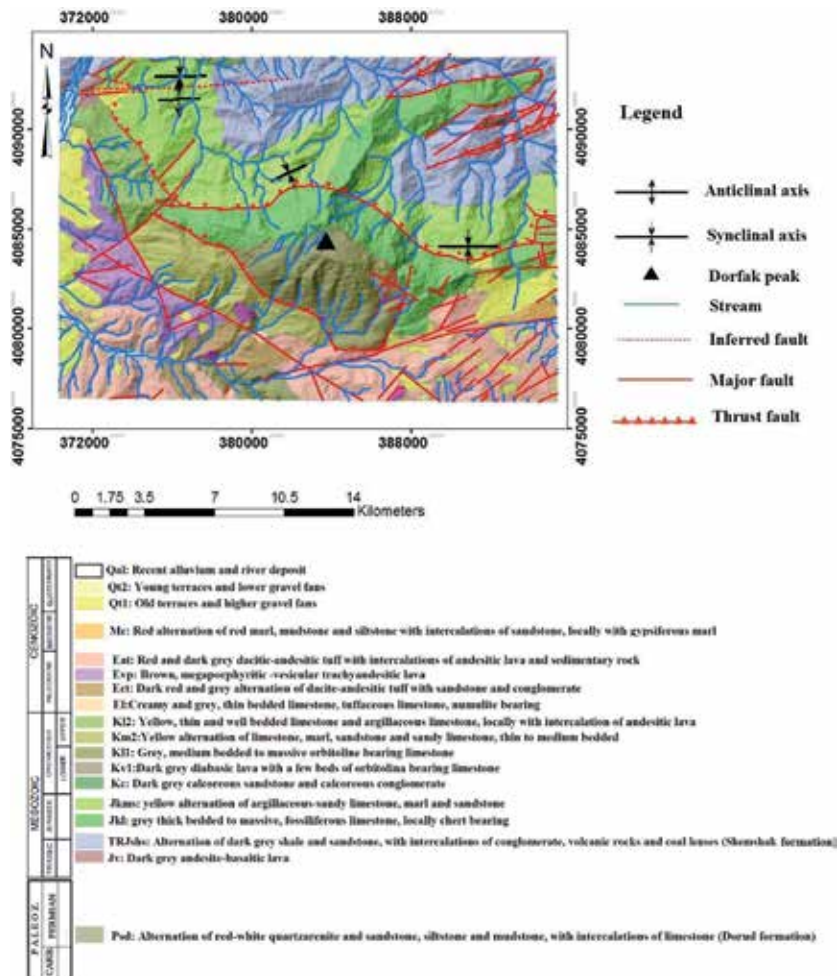

Figure 2.
Geology map of the study area [1].
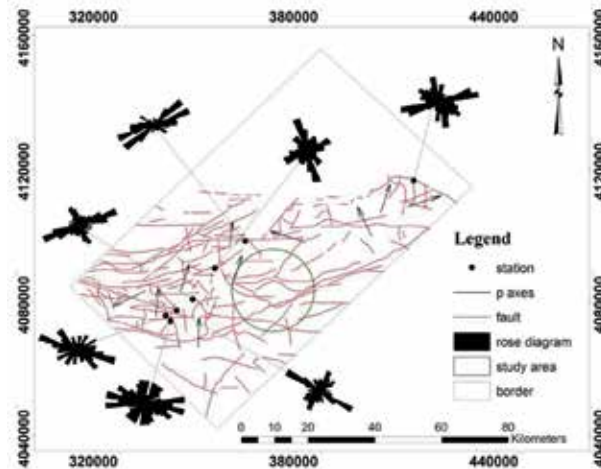
Figure 3.
Structure geology map of the study area (reproduced with the permission from [2]).

rocks with the Paleogene age. The limestone units in the Dorfak karstic area contain gray thick to massive bedded fossiliferous limestone, which is locally chert-bearing (JKL), gray, medium-bedded limestone including Orbitolina fossils (KL1); alternating beds of yellow argillaceous-sandy limestone, marl and sandstone (JKms); alternating beds of thin- to medium-bedded limestone, marl, sandstone and sandy limestone (Km2); and thin and well-bedded limestone and argillaceous limestone, locally with intercalation of andesitic lava (KL2) (**Figure 2**) [1]. The effects of the Arabian Plate's pressure on the Eurasian Plate can be observed in the reported kinetic axes for the West Alborz that is directed from the northeast to the north. In the view of structural geology, the Dorfak karstic area was situated in Lahijan fault shear zone. Safari et al. [2] were reported that the main compression axis for the Lahijan shear zone is N10E. This result is confirmed due to the former measured pressure axis in the area and left-lateral movement of Lahijan fault. The pop-up structure of the Dorfak peak was created by the enclosure between two thrust faults, which are the Dorfak thrust fault with a slope to the south and the Deylaman thrust fault with a slope to the north (**Figure 3**). This structure provides a sui basis for the karst development through creating of the large fractures in rocks of the area [1]. The trend of these faults was almost perpendicular to in this region. The strike of faults was N90s–110 and has reverse movement with a left-lateral component [2].

4. Karst features

One of the main properties of karstification is the existence of karst features. In order to determine the karst extent in the study area, karst features were identified. The critical features of karstic regions such as the presence of sinkholes, karrens, shafts, caves, poljes, and springs can be observed in the Dorfak karst area. The different types of karrens such as grikes, clints, kamenitzas, rinnenkarren, meandering runnels, wall karren, hummocky karren, trittkarren, rainpits, rillenkarren, rundkarren, and cavernous karren are observed in the study area. Sinkholes are prevailing features in the karst region. The types of sinkholes are solution and collapsible. Shafts are prevailing features due to the high abundance of joints with an upright dip in the Dorfak peak. The Dorfak bowl is a polje that its water is supplied through melting snow and drainage of rainfall into the polje. **Figure 4** shows some karst features.
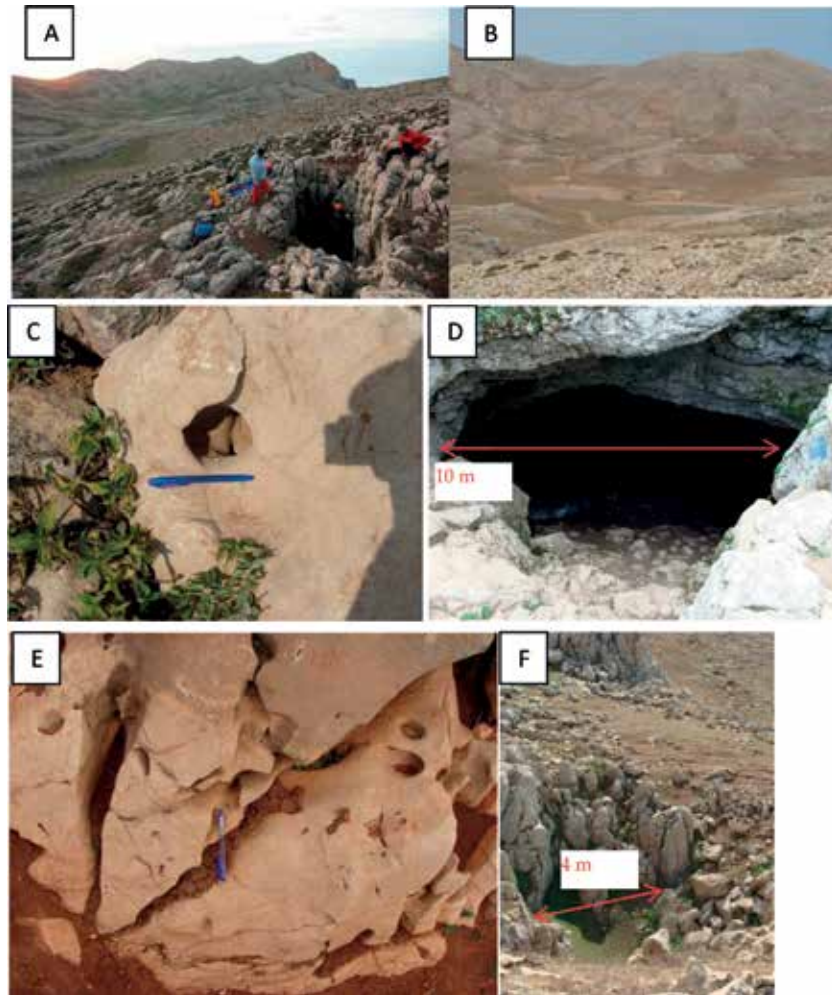
Figure 4.
Images of some karst features in the study area (Dorfak peak), A: a shaft (Afraz scaler group of Rasht city), B: polje, C: Kamenica, D: Dorfak cave, E: Rundkarren, and F: sinkhole.

5. Hydrogeology of the spring

There are several springs in the Dorfak karstic area. The spring's situation is shown in **Figure 5**. In this section, we will investigate Sefidab spring properties as the most important spring of the Dorfak karst area. Sefidab spring operates as the permanent drain of the Dorfak karst aquifer. The Sefidab spring is situated in the west side of the Dorfak peak, in the Sefidab valley, 387 m.a.s.l (**Figure 6**). The annual average discharge of Sefidab spring is 500 l/s that the watershed area of spring was inappreciable against discharge content and it is about 2 km^2. The runoff content of Kharashk watershed is considerably higher than the total content of precipitation because of the high development of karst in this subbasin; the water transition through shafts and sinkholes is situated in the upstream subbasin. The Sefidab spring is a typical fault-bound and limestone karst spring with a dynamic outflow. Since exact measurements done in June 2011, the highest discharge was recorded on December 21, 2013, with more than 2534 l/s. The lowest discharge was recorded on July 14, 2012 with 30 l/s. The mean discharge in this period (2011–2014) reached 500 l/s. The present study investigates the hydrogeochemical attributes of
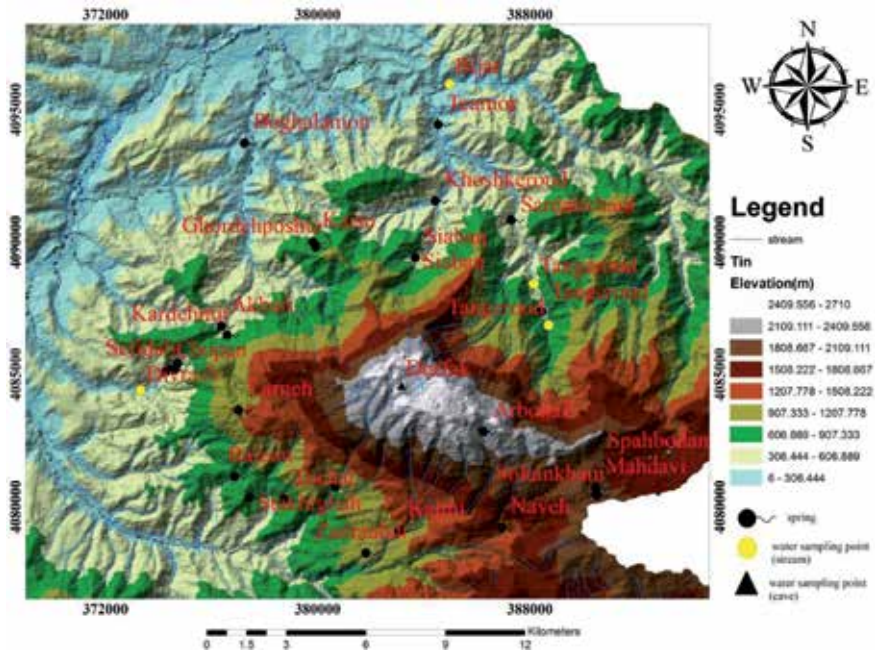
Figure 5.
Situation map of springs and sample point in the study area.

Figure 6.
Images of the Sefidab spring in the study area.

the karst aquifer through the analysis of water samples from karst springs in the area. For achieving this goal, database of the Regional Water Company of Guilan province about the discharge rates of these springs and their chemical analysis was used. Information about various lithologies in the region was obtained using the 1:100,000-scale geological map published by Geological Survey of Iran. A hydrograph analysis method was also used to estimate the degree of karstification in recharge areas.

6. Geochemistry investigation

By plotting a Piper diagram [3] of spring water samples, the water type of all sources of the region was discovered to be the Ca-HCO3 type, demonstrating that all springs in the region were discharged from a karst aquifer (**Figure 7**). Plotting of the Durov diagram of the samples is done to attain an accurate inspection of the chemical attributes of groundwater (**Figure 8**). Compared to Piper diagram, the Durov diagram distinguishes in terms of its ability to showing different types of water and hydrochemical processes such as water mixing of different qualities and ion exchange [4]. The chemical composition of springs is bicarbonate type with the Ca cation being the dominant by using the Durov diagram, which has also confirmed the effects of limestone formations on the quality of groundwater in the region. Also, using the Durov diagram has proven that the springs recharge usually from a single origin. The anionic evolution cycle has more effect on the ion evolutionary cycle of groundwater than the cationic cycle, which has been obviously proven due to the increasing total dissolved solids (TDS) in water sample of springs. The groundwaters of the area are situated into the domain of alkaline springs due to the plotting of the Durov diagram. The statistical parameters of chemical analysis results of elective resource can be observed in **Tables 1** and **2**.
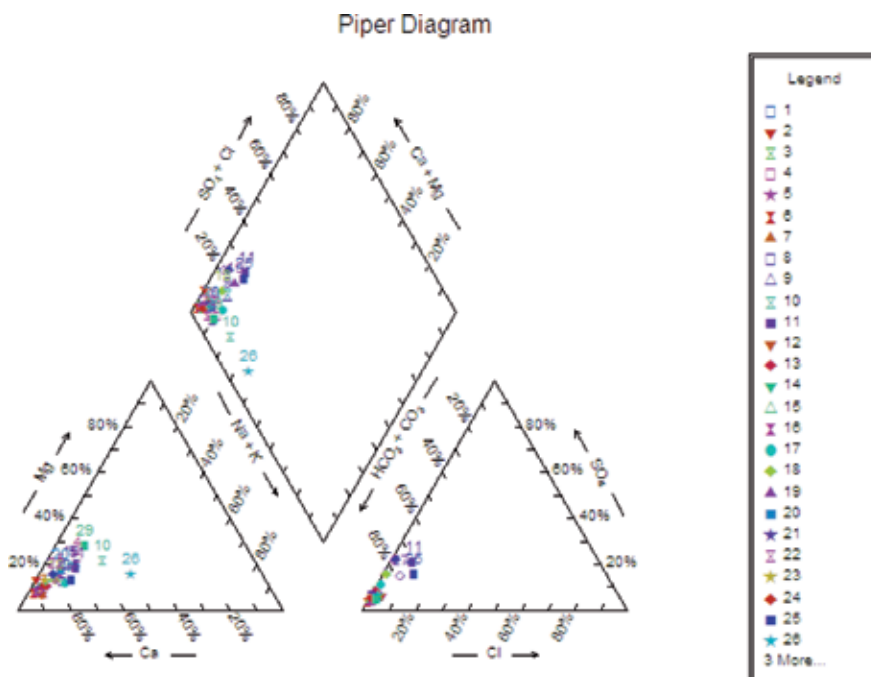
Figure 7.
Piper diagram of water sample.

A Cl-HCO$_3$-SO$_4$ ternary diagram (**Figure 9**) showed distinct zones of alkaline, acidic, and chloride-rich water [6]. As shown in **Figure 9**, all water samples are located in the soda spring zone.

In order to evaluate the controlling mechanisms of water chemistry, the effect of host rock lithology on water quality is estimated, and the mechanism of groundwater flow is determined, and the composition of the main ions in groundwater is applied as per the Gibbs chart (1970) [7]. The effective mechanisms of water chemistry and its evolution are separated into three classes by Gibbs: atmospheric precipitation, rock weathering, and evaporation [8]. Also, he proposed two diagrams of $Na^+/(Na^+ + Ca^{2+})$ and $Cl^-/(Cl^- + HCO_3^-)$ against the TDS to appraise the origin of dissolved chemical constituents in water.
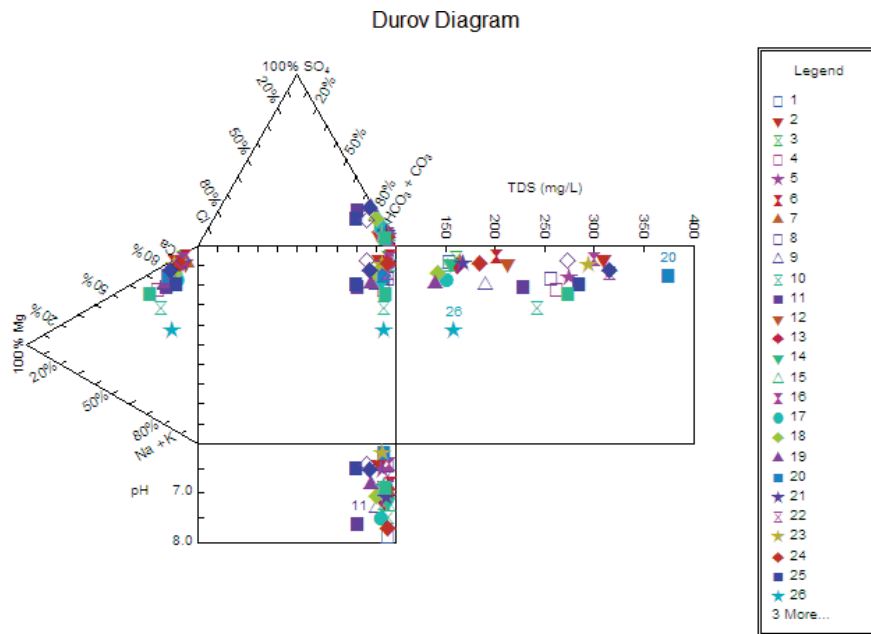
Figure 8.
Durov diagram of water samples.

Dry season

Parameters	Ec (μs/cm)	TDS (mg/l)	pH	meq/l								
				HCO$_3^-$	CO$_3^-$	Cl$^-$	SO$_4^-$	NO$_3^-$	Ca$^+$	Mg^{2+}	Na$^+$	K$^+$
Number of samples	29	29	29	29	29	29	29	29	29	29	29	29
Average	354.34	222.7	6.99	3.48	0	0.07	0.22	0.09	3.08	0.54	0.29	0.04
Maximum	630	375.8	7.9	6.15	0	0.33	0.75	0.61	5	1.37	0.94	0.18
Minimum	159	140.06	6.2	1.94	0	0.01	0.09	0.01	1.38	0.17	0.06	0.01
Standard deviation	124.78	65.52	0.46	1.13	0	0.08	0.15	0.12	1.02	0.32	0.22	0.04
Variation coefficient	0.35	0.3	0.65	0.32	0	1.14	0.68	1.33	0.33	0.59	0.75	1

Table 1.
Statistics parameters of chemical analysis results of elective resource in the dry season [5].

Wet season

Parameters	Ec (µs/cm)	TDS (mg/l)	pH	meq/l								
				HCO$_3^-$	CO$_3^-$	Cl$^-$	SO$_4^-$	NO$_3^-$	Ca$^+$	Mg^{2+}	Na$^+$	K$^+$
Number of samples	30	30	30	30	30	30	30	30	30	30	30	30
Average	334.81	203.28	7.48	3.09	0	0.11	0.18	0.13	2.86	0.47	0.25	0.02
Maximum	595	355.65	8.55	5.96	0	0.72	0.61	1.39	4.83	1.12	2.41	0.1
Minimum	69.7	44.35	6.88	0.6	0	0.03	0.07	0.005	0.4	0.17	0.03	0
Standard deviation	140.51	83.26	0.42	1.32	0	0.13	0.1	0.25	1.28	0.25	0.43	0.02
Variation coefficient	0.42	0.41	0.05	0.43	0	1.19	0.56	1.92	0.45	0.53	1.72	1

Table 2.
Statistics parameters of chemical analysis results of elective resource in the wet season [5].
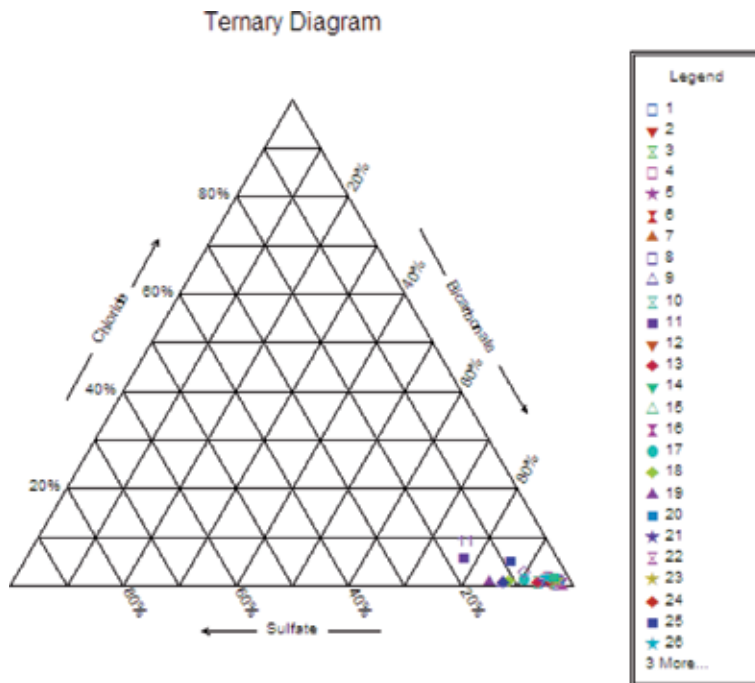
Figure 9.
Ternary diagram (Cl-HCO$_3$-SO$_4$) of the water samples.

In samples with a high ratio of $Na^+/(Na^+ + Ca^{2+})$ or $Cl^-/(Cl^- + HCo_3^-)$ and low amount of TDS, salts derived from rainfall are likely to have a significant effect on the chemistry of water in the study area. In contrast, in samples with a low ratio of $Na^+/(Na^+ + Ca^{2+})$ or $Cl^-/(Cl^- + HCo_3^-)$ and TDS between 100 and 1000 mg/L, rock weathering is likely to affect the groundwater quality. Finally, samples with a higher salinity are likely to be affected by evapotranspiration. Extensive changes in the ratio of $Na^+/(Na^+ + Ca^{2+})$ or $Cl^-/(Cl^- + HCo_3^-)$ with an almost constant TDS probably show that ion exchange affects groundwater quality in the region [1]. During an ion exchange process, 1 mmol/L of calcium was substituted with 2 mmol/L of

sodium, which cannot significantly change the amount of TDS in the water, because the weight of 1 mmol/L of calcium (40 mg/L) was almost two times of 2 mmol/L of sodium (46 = 2 × 23 mg/L) [9]. According to these diagrams (**Figure 10a** and **b**), the water samples were situated in the area with the dominant rock process, suggesting the presence of a significant interaction between rock chemistry and water chemistry in infiltration rainwater.
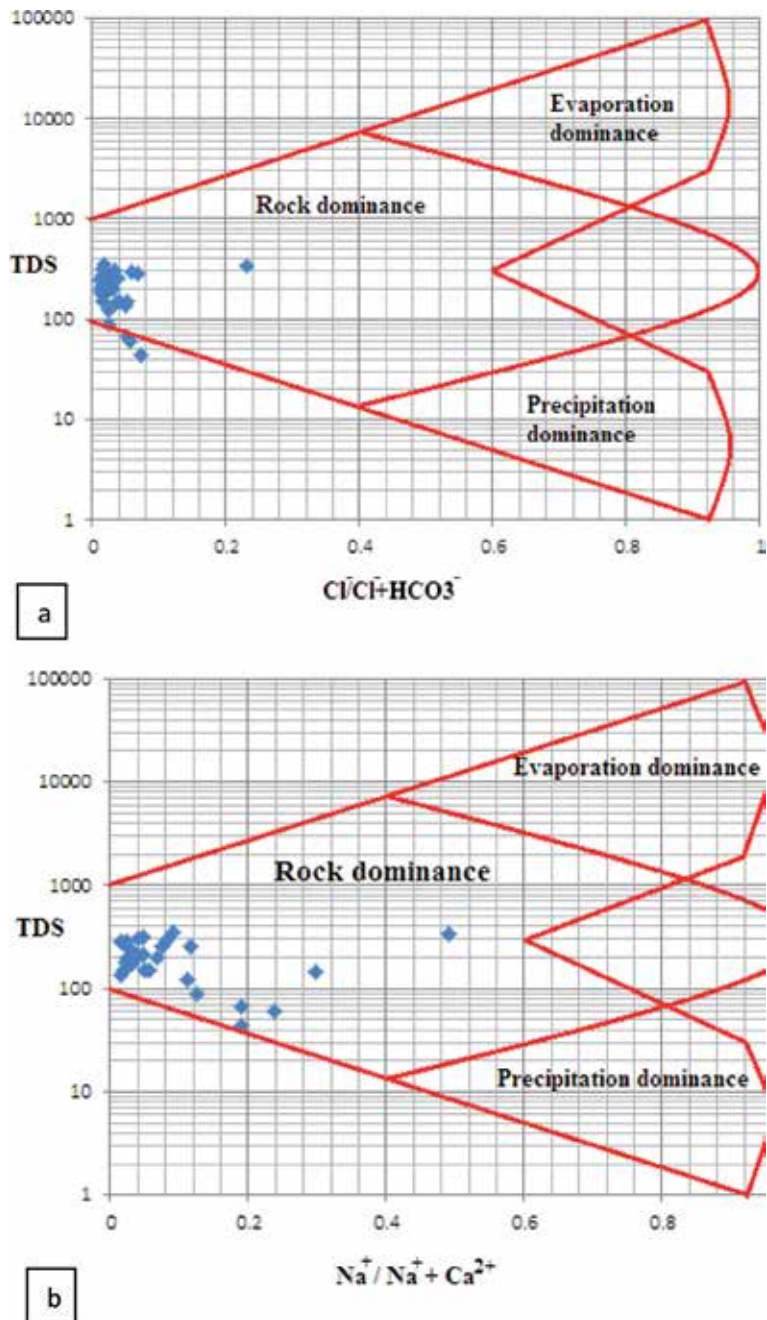
Figure 10.
Gibbs diagram of the spring water samples (a: plots of TDS: $Cl^-/Cl^- + HCO_3^-$, b: plots of TDS: $Na^+/Na^+ + Ca^{2+}$).

7. Saturation indices

To estimate the extent to which groundwater in the karstic aquifer could dissolve of precipitate carbonate minerals, saturation indices (SI) of calcite, dolomite, and CO_2 gas are determined to applying the samples the chemical analysis and PHREEQC software. The water was saturated due to the specified mineral if the saturation indices are zero, and water is undersaturated with mineral if it was negative; thus, the more content of mineral can be dissolved in water. When the water is supersaturated due to the specified mineral, the saturation indices will be positive. Coetsiers and Walraevens [10] represented that the more positive SI shows a higher mineral content in the water and appropriate status to precipitate in this SI. The saturation indices are provided by Eq. (1) as follows [11]:

$$SI = Log \frac{IAP}{K_t} \tag{1}$$

where the ion activity product of the dissociated chemical species in solution with IAP is showed and the equilibrium solubility product of the chemical involved at the sample temperature with K_t is expressed [12]. The SI values due to the calcite, dolomite, and CO_2 gas determined by applying PHREEQC software are shown in **Table 3**.

Spring name	SI_c	SI_d	SI_{CO_2}
Sefidab	−0.22	−1.60	−2.49
Polahaki	0.22	−0.97	−2.16
Chopan	−0.38	−2.19	−2.10
Stakhr	0.09	−0.55	−2.22
Rajeon	0.04	−0.71	−2.02
Larneh	−0.03	−1.01	−2.28
kardemir	−0.09	−1.60	−2.60
Noor-Cheshm	−0.90	−2.88	−1.92
Sardabkhani	−0.19	−1.35	−2.09
Ghordehposhteh	−0.48	−2.09	−2.61
Kaiso	−1.60	−3.87	−2.39
Boghalamon	−0.31	−1.41	−1.36
Arbonaf	0.22	−0.31	−3.02
Naveh	−0.19	−1.34	−1.55
Kalami	−0.26	−1.75	−1.59
Spahbodan	−0.22	−1.42	−2.71
Mirhossieni	0.64	0.21	−2.16
Tochal	0.32	−0.09	−1.76
Stakhrghah	0.27	0.03	−1.89
Khani cheshme	0.62	0.67	−2.90
Rashi river	1.18	1.76	−3.23
Kaiso stream	−0.27	−0.84	−2.78
Alokale	0.27	−0.26	−1.85

Spring name	SI_c	SI_d	SI_{CO_2}
Siyavash	−0.34	−1.57	−1.54
Eshkavari	−0.12	−1.13	−1.70
Kordsara	0.76	0.71	−2.89
Bazmiyaneh	0.62	0.61	−2.62
Siyani	0.09	−0.65	−1.85
Dolisara	−1.29	−2.57	−2.35
Mina cheshme	−1.61	−3.34	−2.51

SI_c, saturation index of calcite; SI_d, saturation index of dolomite; and SI_{CO_2}, saturation index of CO_2.

Table 3.
Saturation index values of water samples (wet season).

In accordance with the saturation index values, most water samples are undersaturated due to calcite, dolomite, and CO_2 in the region; hence, carbonate minerals dissolve to a greater extent. White [13] represented that the springs with negative saturation index values (in the range from −0.2 to −0.4 or lower) have been transmitted through open conduit systems in the temperate and northern climates. A negative saturation index value of CO_2 indicates that they have no potential for travertine formation.

8. Chloro-alkaline indices

The extent to which ion occurs between groundwater and the aquifer matrix is illustrated through the chloro-alkaline indices (CAI) as suggested by Schoeller [14]. When there is an exchange between Ca and Mg in aquifer rocks with Na and K in the water (so-called "normal" ion exchange), the CAI value will be positive. When the CAI value is negative, the ion exchange is a reverse (so-called "reverse" ion exchange) [15].

The CAI value can be used as a diagnostic tool for the source of bicarbonate ion in groundwater. If the weathering of silicate minerals is the source of bicarbonate ions in water, the CAI value will have a positive amount. Conversely, if carbonate minerals were the source of the bicarbonate ions, a negative value of CAI is visible. Also, a negative CAI value shows that the source of bicarbonate can be created from human activities [16]. CAI values are calculated through Eqs. (2) and (3) as below [17]:

$$I_1 = [Cl - (Na + K)]/Cl \qquad (2)$$

$$I_2 = \frac{[Cl - (Na + K)]}{So_4} + HCO_3 + Co_3 + No_3 \qquad (3)$$

The CAI value of spring's water samples was calculated by Eqs. (2) and (3) (**Figure 11a** and **b**). By determining CAI value, the ion exchange in the samples and the source of bicarbonate were investigated. The results show that the four springs (t1, t2, t6, and t8) in this investigation have positive CAI values, suggesting the normal ion exchange and a bicarbonate ion source of silicate minerals. However, in other springs, the source of bicarbonate ions was carbonate minerals.
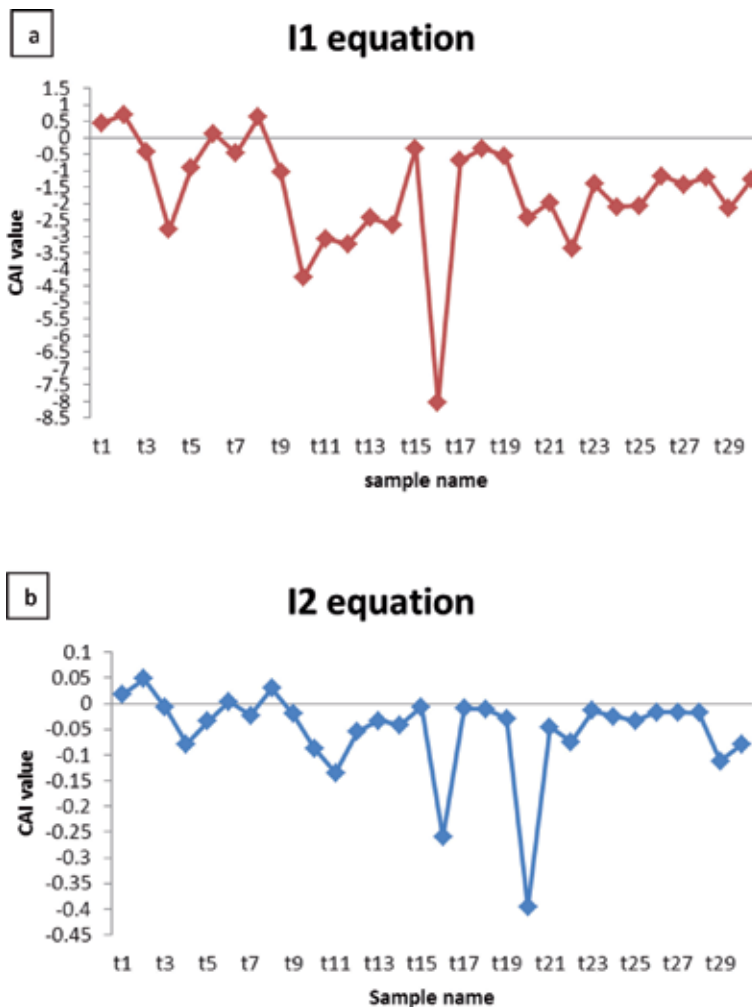
Figure 11.
The graph of chloro-alkaline index (a: relation 1 and b: relation 2).

9. Sources of ionic constituents in groundwater

By plotting the parameters of the water sample analysis on a bivariate diagram (known as a cross diagram), it is possible to interpret the processes that have impressed the chemical quality of groundwater. By plotting cations against anions, it is possible to detect the source in this method [18–22].

The common origin of the ions has been proven by the high determination coefficient between two ions. Diagrams of Ca:TDI (total dissolved ions) and Ca:HCO_3, and diagrams of Mg:HCO_3 and Mg:TDI are made to achieve this goal (**Figure 12a–d**). In order to evaluate the importance of ion exchange and different weathering process, the binary diagrams Ca + Mg:HCO_3 + SO_4 and Ca + Mg:TDI were also plotted (**Figure 12e** and **f**). If the dissolution of calcite, dolomite, and gypsum has provided Ca, Mg, HCO_3, and SO_4, there would be a 1:1 stoichiometric relationship available between Ca + Mg and HCO_3 + SO_4 [23]. The displacement of points to the right side and below the 1:1 line indicates that the ion exchange has occurred. Conversely, the displacement of points to the left side and above the 1:1 line shows the reverse ion exchange [24].
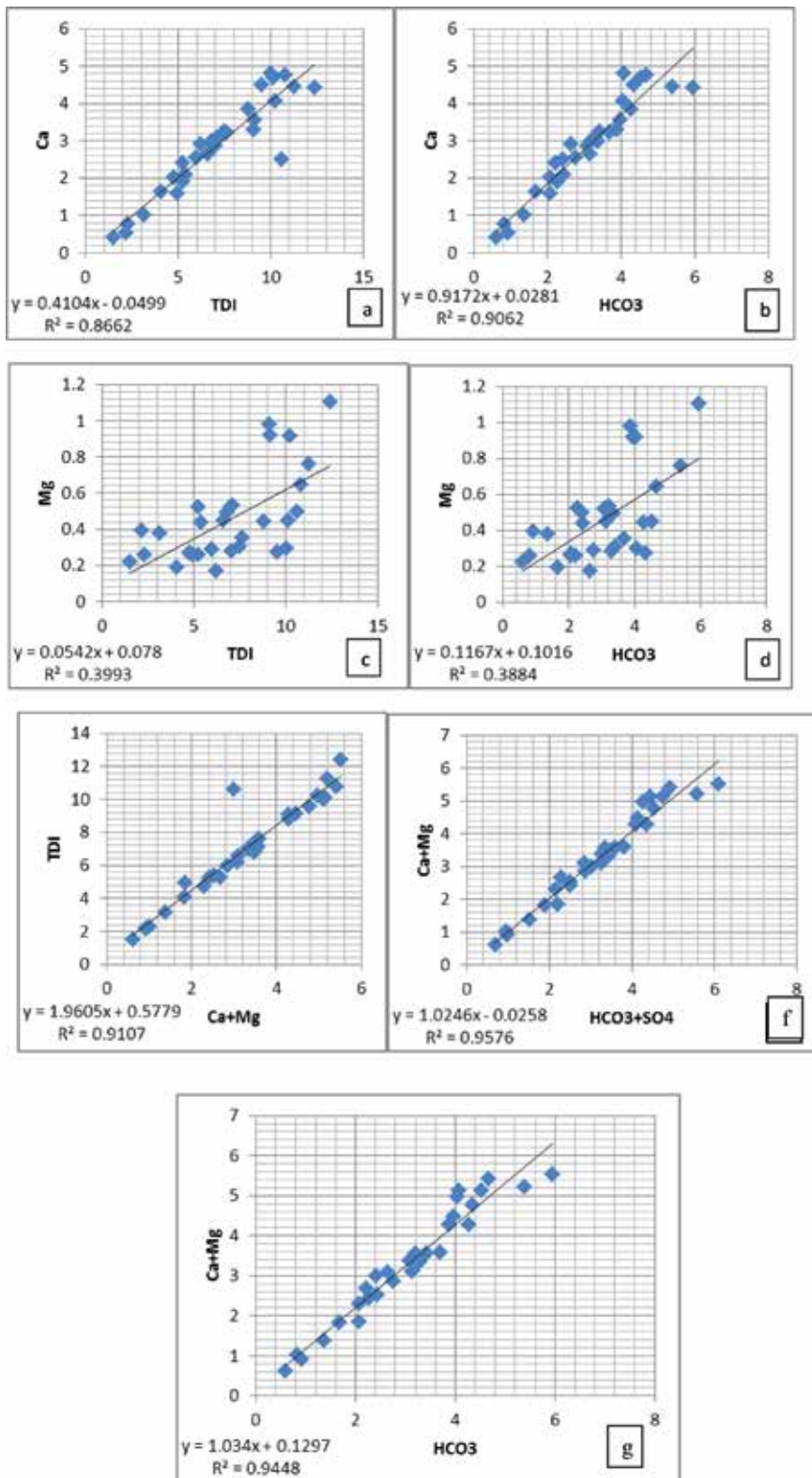
Figure 12.
Cross plot of water samples of springs (a: the plot of Ca: HCO_3, b: the plot of Ca: TDI, c: the plot of Mg: HCO_3, d: the plot of Mg: TDI, e: the plot of Ca+Mg: HCO_3+SO_4, f: the plot of Ca+Mg: TDI, g: the plot of Ca+ Mg: HCO_3).

Information about the stoichiometric process existence in groundwater provides the evaluation of Ca + Mg against HCO_3. The evaluation of the water quality data represents that the main source of Ca and Mg in groundwater was the dissolution of carbonate minerals, while the source of HCO_3 is likely to be the weathering of both silicate and carbonate minerals [25]. The simple dissolution was the very common weathering process for carbonates. Zhang et al. [26] presented a 1:1 ratio of Ca + Mg:HCO_3 or 1:2 molar ratio of Ca:HCO_3. As a result, through the ion exchange process of calcium and magnesium in water by the sodium in the clay, or by the cationic exchange or HCO_3 enrichment from weathering, the silicates create the low molar ratio of Ca:HCO_3 (<0.5) in groundwater [27], whereas the high ratios (>0.5) indicate the other sources of calcium and magnesium, such as reverse ion exchange, which is also created in hard rock formations with increasing salinity.

A high determination coefficient in plotting the Ca against the HCO_3 and TDI suggests that the calcium is originated from the dissolution of calcite (**Figure 12a** and **b**). Moreover, the moderate determination coefficient (classification of R^2: 0–0.3: low, 0.3–0.6: moderate, 0.6–0.9: high, and 0.9–1: very high) due to plotting the Mg against HCO_3 and TDI implies that magnesium ions may have been derived from the dissolution of dolomite (**Figure 12c** and **d**). Besides, the binary plot of Ca + Mg versus HCO_3 + SO_4 represented that 48.27% of groundwater samples shows a reverse ion exchange and 51.72% shows the ion exchange process (**Figure 12e**). The high determination coefficient due to the plotting of composite diagrams of Ca + Mg against HCO_3 indicates that these two ions have a common source, i.e., dissolution of carbonates and silicate weathering (**Figure 12g**).

10. Evaluation of the degree of karstification in recharge areas

The multiple hydrodynamic behaviors of karst aquifers were created by the development of epikarst geomorphology and the existence of sinkholes and abundant joints in limestones. Factors such as the flow hierarchy, the setting of the output, and drainage network organization in an unsaturated area have impressed the flow condition in karst systems, which are determined by the karst system structure [28]. The hydrographs of springs represent all the physical processes that have impressed groundwater flow in a karst aquifer [29]. The important method for determining the hydrological characteristics of karst aquifers is done by the analysis of hydrograph recession curves [30]. The period between peak discharge and next peak discharge at the end of the period forms the recession curve [31].

The perpetual drain of the Dorfak karst aquifer is done through the Sefidab spring, while the temporal spring is the Norcheshme spring. In the western part of the Dorfak karst area, the Sefidab spring is presented as a fault-bound spring that is situated in a fracturing zone created due to the faulting of bedded limestone. That way, the hydrograph plot was made to investigate the characteristics of the springs that include the extent of the reservoir, discharge rates, and discharge variability over time. Accordingly, the recession coefficient (α) and dynamic storage volume (as a determinant agent of aquifer development) were obtained. The discharge capacity of Sefidab spring was very variable that is related to the magnitude and duration of a precipitation event. The dynamic storage volume and recession coefficient (α) of Sefidab spring are determined through the following equations [32, 33] (**Table 4**).

$$\alpha = \frac{\log Q_0 - \log Q_t}{0.4343(t)} \quad (4)$$

Coefficient	α_1	α_2	β_1	V (m³)
Sefidab spring	0.0771	0.05795	0.11331	2467838.95

Table 4.
Parameters associated with recession curve [1].

where α is the recession coefficient, Q_0 (m³/s) is a previous discharge at t = 0, Q_t (m³/s) is discharged at t, and t is the period of time between primary and secondary discharge (day).

$$V = 86400\left(\frac{Q_{01}}{\alpha_1} + \frac{Q_{02}}{\alpha_2} + \cdots + \frac{Q_{0n}}{\alpha_n}\right) \tag{5}$$

where V is the dynamic storage volume (m³), Q_{0n} is the primary discharge at n part of hydrograph plot, and α_n is the recession coefficient at n part of hydrograph plot.

The karstification degree in the recharge areas of Sefidab spring is determined through its 1-year hydrograph (due to the data loss in the monthly discharge hydrographs) and information from Malík and Vojtková [31]. Therefore, the degree of karstification of the spring is estimated to be 5.5 due to the methodology described above.

The results of the investigation are represented that Sefidab spring has a complex discharge regime, with a combination of one subregime with turbulent flow and two subregimes with the laminar groundwater flow (**Figure 13**). The impact rate of the turbulent flow subregime was short time in comparison with overall groundwater discharge. Usually, such a situation is created when there are many open medium-sized fissures (both karstified and nonkarstic) in the phreatic zone of a fissure karst aquifer (according to α_1) and with a smaller influence of connected conduits (groundwater of large karstic channels, according to β_1).

The hydrograph of Sefidab spring (the most important spring in terms of discharge) is compared with a histogram of precipitation over a 4-year period from 2011 to 2014 to investigate the precipitation effects on the karst aquifer in the study area (**Figures 14 and 15**). Three peaks can be observed in the hydrograph that the initial and tertiary peaks have occurred after two maximum rainfall events, while the second peak occurred after a period of continuous rainfall.

$$Q_t = Q_{01}e^{\alpha_1 t} + Q_{02}e^{\alpha_2 t} + Q_{04}(1 - \beta_1 t)$$
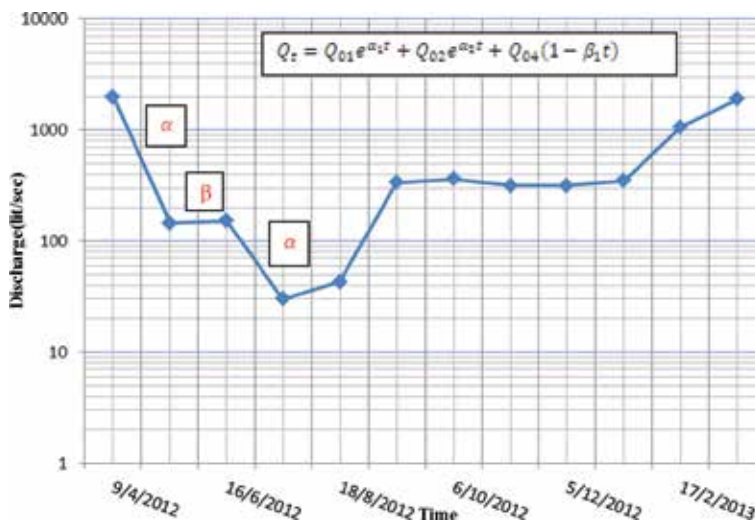
Figure 13.
The 1-year-old hydrograph of Sefidab spring [1].
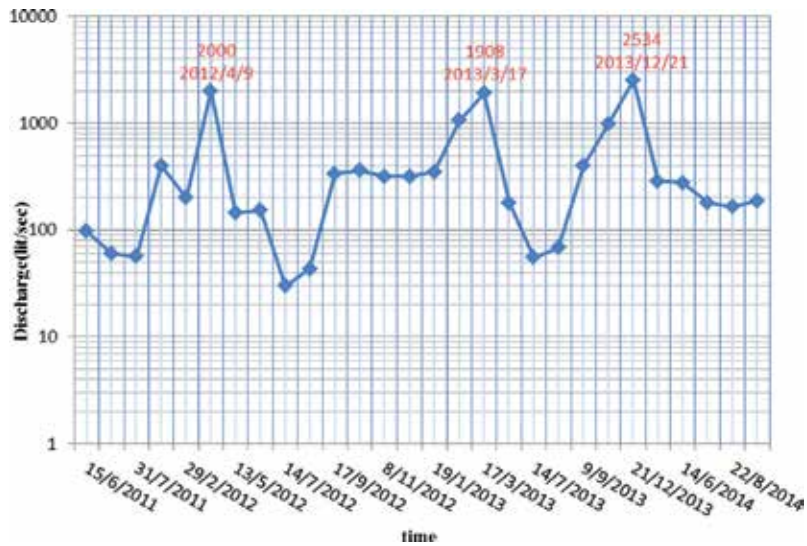
Figure 14.
The 1-year period hydrograph of Sefidab spring [1].
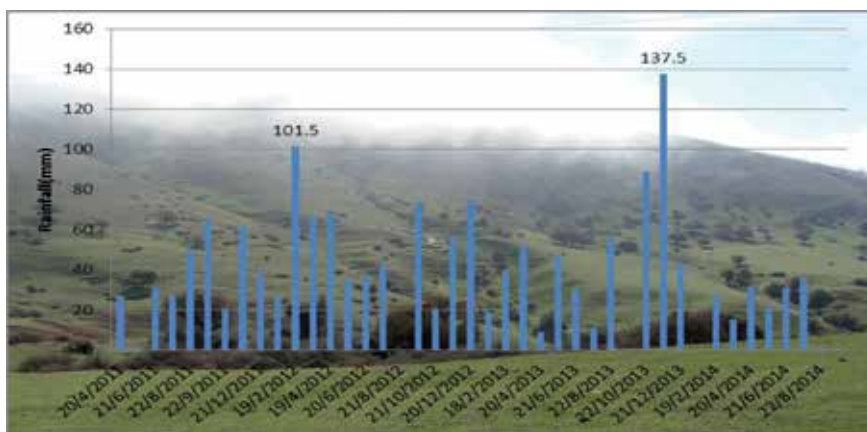
Figure 15.
The 4-year period histogram of Sefidab spring (image of Shaheshahidan pasturage) [1].

11. Chemical and microbial spring water quality

Chemical parameters and microbial agents existing on the groundwater can have a natural and human origin. The nitrate ion (NO_3) is the most important chemical parameter that shows the effect of human activity on the groundwater quality. The nitrate ion in the groundwater originates from urban wastewater influx, industrial, fertilizer, and animal excreta. Based on our measurements, the highest value of the nitrate ion was 1.392 meq/l for Soltankhani spring that is higher for world hygiene organization's limit. The high nitrate value was due to the occurrence of some cottage and pasture in the upstream of the Soltankhani spring due to the animal and human excreta influx. Except for the Soltankhani spring, all appointive samples of the nitrate values have a favorable value in both wet and dry seasons. The water microbial contamination is usually determined based on the number and frequency of the special type of bacteria. The coliforms are the dominant index of microbial quality of the water resource that is frequently found in the human excreta and

other endotherm animals. The most prevalent bacteria in the coliform group are *Escherichia coli* that are excreta contamination index of the water. The microbial contamination can be observed in all samples due to the intense development of karst, lack of self-purification in the karst system, and lack of an adequate cover layer on carbonate formation. Although the major elective samples have the better status of microbial contamination in the wet season than the dry season, the accomplishment of sanitary preparation and infiltration before consumption (among boiling of water and surcharge of chlorine) is of great necessity.

12. Contamination hazards in the spring catchment and vulnerability mapping

Potential hazards to the karst aquifer were created mainly from forestry, pasture, tourism, and an unnaturally high game population (mainly, chamois and deer) except airborne pollution. The input from tourism, pasture, and the game population was mainly feces with their microbial contaminations [34]. Karst systems with joints and clefts and without a self-purification inexistence pose a high vulnerability to human activities. The high hydraulic conductivity, transmissivity, and intense heterogeneity and anisotropy of karst aquifers enhance their vulnerability to dopants. Various methods can be applied to the vulnerability analysis of karst aquifers. Kardan Moghadam et al. [35] applied the EPIK vulnerability index that consists of four parameters: epikarst, the preservative cover layer, permeation condition, and developed karst system. Preparation, weighing operation, and incorporation of the suitable parameters map was accomplished in the ArcGIS environment [35]. The Dorfak peak Polje can enhance the vulnerability level of karst aquifer due to livestock aggregation in the spring and summer seasons. The risk map is provided through incorporating this information with vulnerability index [35]. In general, carbonates in the study area were very well karstified throughout and covering layers were mostly absent, not protective, and sometimes even increased the point recharge. Vulnerability, according to the EPIK method (**Figure 16**), is high in 20% of the area (20% high vulnerability, 35% moderate vulnerabilities, and 45% low vulnerabilities) [35].
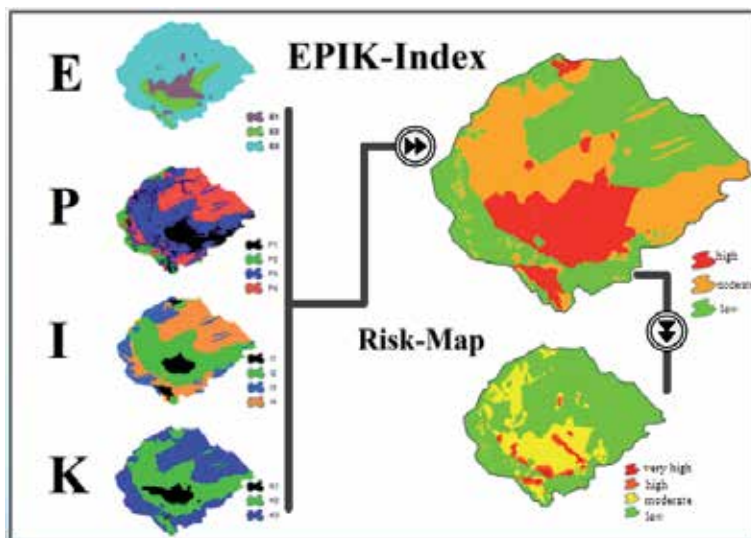

Figure 16.
Risk map of the study area (reproduced with the permission from Kardan Moghadam et al. [35]).

Acknowledgements

Glossary

m.a.s.l:	abbreviation of meters above sea level, elevation
Csa:	hot dry-summer" Mediterranean climates
Bsk:	cold semiarid Mediterranean climates
TDS (total dissolved solids):	it is a measurement of the soluble composed of amount of all organic and inorganic materials existing in a liquid in a microgranular (colloidal sol) suspended form, ionized or molecular.
Karren:	these are channels or furrows that were created due to dis solution on massive bare limestone surfaces; their depth changes from a few millimeters to more than a meter and is discredited by ridges.
Shaft:	it is a cylindrical tube commonly steep-sided, which is created due to dissolution and (or) collapse.
Polje:	it is a Slavic word for field. They are a very large closed depression in areas of karst topography; their length and width vary by several kilometers in some places, having a flat floor, both covered by alluvium or bare Limestone, and blockaded generally by steep walls of limestone.
Grike:	these are vertical or subvertical fissures in a limestone pavement that are created through solution along with a joint. Their synonym is Kluftkarren (in the German language).
Clint:	these are slabs of limestone, parallel to the bedding, forming a pavement. Widened joints, or grikes, are isolated individual clints. The synonym term is Flachkarren.
Kamenitzas:	the form of the kamenitzas (solution pans) looks like a dish or a plate.
Rinnenkarren:	these are the solution grooves named in the German language and are created where the runoff water has gathered in streams. If the total surface is wetted, the content of water increases downward, and in this case, the grooves were broadened and deepened at their bottom.
Meandering runnel:	their cross section were asymmetrical. They are sometimes meandering and are frequently created as isolated features on gentle slopes (less than 10°).
Wall karren:	these are formed on vertical walls as a result of water flowing down the walls without any wide-spreading moistening although wide-spreading wet down ing occasionally impresses their development.
Hummocky karren:	these are constructed due to bulge and depression created by solution on the rock surface.
Trittkarren:	these are best characterized as heel-print karren because they look like the imprint of a heel. They are linked nearly with subhorizontal, adjacent, flat plains, and immigrated upslope by cutting "steps" through the process of retrogres sive corrosion.

Rainpit:	their depth and diameter vary by several centimeters. The shape of the rainpit is circular (from above) and spherical calotte (in lateral view). According to Jennings (1985), they are formed by raindrops (e.g., falling from leaves).
Rillenkarren:	these occur only in places where fresh unspent precipita tion is active and end where the water attains too high a content of lime or where water is added.
Rundkarren:	these are solution channels or furrows, which are devel oped beneath a soil cover.
Cavernous karren:	these are pitted, rubbly limestone most commonly found in relatively recent and tertiary limestones of the humid tropics.

Author details

Maryam Dehban Avan Stakhri[1*], Mohammad Hossien Ghobadi[2] and Ali Mirarabi[3]

1 Engineering Geology, Faculty of Sciences, Bu-Ali Sina University, Hamedan, Iran

2 Department of Geology, Faculty of Sciences, Bu-Ali Sina University, Hamedan, Iran

3 Hydrogeology, Faculty of Sciences, Shahid Beheshti, Tehran, Iran

*Address all correspondence to: mdehban84@gmail.com

IntechOpen

References

[1] Ghobadi MH, Dehban Avan Stakhri M, Mirarabi A. Investigating the hydrogeological properties of springs in a karstic aquifer in Dorfak region (Guilan Province, Iran). Environmental Earth Sciences. 2018;**77**:96. DOI: 10.1007/s12665-018-7270-4

[2] Safari HO, Ghassemi MR, Razavi-Pash R. Determination and structural analysis of the Lahijan transverse fault in forestall region of Alborz mountains, Iran: A geospatial application. International Journal of Remote Sensing Applications. 2013;**3**(4):215-224. DOI: 10.14355/ijrsa.2013.0304.06215

[3] Piper AM. A graphic procedure in the geochemical interpretation of water analyses. American Geophysical Union, Transactions. 1944;**25**:914-923

[4] Singhal BBS, Gupta RP. Applied Hydrogeology of Fractured Rocks. Kluwer Academic Publisher; 1999. p. 400

[5] Giggenbach WF. Geothermal solute equilibria. Derivation of Na–K–Mg–Ca geoindicators. Geochimica et Cosmochimica Acta. 1988;**52**:2749-276

[6] Mirarabi A. The identification of Dorfak karstic regions, Divrash and Shahr-e-Bijar watersheds. Report of Regional Water Company of Guilan Province. 2015 (in Persian)

[7] Subba Rao N. Geochemistry of groundwater in parts of Guntur district, Andhra Pradesh, India. Environmental Geology. 2002;**41**:552-562

[8] Gibbs RJ. Mechanism controlling world water chemistry. Science. 1970;**170**:1088-1090

[9] Li PY, Qian H, Wu JH, Ding J. Geochemical modeling of groundwater in southern plain area of Pengyang County, Ningxia, China. Water Science and Engineering. 2010;**3**(3):282-291

[10] Coetsiers M, Walraevens K. Chemical characterization of the Neogene Aquifer, Belgium. Hydrogeology Journal. 2006;**14**:1556-1568

[11] Garrels R, Mackenzie F. Origin of the chemical compositions of some springs and lakes. In: Ground RF, editor. Equilibrium Concepts in Natural Water Systems. Washington: American Chemical Society Publications; 1967

[12] Singh EJ, Gupta A, Singh NR. Groundwater quality in Imphal West district, Manipur, India, with multivariate statistical analysis of data. Environmental Science and Pollution Research International. 2013;**20**:2421-2434

[13] White WB. Thermodynamic equilibrium, kinetics, activation barriers, and reaction mechanisms for chemical reactions in karst terrains. Environmental Geology. 1997;**30**:46-58

[14] Schoeller H. Geochemistry of groundwater. In: Groundwater Studies—An International Guide for Research and Practice. Vol. 15. Paris: UNESCO; 1977. pp. 1-18

[15] Aghazadeh N, Asghari Moghaddam A. Investigation of hydrochemical characteristics of groundwater in the Harzandat aquifer, Iran. Environmental Monitoring and Assessment. 2011;**176**:183-195

[16] Chidambaram S, Karmegam U, Prasanna MV, Sasidhar P, Vasanthavigar M. A study on hydrochemical elucidation of coastal groundwater in and around Kalpakkam region, Southern India. Environmental Earth Sciences. 2011;**64**:1419-1431

[17] Schoeller H. Geochemistry of Groundwater: An International Guide for Research and Practice Book. India: UNESCO; 1965. pp. 1-18

[18] Howard FWK, Mullings E. Hydrochemical analysis of groundwater flow and saline intrusion in the Clarendon basin, Jamaica. Groundwater. 1996;**34**:801-810

[19] Stossel RK. Delineating the chemical composition of the salinity source for saline groundwater: An example from east central Canadian Parish, Louisiana. Ground Water. 1997;**35**:409-417

[20] Stober I, Bucher K. Deep groundwater in the crystalline basement of the Black Forest region. Applied Geochemistry. 1999;**14**:237-254

[21] Timms W, Acworth RI, Jankowski J, Lawson S. Groundwater Quality Trends related to Aquitard Salt Storage at Selected Sites in the Lower *Murumbidgee alluvium*, Australia. Groundwater. 2000;**25**:655-660

[22] Marie A, Vengosh A. Sources of salinity in groundwater from Jericho area, Jordan Valley. Ground Water. 2001;**39**:240-248

[23] McLean W, Jankowski J, Lavitt N. Groundwater quality and sustainability in an alluvial aquifer, Australia. In: Sililo O et al., editors. Groundwater, Past Achievements and Future Challenges. Rotterdam: A Balkema; 2000. pp. 567-573

[24] Krishnaraj S, Murugesan V, Vijayaraghavan K, Sabarathinam C, Paluchamy A, Ramachandran M. Use of hydrochemistry and stable isotopes as tools for groundwater evolution and contamination investigations. Geosciences. 2011;**1**(1):16-25. DOI: 10.5923/j.geo.20110101.02

[25] Srinivasamoorthy K, Vasanthavigar M, Vijayaraghavan K, Sarathidasan R, Gopinath S. Hydrochemistry of groundwater in a coastal region of Cuddalore district, Tamilnadu, India: Implication for quality assessment.

Arabian Journal of Geosciences. 2011. DOI: 10.1007/s12517-011-0351-2

[26] Zhang J, Huang WW, Letolle R, Jusserand C. Major element chemistry of the Huanghe (Yellow River), China—Weathering processes and chemical fluxes. Journal of Hydrology. 1995;**168**:173-203

[27] Drever JI. The Geochemistry of Natural Waters. 3rd ed. New Jersey: Prentice Hall; 1997. p. 436

[28] Lastennet R, Mudry J. Role of karstification and rainfall in the behavior of a heterogeneous karst system. Environmental Geology. 1997;**32**(2):114-123

[29] Kuhta M, Brkić Ž, Stroj A. Hydrodynamic characteristics of Mt. Biokovo foothill springs in Croatia. Geologia Croatica. 2012;**65**(1):41-52

[30] Kresic N, Bonacci. Spring discharge hydrograph. In: Groundwater Hydrology of Springs: Engineering, Theory, Management, and Sustainability. Elsevier; 2010. pp. 129-163. Ch. 4

[31] Malík P, Vojtková S. Use of recession-curve analysis for estimation of karstification degree and its application in assessing overflow/ underflow conditions in closely spaced karstic springs. Environmental Earth Sciences. 2012;**65**(8):2245-2257

[32] Castany G. Prospection et Exploitation des Eaux Souterraines. Paris: DUNOT; 1968

[33] Mijatovic B. A Method of Studying the Hydrodynamic Regime of Karst Aquifers by Analysis of the Discharge Curve and Level Fluctuation During Recession. Beograd: Institute for Geological and Geophysical Research; 1970

[34] Plan L, Kuschnig G, Stadler H. Kläffer Spring—The major spring of

the Vienna water supply (Austria).
In: Kresic N, Stevanovic Z, editors.
Groundwater Hydrology of Springs.
Butterworth-Heinemann: Elsevier;
2010. pp. 592-411. DOI: 10.1016/
C2009-0-19145-6

[35] Kardan-Moghadam H, Javadi
S, Kavosi-Hydari A, Mirarabi A.
Evaluation of Dorfak Karst Aquifer
intrinsic vulnerability with EPIK
method in the North of Iran. In:
First International Conference on
Water Environment and Sustainable
Development; 27-29 September 2016;
Ardabil, Iran. 2016. in Persian

Fluoride Levels in the Groundwater and Prevalence of Dental Fluorosis in the Municipality of Santana, in Region Karstic of West Bahia, Brazil

Manuel Vitor Portugal Gonçalves, Rodrigo Alves Santos,
Carlos Alberto Machado Coutinho
and Manoel Jerônimo Moreira Cruz

Abstract

This chapter was aimed to investigate the relationship between the consumption of water of Bambuí Aquifer with natural fluoride levels and the prevalence of dental fluorosis in the municipality of Santana, Bahia, Brazil. Hydrochemistry and cluster analysis indicated that there were two groups differentiable in relation to TDS, pH, F-, rNa^+/rCa^{2+}, and saturation indexes of minerals. The fluoride concentration varied from 0.05 to 9.16 mg.L^{-1} in the samples and the prevalence of dental fluorosis was 53%, 17% moderate, or severe, which was associated of the consumption of groundwater. The toxic levels of fluoride reached 47% of the samples, where the risk of skeletal fluorosis (20%) and incapacitating fluorosis (20%) was estimated. The water supply service should include the monitoring of fluoride in groundwater, the implementation of sanitary and environmental health surveillance of endemic fluorosis, and the continuing training of professionals for health in this municipality.

Keywords: medical geology, fluoride-health, drinking water, bambuí aquifer

1. Introduction

The care with water quality should be universal because human dignity and health public depends on the access to drinking water. The quality of natural waters can naturally be modified by the enrichment of dissolved ions, such as fluoride, which may reach adverse amounts to human health [1]. The fluoride-health relationship has a worldwide relevance because the main route of exposure is the ingestion of water with toxic levels of fluorine [2].

Dental fluorosis is the first sign of chronic fluoride poisoning; it is related to discoloration and the appearance of blemishes on the enamel of homologous teeth [3]. It is a chronic intoxication from exposure to toxic doses of fluoride, a hypomineralization of the enamel, which has esthetic and morphofunctional repercussions [4].

The severity of dental fluorosis is dependent on both the dose and time of exposure to fluoride levels [5]. It refers to the chronic intake of toxic doses of fluoride during enamel formation, whose critical period extends until 6 years of age, although it depends on individual differences in amelogenesis [6].

The continuous consumption of water with optimal fluoride content represents a protection factor against caries or dental fluorosis, whereas the excess represents a risk factor for fluorosis and the deficiency is a risk factor for dental caries [5]. The changes in the constitution of the enamel, which cause staining or loss of its structure, can provide esthetic, functional, and psychological problems [7]. Due to the epidemiological relevance of fluorosis, consumption with toxic levels of fluoride, the World Health Organization [8] recommended a maximum limit of 1.5 mg.L^{-1} of fluoride in drinking water. Other factors may aggravate the distribution and severity of fluorosis, such as metabolic disorders [9], nutritional status that accompanies the socioeconomic context [10], and temperature [11].

Fluorine, very electronegative, reacts easily with cations, for example, calcium ion. This behavior explains why most of the fluorine in the matrix of bones and teeth is associated with fluorapatite crystals, $Ca_5 (PO_4)_3 F$, combined as a solid solution with hydroxyapatite, $Ca_5 (PO_4)_3 OH$ [12]. The dental enamel is composed of a prismatic mineral, which in the absence of fluoride (F^-) is known as hydroxyapatite $[Ca_{10} (PO_4)_6 (OH)_2]$. Fluoride in the diet during odontogenesis favors the conversion of part of the hydroxyapatite into fluorapatite $[Ca_{10} (PO_4)_6 F_2]$ by replacing the OH^- group. Fluorapatite, less soluble in oral acids than hydroxyapatite, gives teeth a protection against the erosional action of caries.

Chronic ingestion of natural waters containing fluoride levels greater than 3.0 mg.L^{-1} correlates with the prevalence of dental fluorosis or skeletal fluorosis and represents a risk of deformities in the hips and incapacitating fluorosis [13, 14]. In this way, the importance of the epidemiological and environmental health surveillance of the contents of fluoride in the waters of human consumption as a preventive measure of endemic fluorosis is evidenced.

Fluoride occurs in natural waters mainly in the form of fluoride (F^-), who's levels vary from residual amounts up to 2800 mg.L^{-1} [15]. In the rocks, fluorine is release mainly from the fluorite mineral phase, occurring also in amphiboles, micas, fluorapatite, topaz, cryolite, certain clays, and villiaumite [16]. The chemical weathering of rocks bearing fluorine minerals releases this halogen to the atmosphere, biota, soils, dust, and water [17]. The weathering of the fluorine-containing minerals promotes the leaching of this halogen, which has high mobility, through the water-rock interaction [18]. Fluoride levels are high in groundwater where the source minerals abound in the geological substrate [19].

In this context, the application of hydrochemical methods and techniques can help the management of water quality. The knowledge about the origin and behavior of major ions (Ca^{2+}, Mg^{2+}, Na^+, K^+, CO_3^{2-}, HCO_3^-, Cl^-, SO_4^{2-}) in groundwater allows the elucidation of the hydrogeochemical composition [20]. This varies depending on the solubility of the chemical elements from the dissolution of the mineral constituent of the rocks that host the aquifer.

Fluorite deposits and sulfide levels have a widespread occurrence in the carbonate rocks of the Bambuí Group, in the western Bahia, Brazil [21]. These carbonate rocks shelter the Bambuí Aquifer, whose waters complement the public supply of several municipalities, including Santana (**Figure 1**). In turn, information on hydrochemistry could guide water and health planners.

The chemical composition of the waters of the Bambuí Aquifer varies as a function of the mineral composition of the rocks of the Bambuí Group [23]. The hydrochemical of karstic environments varies according to the climate, water circulation, residence time, and mineralogy of the rocks of the aquifer [24]. In this perspective,
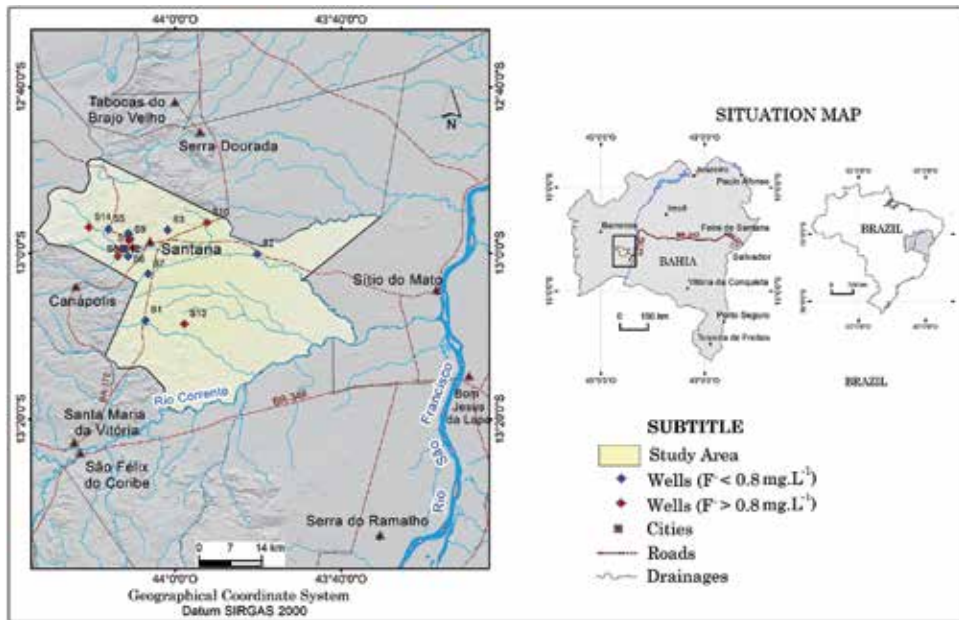
Figure 1.
Map of location of the municipality of Santana, based on the data of IBGE/SEI (2008) [22].

it is expected that the integration of geochemical and statistical techniques helps elucidate the basic aspects of water-rock interaction, groundwater flow, and hydro-chemical evolution [25].

In the municipality of Santana, in the karst province of western Bahia (**Figure 1**), the prevalence of dental fluorosis could relate to the consumption of groundwater with toxic levels of fluoride, which complemented the public supply [26]. This research aimed to investigate the relationship between the consumption of water of Bambuí Aquifer with natural fluoride levels and the prevalence of dental fluorosis in the municipality of Santana, Bahia, Brazil.

2. Area of study, climate, and hydrogeology

The Santana municipality is situated in the western Bahia (**Figure 1**) and has an area of 1909,352 km^2, gross domestic product (GDP) of R$130,550, and a population of about 24,750 inhabitants [27]. In 2010, this municipality had a Human Development Index of the Municipality (HDI-M) of 0.608 [28] ranking 125th in relation to the other 417 municipalities of Bahia. This municipality occupies 133rd position in relation to income (economic aspect) and 151rd position in relation education (socio-cultural aspect), which represent the fundamental conditions to dealing with health as an individual responsibility. The individual and public power revealed a municipal profile with inequalities of conditions of human development.

The region presents a subhumid to semiarid climate, with average temperature of 24.3°C and precipitation between 800 and 1000 mm/year (1961–1990), concentrated between November to April and the dry season from May to September (IMNET, 2016) [29]. It is important to note that from 2011 to 2012, the precipitations fell from 498 to 821 mm/year (**Figure 2**).

The geology includes pelitic, calcareous, and dolomitic rocks of Neoproterozoic age belonging to the Bambuí Group [30]. In addition, there are pelitic rocks (silt-stones, shales, argillites, and slates) with subordinate limestones. This sedimentary

Figure 2.
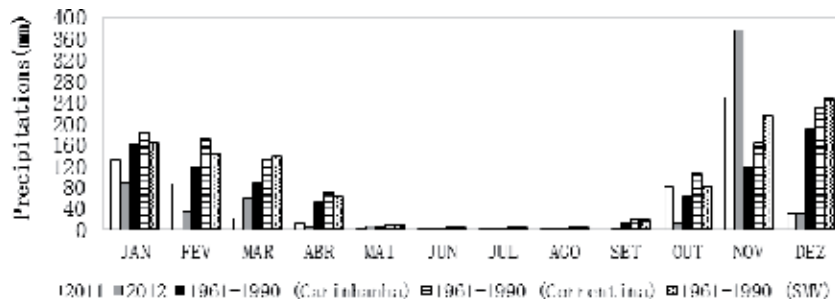*Distribution of monthly precipitation averages in the stations Carinhanha, Correntina, and Santa Maria da Vitória (SM) (2011–2012 and 1961–1990), based on the data available by INMET [29].*

set was deposit in the gneiss-migmatite complex Arqueano. The Urucuia Group sandstones and alluvial and detrital coverings were deposit on the Bambuí Aquifer. The wells drilled in the municipality of Santana cross the rocks of the Bambuí Group, which hosts the Bambuí Aquifer. The Urucuia Aquifer contributes to the recharge of the Bambuí Aquifer, in consortium with the infiltration of rains [31]. The main direction of the displacement of the groundwater follows from west to east, in the direction of the San Francisco River.

3. Materials and methods

3.1 Hydrogeochemical and (geo)statistical

Epidemiological data on dental fluorosis in the municipality of Santana have been compiled from Coutinho's master dissertation [32]. The hydrochemical data have been obtained from of the thesis of Gonçalves [33] and the study of Coutinho [32]. Data collection included the methodological procedures described below.

Water samples were collected from 41 tubular wells in the years 2011 (rainy season) and 2012 and 2014 (dry) in the municipality of Santana. In the 2014 sample campaign, only the fluoride levels have been measured in the locality where epidemiological information have been obtained. The hydrogenation potential (pH) and total dissolved solids (STD) were determined in situ, using a multiparameter probe (*Horiba U-50*), and aliquots have been taken for laboratory analyses. The aliquots were stored in polyethylene (0.5 and 1 L), according to APHA [34].

The cation (Na^+, K^+, Ca^{2+}, and Mg^{2+}) reading was performed by inductively coupled plasma optical emission spectrometry (ICP OES *700 Agilent Technologies*), performed in duplicate, counting with 20% in triplicates to improve the analytical quality. Anion analyzes were performed by titrimetric (HCO_3^-, Cl^-), UV-Vis spectrophotometric (*Varian*) ($N–NO_3^-$, SO_4^{-2}), and colorimetric (SPANSD) (F^-) methods using a fluorometer (LS 4000), in the Plasma Laboratory, Institute of Geosciences, of the Federal University of Bahia.

The use of the PHREEQC software allowed saturation index (SI) calculations [35]. These were grouped as subsaturated (IS <−0.5), in chemical equilibrium (SI: −0.5 and 0.5), and supersaturated (SI > −0.5). Merkel and Planer-Friedrich [36] recommend the admission of SI values of the interval 0 ± 0.5, due to the uncertainties inherent in the calculation of this or the equilibrium constant of the dissolved mineral and of the chemical analyses.

The statistic includes a descriptive and using test of normality (Shapiro–Wilk), with significance of 95%, and cluster analysis, which uses the similarity

between individuals to classify the samples hierarchically into groups [37]. The Euclidean distance was chosen as a measure of similarity between the sample points, along with the Ward method, for the connection between the groups. The geostatistical was estimated by ordinary kriging by the application of ArcGIS 9.0 program. In addition, it included selected data from the well data from the Groundwater Water Information System (SIAGAS) of the Geological Survey of Brazil (CPRM).

3.2 Health research and statistical analysis

The prevalence and severity of dental fluorosis were obtained by cross-sectional study, whose research had a descriptive design, starting from an epidemiological survey that included 159 schoolchildren, of both genders, with age of 12, of the municipal schools of the Santana. Children 12 years old are chosen because they have the majority of permanent teeth erupted [38]. The schoolchildren were examined in 2014 by dental surgeon Dr. Carlos Alberto M. Coutinho, who registered the study by the research ethics committee through the website of Brazil Platform (Ministry of Health). All the steps for clinical analysis to assess the prevalence and severity of fluorosis were previously informed those involved in the study by free informed term of consent (FITC).

The schoolchildren were examined in public or private schools, according to the criteria of inclusion of sample selection: (i) born and resided in the municipality of Santana until the date of the tests according to the Department of Education; (ii) the presence of the person responsible at the time of examination and interview; and (iii) the sample included only the children whose parents signed the IC, according to Resolution 196/96 of the National Health Council [39].

Oral examinations in schools followed recommendations from the Dean index, advocated by the WHO [40] (**Table 1**). The oral examinations were performed by dentist previously calibrate and trained, using images available through the national oral health research of SB Brazil 2010 [42], in the school environment with natural light, aided by spatula and wooden gauze. In the calibration, the agreement of the results was evaluated by the Kappa statistic [43], until a suitable inter-examiner agreement was reached (Kappa = 0.85). A sample of 118 individuals was estimated by simple finite random sample, without repetitions, with proportion estimator (prevalence

Rating	Value	Diagnostic criteria
Normal	0	Enamel presents usual translucency with semi-vitric structure. The surface is smooth and polished and has bright cream color
Questionable	1	Enamel reveals little difference from the normal translucency, with occasional white spots. Use this code when the "normal" classification is not justified
Very light	2	Areas are whitish and opaque; small spots scattered irregularly by the tooth but involving no more than 25% of the surface. It includes clear opacities with 1 mm to 2 mm at the tip of the cusps of molars (snowy peaks)
Light	3	The opacity is more extensive but involves no more than 50% of the surface
Moderate	4	All tooth enamel is affected and the areas subject to attrition show up worn. There may be brown spots or yellowish often disfiguring
Severe	5	Hypoplasia is widespread and the very shape of the tooth may be affected. The most obvious sign is the presence of depressions in the enamel, which seems eroded. Generalized brown spots

Table 1.
Criteria and values for fluorotic teeth classification according to Dean index [41], adapted from SB Brazil Project [42].

or incidence) and a 95% confidence level and prevalence of 0.815, extracted from Velásquez et al. [44] at the age of 12. The sample was obtained from a population of ±423 adolescents at 12 years of age, according to information of IBGE [27].

4. Results and discussion

4.1 Hydrochemistry, source the fluoride, and cluster analysis

The analysis of **Figure 3** revealed that calcium bicarbonated (40%), mixed calcium (20%), sodium bicarbonated (27%), and sodium chlorinated (13%) hydrochemical facies were representative. The uncertainty of ionic balance was at most 20%, based on practical error [46]. For the calcium bicarbonated or calcium mixed facies, the content of the ions was in decreasing order: $rCa^{2+} > rNa^+ > rMg^{2+} > rK^+$ and $rCO_3^{2-} - rHCO_3^- > rCl^- > rSO_4^{2-} > rF^- > rN-NO_3^-$. While in the sodium facies, the cation contents followed in the order $rNa^+ > rCa^{2+} > rMg^{2+} > rK^+$. There is a clear relationship between the sodium hydrochemical facies and the fluoride levels above the optimum limit (0.8 mg.L^{-1}) of the groundwater sample.

Table 2 presents the statistical summary of the hydrochemical variables, whose calcium levels exceeded the limit recommended by the WHO [47], for 40% of the wells. These calcium contents have been derived from the interaction between the water and the rocks of the Bambuí Group. The hydrochemistry of karstic aquifers reflects the dissolution of the minerals calcite and dolomite, residence time, and water circulation in the aquifer [48].

The cluster analysis was used to classify the samples into groups (G1 and G2), with the aid of visual observation of the dendrogram, inserting the hydrochemical facies (**Figure 4**). The cut line was marked on the dendrogram at a distance of 80, whose samples that showed lower bond distance belonged to the same category. In the samples, the increase of mineralization accompanies the evolution of bicarbonate calcium facies to the bicarbonate or sodium chlorate facies.
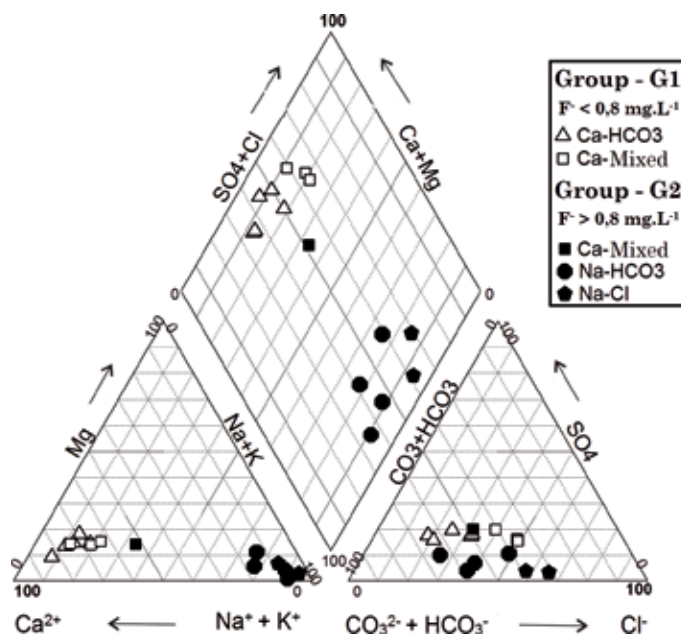

Figure 3.
Diagram of Piper [45] for groundwater classification and indication of hydrochemical groups and fluoride contents.

Parameters	VMP*	Min.	Max.	Mean	Median	EP	CV (%)	p-valor**
pH	6.5–9.5	7.26	8.93	7.92	7.65	0.15	7.32	0.04**
STD (mg.L^{-1})	1000.00	440.00	1110.00	625.00	597.00	43.73	27.09	0.001**
Na$^+$ (mg.L^{-1})	200.00	18.80	238.30	58.05	35.96	19.92	90.71	0.001**
K$^+$ (mg.L^{-1})	—	1.30	5.21	2.69	2.70	0.27	39.20	0.15*
Ca^{2+} (mg.L^{-1})	75.00	5.45	197.27	77.65	93.21	15.23	75.96	0.13*
Mg^{2+} (mg.L^{-1})	50.00	1.22	16.86	10.74	13.50	1.33	47.82	0.01**
Cl$^-$ (mg.L^{-1})	250.00	40.39	300.50	113.74	95.69	16.46	56.05	0.01**
HCO$_3^-$ (mg.L^{-1})	—	178.00	366.00	234.92	232.50	11.60	19.13	0.01**
SO$_4^{2-}$ (mg.L^{-1})	250.00	10.57	85.53	50.09	53.74	6.06	46.84	0.44*
N-NO3$^-$ (mg.L^{-1})	10.00	0.04	5.40	1.05	0.56	0.36	133.71	0.01**

Non-Gaussian distribution.
**Gaussian distribution.

Table 2.
Statistical summary of the hydrochemical and isotopic variables.

Grupo 1a: Ca-HCO3 (1-5 e 9) e Ca-HCO3-Cl (6-8)
Grupo 2a: Na-HCO3 (10-11 e 13-14) e Na-Cl (12 e 15)
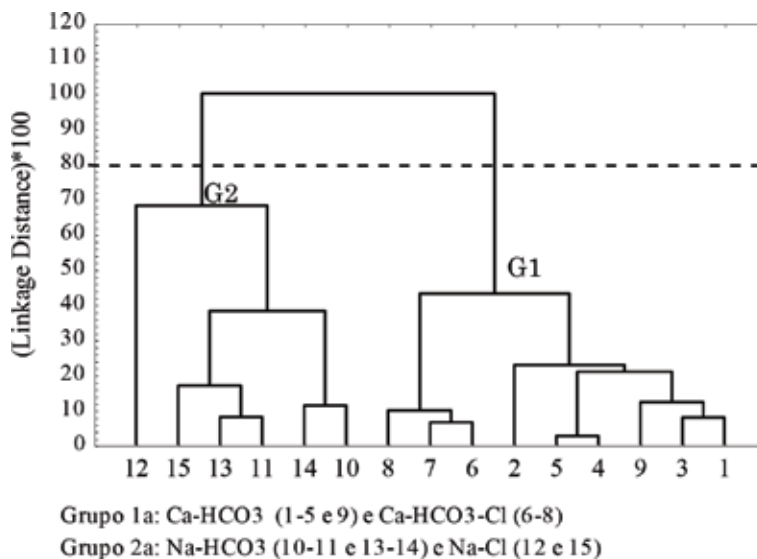
Figure 4.
Dendrogram and hydrochemical classification of the groundwater of Santana.

The formed hydrochemical groups showed differences in TDS values, pH, and calcite and dolomite saturation indexes (**Table 3**). This trend was also indicated by the geochemical reasons rNa$^+$/rCa^{2+} and rHCO$_3^-$/rCa^{2+}, which modeled that the base-exchange processes and the chemical weathering of pellets could add lithogenic Na$^+$ and rHCO$_3^-$ to the groundwater and remove Ca^{2+} from them.

The values of the rHCO$_3^-$/rCa^{2+} ratio were lower than 1.5 for the G1 group, reflecting the importance of the water-rock interaction. The values of this ratio less than 1.5 result from the dissolution of the calcite and solutions subsaturated in calcite [49]. The values of the rHCO$_3^-$/rCa^{2+} ratio were greater than 1.5 in the G2 group, corroborating the relevance of the water-rock interaction, whose chemical

Well	Facies	$SI_{Calcite}$	$SI_{Dolomite}$	SI_{Gypsum}	$SI_{Fluorite}$	$[rCl^- - (rNa^+ + rK^+)]/rCl^-$	rNa^+/rCa^{2+}	$rCl^-/(rCl^- + HCO_3^-)$
Group 1 (G1): the hydrochemical facies presented fluorine contents lower than 0.8 mg.L⁻¹								
P1	Ca-HCO₃	0.71	0.96	−1.75	−1.5	0.39	0.13	0.39
P3	Ca-HCO₃	0.39	0.25	−1.7	−1.79	0.39	0.26	0.39
P9	Ca-HCO₃	0.19	−0.06	−2.02	−0.91	0.39	0.63	0.39
P4	Ca-HCO₃	0.67	0.89	−1.83	−2.23	0.22	0.18	0.22
P5	Ca-HCO₃	0.91	1.4	−1.6	−1.92	0.24	0.17	0.24
P2	Ca-HCO₃	0.57	0.37	−1.44	−1.82	0.31	0.09	0.31
P6	Ca-HCO₃-Cl	1.01	1.47	−1.79	−1.46	0.49	0.15	0.49
P7	Ca-HCO₃-Cl	0.43	0.35	−1.65	−1.42	0.57	0.26	0.57
P8	Ca-HCO₃-Cl	0.33	0.1	−1.9	−2.06	0.58	0.32	0.58
Mean		0.35	0.58	−1.74	−1.68	0.40	0.24	0.40
Median		0.40	0.57	−1.75	−1.79	0.39	0.18	0.39
Group 2 (G2): the hydrochemical facies presented fluorine content higher than 0.8 mg.L⁻¹								
P10	Na-HCO₃	0.73	1.54	−3.48	−0.5	0.54	5.53	0.54
P11	Na-HCO₃	0.15	0.19	−2.83	−0.91	0.42	11.96	0.42
P13	Na-HCO₃	0.3	−0.16	−2.72	−0.26	0.29	11.27	0.29
P14	Na-HCO₃	0.37	0.3	−3.06	−0.46	0.39	4.59	0.39
P12	Na-Cl	1.02	2.12	−2.94	−0.06	0.68	10.04	0.68
P15	Na-Cl	0.07	0.18	−3.48	−0.75	0.60	28.36	0.60
Mean		0.54	0.44	−3.09	−0.49	0.49	11.96	0.49
Median		0.60	0.34	−3.00	−0.48	0.48	10.66	0.48

Table 3.
Values of the saturation indexes (SI) and the geochemical ratios of the samples.

weathering of the minerals of the pelitic lithophytes would supply bicarbonate and sodium ions to the solution.

The analysis of **Table 3** allows the proposition that part of the samples of G1 group are located under the influence areas of the meteoric recharge zones of the aquifer, presenting a shorter transit time. The higher ionic contents and values of the geochemical ratios rNa^+/rCa^{2+} and $rHCO_3^-/rCa^{2+}$ related to the G2 group were verified, which were attributed to the influence of the water-rock interaction processes and the action of the base-exchange reactions. The hydrogeochemistry of karstic aquifers reflects the dissolution of calcite and dolomite minerals, the transit time, and the water circulation in the aquifer [50].

In the G2 group, related to the fluorine content higher than 0.8 mg.L⁻¹, most alkaline and sodium geochemical conditions favor the addition of alkalinity and the dissolution of fluorite, a hypothesis corroborated by the saturation conditions of fluorite, calcite, and dolomite revealed in **Figure 5**. These hydrochemical conditions explain the relationship between sodium waters and fluoride levels above 0.8 mg. L⁻¹ as was as shown in Piper's diagram in **Figure 3**.

In the natural waters, the saturation of the solution in calcite controls the solubility and the precipitation of the fluorite [51]. In the karstic province of western Bahia, Brazil, the fluorite is the main source of fluorine for groundwater. Gonçalves et al. [33] have shown that the Handa [41] model can be adapted for geochemical investigation of the Bambuí Aquifer. This model elucidates the relationship between F^-, Ca^{2+}, and HCO_3^- ions relatively constant for pH conditions.
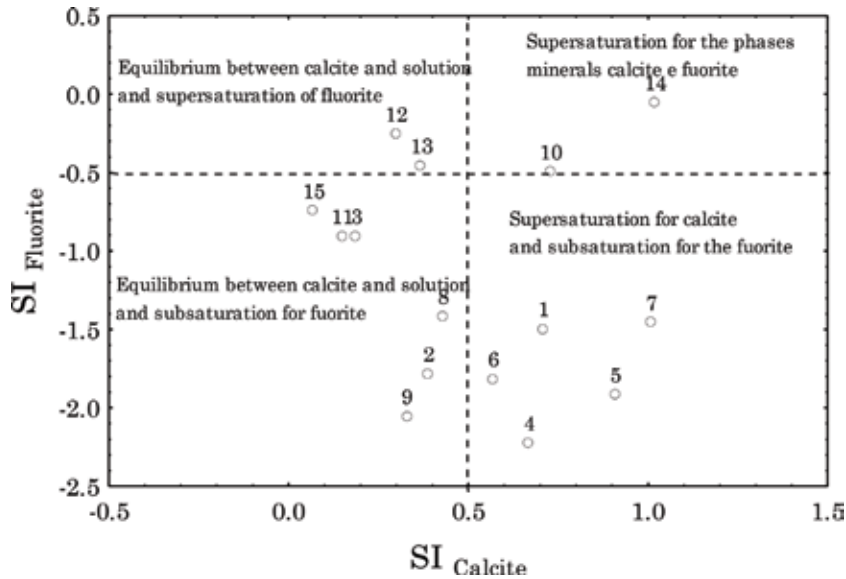
Figure 5.
Dispersion of saturation indices (SI) of calcite and fluorite minerals.

Handa [52] proposed a model for the hydrogeochemistry of fluorine, synthesized in Eq. (1), which covers the solubility constant (**K**) and ionic activity (α). It predicts that the precipitation of the calcite in consortium with the base-exchange reactions adds Na^+ and HCO_3^- to the solution, a condition that favors the solubility of the fluorite. This model has been applied to the hydrogeochemical investigation of crystalline aquifers [52]:

$$KCaF_2 \leftrightarrow CaCO_3 = \left[\alpha\left(HCO_3^-\right)\right] / \left[\alpha\left(H^+\right).\left(F^-\right)_2\right] \tag{1}$$
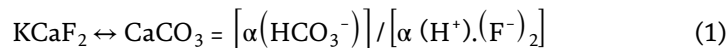
Costa [53] proposed that the plagioclase mineral phases would provide lithogenic Na^+ to the waters of the Bambuí Aquifer in the north of Minas Gerais. The interaction of the waters with the clay minerals (M), due to the weathering of impure carbonates and pelitos, removes Ca^{2+} and provides Na^+ to the solution by the base-exchange reactions (Eqs. (2)–(5)). The ionic activity of sodium interferes with the alkalinity, saturation, and calcification conditions of the precipitation and the solubility of the fluorite [15]:

$$(M) \ SiO_3 + CO_2 + H_2O \leftrightarrow M^{2+} + SiO_2 + 2HCO_3^- \tag{2}$$

$$Na\,(M)\,(S) + Ca^{+2} \leftrightarrow Ca\,(M)\,(S) + 2Na^+ \tag{3}$$

$$CaF_2 + Na2\,CO_3 \leftrightarrow CaCO_3 + 2F^- + 2Na^+ \tag{4}$$

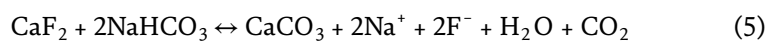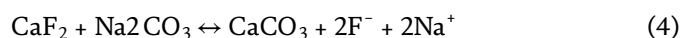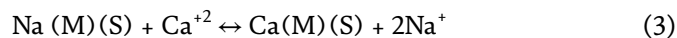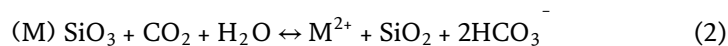$$CaF_2 + 2NaHCO_3 \leftrightarrow CaCO_3 + 2Na^+ + 2F^- + H_2O + CO_2 \tag{5}$$

Figure 6 shows the Gibbs diagram and indicates basic processes for hydrogeochemical evolution. The samples reported the influence of the water-rock interaction. The increase in the ratio $rCl^-/(rCl^- + rHCO_3^-)$ accompanies the hydrochemical composition

Figure 6.
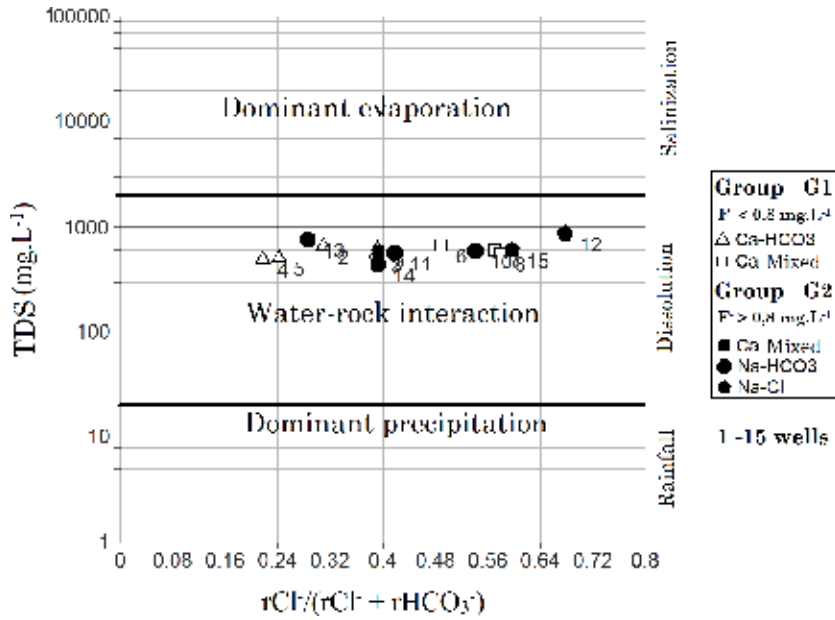*Diagram of Gibbs [54] indicating the controls the hydrochemistry.*

of the local flow to the regional (Ca–HCO_3 → Ca–Cl–HCO_3 → Na–HCO_3 → Na–Cl). The transition from calcium to sodium facies also reflects the action of base exchange and weathering of the pellets. These processes add lithogenic sodium and bicarbonate to groundwater while removing calcium.

Miranda et al. [55] and Conceição Filho et al. [56] studied the fluorite in the carbonates of the Bambuí Group, in Bahia (BR). Conceição Filho et al. [57] conducted a statistical analysis of the physical-chemical data of current sediments of the Bambuí Geochemical Projects (PGB) [58] and São Francisco Basin (PBSF) [56]. Fluoride contents were 25–6500 mg.L^{-1}, with geometric means of 235.78 (PGB) and 303.85 mg.L^{-1} (PBSF), whose pH values were predominantly alkaline. The anomalous content ranged from 900 to 1600 mg.L^{-1} (PGB). In these sediments, the pH values were predominantly alkaline.

Costa [54] analyzed fluoride in rocks of the Bambuí Group in northern Minas Gerais (BR). The mean values of fluoride in pelitic rocks ranged from 120 to 620 mg.L^{-1} and in carbonate rocks ranged from 320 to 508 mg.L^{-1}. The fluoride values of the rocks of the Bambuí Group were higher than the average level of this element in carbonate rocks (300 mg.L^{-1}) [59]. The rocks of the Bambuí Group may represent relevant geogenic sources of fluorine for groundwater.

4.2 Fluoride levels, epidemiology, and medical geology

The optimum content of fluoride (C) in solution for public water supply in the region was obtained according to Galagan and Vermilion [60] (Eqs. (6) and (7)), as a function of the regional average air temperature (T). This optimum limit was recommended by Ordinances n°. 2,914/11 [61] and WHO. [47]. From this premise, fluoride content of 0.78 mg.L^{-1} as optimum limit for water of human consumption of Santana and of the neighboring municipalities can be proposed:

$$€(T) = 10.3 + 0.725T \tag{6}$$

$$C = 22.2/€ \tag{7}$$

Table 4 presented a statistical summary for the fluoride values obtained in the current research in the municipality of Santana and the SIAGAS data. The fluoride contents varied between 0.05 and 9.16 mg.L^{-1}, which could be compared to the levels of the groundwater of the Canápolis, Serra Dourada, and Sítio do Mato. Gonçalves et al. [62] found fluorine levels of 0.11–2.15 mg.L^{-1} in the groundwater of the Bambuí Aquifer in municipality of Serra do Ramalho, Bahia.

Velásquez et al. [44] analyzed the contents of fluorine in waters of 78 wells drilled in the Bambuí Aquifer, in the municipality of São Francisco, northern Minas Gerais, Brazil. Fluoride contents ranged from 0 to 3.9 mg.L^{-1}, with 13 wells (17%) exceeding the local optimum limit (0.8 mg.L^{-1}). The municipalities of Santana (Bahia) and São Francisco (Minas Gerais) have similar geological, climatic, and precipitation index. The municipalities of Santana and São Francisco represent endemic areas of dental fluorosis, which require the identification of sources and understanding of hydrogeochemistry.

The samples were classified according to fluoride levels and risk for oral health and with the SIAGAS well data for a regional perspective (**Figure 7**). The groundwater classified in the protection factor category may assist in the promotion of oral health, which included only 20% of the samples in Santana. The municipalities of Canápolis, Santa Maria da Vitória, and Serra Dourada have a higher percentage of groundwater samples with optimal natural fluorine content, which may represent a viable alternative to public water supply.

The risk category of dental fluorosis comprised 47% of the groundwater samples of the municipality of Santana, being equable only to the percentages found in the municipalities of Serra Dourada and Sítio do Mato (**Figure 7**). The chronic exposure of children up to 6 years of age at high fluoride levels during tooth germ formation has epidemiological relevance and health surveillance [63].

A portion of the samples (40%) had fluoride contents higher than 3.0 mg.L^{-1}, whose prolonged consumption represents a risk of bone fluorosis or deformities in the hips and incapacitating fluorosis (**Table 5**). This risk also includes the municipalities of Canápolis, Serra Dourada, and Sítio do Mato. The chronic ingestion of natural waters containing fluoride levels greater than 3 mg.L^{-1} correlates with the prevalence of dental fluorosis or skeletal fluorosis [14].

The fluoride levels in the groundwater of the municipality of Santana presented epidemiological relevance. Rouquayrol [64] defined epidemiology as the science that studies the health-disease process, population distribution, and determinants of diseases and damage to health and events associated with public health, proposing specific measures to prevent, control, or eradicate diseases and provide indicators that support the planning, administration, and evaluation of health actions. This observational science is based on the concept of risk (incidence and prevalence), defined as the probability of members of a given population developing a specific disease or

Municipality	Size (n)	Minimum	Maximum	Mean	Median	CV (%)
Santana (current)	41	0.05	9.16	1.41	0.54	135
Canápolis (SIAGAS)	21	0.15	7.0	1.02	0.66	141
Santa Maria da Vitória (SIAGAS)	39	0.02	3.5	0.73	0.53	89
Serra do Dourada (SIAGAS)	28	0.17	5.20	1.43	0.95	87
Serra do Ramalho (SIAGAS)	08	0.11	1.95	0.52	0.13	127
Sítio do Mato (SIAGAS)	10	0.16	6.12	2.39	1.46	96

Table 4.
Statistical summary of fluorine levels in the groundwater of Santana (current) and neighboring municipalities (SIAGAS).
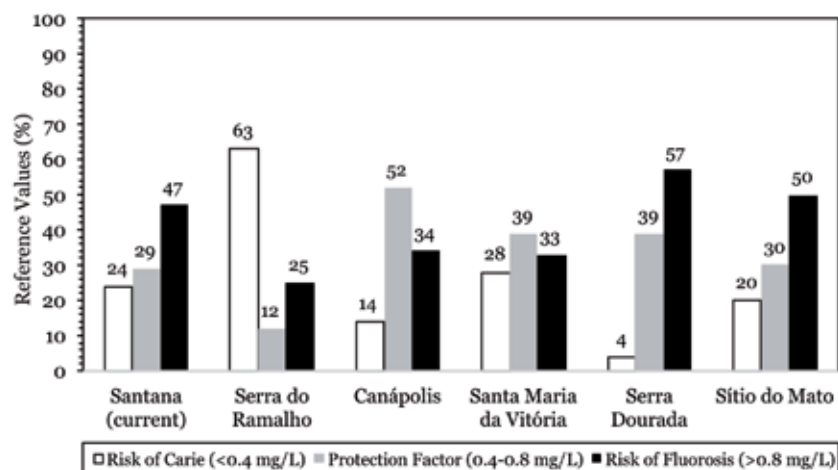
Figure 7.
Classification of samples according to fluoride values and health risk.

health-related event at a time interval. The prevalence of fluorosis is an epidemiological indicator that represents the number of cumulative cases over a period (new and old), and the incidence quantifies the number of people who lost health over a period [65].

Table 6 presents the descriptive analysis of the fluorosis condition in 159 12-year-old schoolchildren (87% resided in rural); 53% had dental fluorosis (Dean index) and 17% in moderate to severe forms. It obtained 60% of the examined in the female gender and was observed (interviews or clinical examination) that the male students were less likely to be examined, which configured a bias to obtain the sample. The prevalence and severity of dental fluorosis in this study are in disagreement with the national oral health survey of the SB Brazil Project [42]. This national survey found a prevalence of dental fluorosis at 12 years of age of 17% (Dean index), with 15% very light or light and 1.5% moderate or severe.

Clinical examination revealed that moderate to severe forms of dental fluorosis were the most relevant, with clinical aspects presented in **Figure 8D**. The clinical aspect of the dental fluorosis includes emergence opaque spots on the enamel, teeth counterparts, to yellowish or brown areas in cases of severe changes [38]. In the most severe forms, the detachment of the enamel portions can occur, after eruption. This leads to the appearance of dental surface depressions observed in

Meenakshi and Maheshwari [12]	WHO [8]	Risk to health	%				
			Santana (current)	A*	B*	C*	D*
<0.40	<0.50	Caries risk	24	14	28	3.5	20
0.4–0.8	0.5–1.5	Local optimal limit	29	52	39	39	30
0.8–3.0	1.5–3.0	Risk of dental fluorosis	10	29	31	47	0
3.0–4.0	>3.0	Bone and joint Problems	17	0	2	3.5	10
4.0–6.0 (or >6.0)	—	Deformities in the knees and hips and disabling fluorosis	20	5	0	7	40

Hydrochemical data of the Bambuí Aquifer, Bahia (BR), from SIAGAS wells: (A) Canápolis; (B) Santa Maria da Vitória; (C) Serra Dourada; and (D) Sítio do Mato.

Table 5.
Fluoride (F^-) $(mg.L^{-1})$ levels in drinking water and risks related to human health.

Fluorosis	Male		Female		Total	
	N	%	N	%	N	%
Absent (0)	35	22	38	24	79	46
Contestable (1)	4	2.5	5	3	9	5.5
Very light (2)	11	7	17	11	28	18
Light (3)	5	3	17	11	22	14
Moderate (4)	5	3	10	6	15	9
Severe (5)	4	2.5	8	5	12	7.5
Total	64	40	95	60	159	100

Table 6.
Absolute and relative frequency of the gender and categories indicated by the Dean index in a sample of 12-year-old schoolchildren from the municipality of Santana.

severe forms (**Figure 8D**). The several degrees of fluorosis can be related to whitish, yellow, and brownish spots (severe) [4]. Severe fluorosis often produces painful hypersensitivity to the teeth and esthetic disharmony, compromising the individual's quality of life [26], [66–67].

Figure 9 showed a correlation between the prevalence and severity of dental fluorosis in schoolchildren at 12 years of age examined and the consumption of groundwater with toxic levels of fluoride from the Bambuí Aquifer, in the municipality of Santana. The proportions of the prevalence and severity of dental fluorosis

(A- Normal)   (B - Light)

(C - Moderate)   (D - Severe)
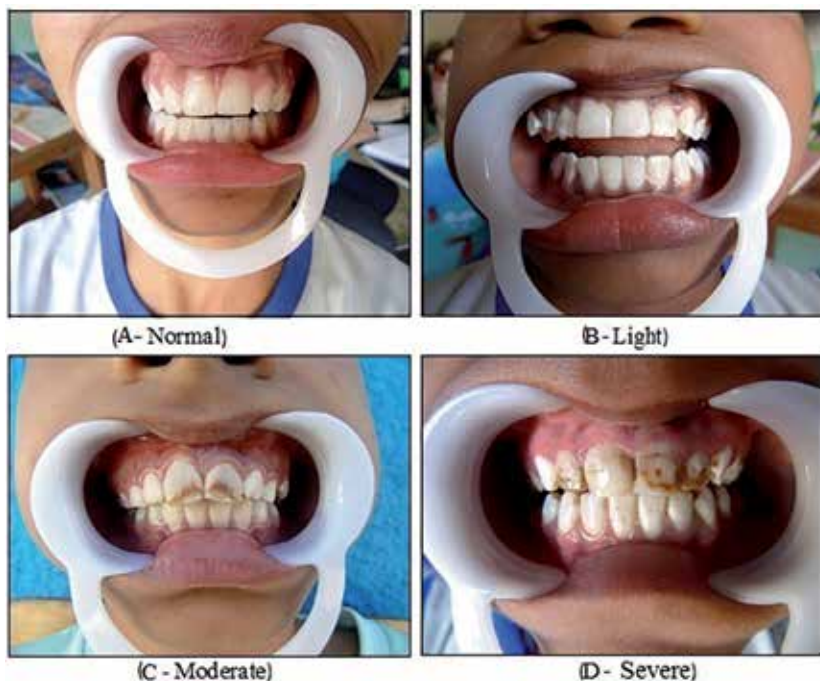
Figure 8.
*Clinical aspects of dental fluorosis, obtained in the municipality of Santana by Coutinho, 2014, according to Dean's classification [44]. **A**: Enamel presents usual translucency with semi-vitric structure, with surface is smooth, polished and has bright cream color. **B**: The opacity is more extensive but involves no more than 50% of the surface. **C**: All tooth enamel is affected and the areas subject to attrition show up worn, with may be associate the brown spots or yellowish often disfiguring. **D**: Hypoplasia and brown spots are widespread, the shape of the tooth may be affected and the most obvious sign is the presence of depressions in the enamel.*

Figure 9.
Prevalence and severity of dental fluorosis versus fluoride contents.

increase significantly from fluoride values in the range of 1.2–1.6 mg.L^{-1}. The propagation of severe fluorosis, grade 5 (**Figure 10D**), increases sharply from the range of fluoride values greater than 2 mg.L^{-1} (>2).
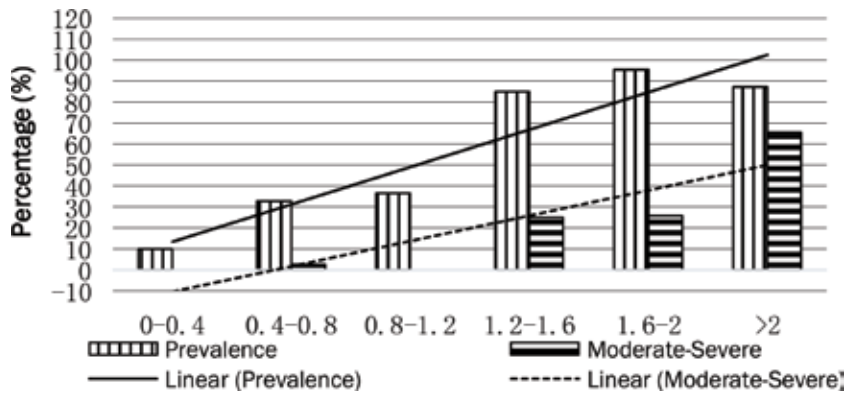
   Figure 10 shows the map of spatial distribution of fluoride levels in groundwater of the municipality of Santana, based on data from the field survey or selected from the SIAGAS registry. This figure also spatializes the risk categories of fluorosis and indicates the locations where the epidemiological information was obtained. The fluoride contents of the groundwater collected in tubular wells drilled in the localities of Areão, Cachoeira, Canabrava, Caracol, Olhos d'Água, Pedra Preta, Sossego, and Várzea do Mourão presented epidemiological relevance for children up to 6 years of age, since they ingest these waters for a chronic exposure.
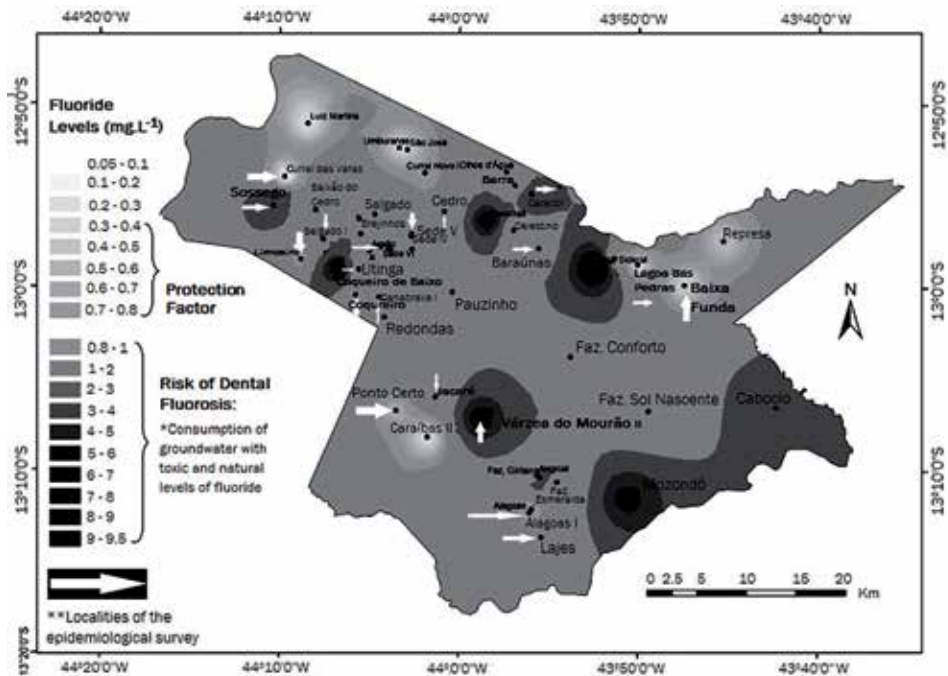

Figure 10.
Map of distribution of fluoride levels in groundwater and indication the spatial information of the dental fluorosis. The categories of epidemiological risk were protection factor (0.4-0.8 mg.L^{-1}) and risk of fluorosis dental (> 0.8 mg.L^{-1}).

The spatial analysis of fluoride isoteores revealed epidemiological relevance and allowed the indication of Santana as an endemic area of dental fluorosis, whose consumption of water with toxic and natural levels of fluoride is the main risk factor. It is expected that water resource managers in city of Santana could apply viable cost-benefit technologies for defluoroating in groundwater with toxic levels of fluoride used in public water supply. The technical-scientific literature offers several technologies for the natural deflowering of water [68–78], which cover the use of activated alumina, activated carbon, ion exchange resins, reverse osmosis systems, electrodialysis and nanotechnology.

Table 7 presents the prevalence and severity of dental fluorosis and fluoride levels of groundwater used in the public supply of endemic areas. Churchill [85], in a study conducted in the United States, observed a direct correlation between permanent tooth enamel patches or dental fluorosis and the presence of high levels of fluoride in the water supply. Dean et al. [86] discussed the correlation between the prevalence of dental caries or fluorosis and fluoride values in the water supply of four cities in the United States. The proportions of dental fluorosis in the moderate or severe forms are higher in the endemic areas, attributed to the consumption of natural waters with toxic levels of fluoride [87].

In this context, it is imperative to emphasize that the presence of dental fluorosis and its influence on the self-esteem of the people may not affect equally the population of the municipality, because the access to drinking water and the socioeconomic conditions to individually deal with the dental fluorosis impacts in esthetics and self-esteem are unequal. Funtowicz et al. [88] call attention to the complexity dimension in epidemiology and other health sciences, as well as to the technical, methodological, and epistemological uncertainties that accompany the risk assessments.

Author/year	Study area	Prevalence (%)	Severity	F^- (mg.L^{-1})
Costa et al. [75]	São Francisco, Minas Gerais, Brazil	56–67	35% moderate/severe[B]	0–3.9
Cruz et al. [26]	Santana, Bahia, Brazil	53	18% moderate/severe[B]	0.1–6.20
Azcurra et al. [3]	Sampacho, Córdoba, Argentina	78	25% moderate/severe[A]	9.0
Loyola-Rodríguez et al. [76]	San Luis Potosí, Mexico	78	46% moderate/severe[A]	0.7–3.1
Dozal et al. [77]	Chihuahua, Mexico	82	41% moderate/severe[A]	0.7–8.6
Yadav et al. [78]	Distrito de Haryana, India	45–60	22–39% moderate/severe[A]	1.52–4.0
Vazquez-Alvarado et al. [79]	San Miguel Vindhó, Mexico	85	41% moderate/severe[A]	0.7–2.0
Ding et al. [80]	Inner Mongolia, China	42.6	20% moderate[A]	0.24–2.84
Gallará et al. [5]	Córdoba, Argentina	76–87	17–22% moderate/severe[A]	1.4–7.0
Jarquín-Yañez et al. [81]	Hidalgo, Mexico	100	95% severe[A]	4.1
Larquin et al. [82]	Camagüey (Cuba)	51	47% moderate/severe[A]	1.7–2.0
Haritash et al. [83]	Haryana, India	23–32	29–44 moderate/severe[A]	0.5–2.40
Chaudhry et al. [84]	Uttar Pradesh, India	14–24	30% moderate/severe [A]	0.20–25.0

[A]*Dean index.*
[B]*Index of Thylstrup and index of Fejerskov.*

Table 7.
Epidemiology of dental fluorosis and fluoride contents in waters of endemic areas.

The collective health paradigm expands the health-environment relationship and contemplates the biomedical and sanitation paradigms, as well as the political, cultural, economic and ecological dimensions of health [89].

The integrated analysis of the hydrochemical research and multivariate and epidemiological statistics indicated that the chemical weathering of the rocks of the Bambuí Group and the leaching of its constituent mineral phases provide fluorine to the groundwater in the municipality of Santana. In this way, the minerals that make up the rocks provide fluorine and other chemicals for the biogeochemical cycles, which if conducted by natural waters can influence human health. This perspective, according to Selinus [90], defines medical geology, an interdisciplinary science that gathers professionals of geosciences, health, and biosciences around the understanding of the interaction between environmental geological factors and the geographical distribution of diseases, such as fluorosis.

An environmental health and education program would provide information for the population and for municipal accountability regarding the identification and reception of those affected by endemic fluorosis. Future research would help promote health in this municipality and encourage collaboration between geoscientists, ecologists, and health professionals to develop studies that relate geological processes to the ecosystem and human health. In addition, it would guide water quality managers, public health planners, and educators.

5. Conclusions

The groundwater samples were predominantly alkaline. The hydrochemical characterization indicated that there were two aquifers, with different levels of sodium, calcium, and fluoride. The most representative aquifer covered the bicarbonated calcium and mixed calcium waters (66%) and the lower levels of fluoride. The pelito-carbonático aquifer contemplated the sodium bicarbonated and sodium chlorinated waters, whose fluoride levels exceeded the local optimum limit. Analysis of clusters also indicated that there were two hydrochemical groups (G1 and G2) that differed in STD, pH, F^-, rNa^+/rCa^{2+} ratio, and saturation indexes of the mineral phases calcite, dolomite, and fluorite minerals.

The risk category for dental fluorosis comprised 47% of the samples. A portion of the samples presented fluoride levels representative of the category of risk of skeletal fluorosis (20%) or associated with the risk of incapacitating fluorosis (20%). The descriptive analysis of the dental fluorosis condition in the sample universe revealed a prevalence of dental fluorosis of 53%, with a 17% prevalence of moderate to severe forms. These proportions were associated to the consumption of groundwater with high toxic levels of fluoride.

The monitoring of fluoride levels in groundwater, application of defluoridation techniques, and environmental health surveillance and sensitization programs for endemic fluorosis in the municipalities of Santana and neighboring (Canápolis, Serra Dourada and Sítio do Mato) are recommended. Future research in medical geology would help encourage studies that link geological processes to the ecosystem and human health. They would also guide the management of water quality and the decisions of municipal public health managers.

Acknowledgements

Author details

Manuel Vitor Portugal Gonçalves*, Rodrigo Alves Santos,
Carlos Alberto Machado Coutinho and Manoel Jerônimo Moreira Cruz
Geochemical Group of Interfaces, Federal University of Bahia, Salvador, Brazil

*Address all correspondence to: hidrovitor81@gmail.com

IntechOpen

References

[1] Raju NJ. Prevalence of fluorosis in the fluoride enriched groundwater in semi-arid parts of eastern India: Geochemistry and health implications. Quaternary International. 2017;**443**:265-278. DOI: 10.1016/j.quaint.2016.05.028

[2] Komati SH, Figueiredo BR. Flúor em água e prevalência de fluorose em Amparo (SP). Geociências (São Paulo). 2013;**32**(3):547-559

[3] Azcurra AI, Battellino LJ, Calamari SE, Dorronsoro de Cattoni ST, Kremer M, Lamberghini FC. Estado de salud bucodental de escolares residentes en localidades abastecidas con agua de consumo humano de muy alto y muy muy bajo contenido de fluoruros. Revista de Saúde Pública. 1995;**29**:364-375. DOI: 10.1590/S0034-89101995000500005

[4] de Parreiras PM, Silva APA, Zocratto KBF. Fluorose Dentária: Percepção dos portadores e seus responsáveis. Revista da Faculdade de Odontologia (UPF). 2009;**14**(1):18-22. DOI: 10.5335/rfo.v14i1.688

[5] Gallará RV, Piazza LA, Piñas ME, Barteik ME, Moncunill I, Ponce RH. Endemic fluorosis in Northern and Northwestern rural areas in the Province of Cordoba, Argentina. Revista de Salud Pública. 2011;**XV**(1):40-48

[6] Soares FF, Valverde LF, Silva RDCR, Cangussu MCT. Prevalência e severidade de fluorose em escolares do município de São Francisco do Conde-BA, 2010. Revista de Odontologia da UNESP. 2012;**41**:318-323. DOI: 10.1590/S1807-25772012000500004

[7] Rigo L, Sabadin CS, Wietholter P, Solda C, Flores RA. Prevalência de fluorose dentária em crianças de uma escola municipal de Passo Fundo/RS. Full Dentistry in Science. 2014;**5**(19):472-476

[8] World Health Organization (W.H.O.). Guidelines for Drinking Water Quality. Geneva: Word Health Organization; 1996

[9] Evans RW, Darvell BW. Refining the estimate of the critical period for susceptibility to enamel fluorosis in human maxillary central incisors. Journal of Public Health Dentistry. 1995;**55**(4):238-249. DOI: 10.1111/j.1752-7325.1995.tb02376.x

[10] Ellwood RP, O'Mullane DM. The demographic and social variation in the prevalence of dental enamel opacities in North Wales. Community Dental Health. 1994;**11**(4):192-196

[11] Horowitz HS. Fluoride and enamel defects. Advances in Dental Research. 1989;**3**(2):143-146. DOI: 10.1177/08959374890030021201

[12] Meenakshi, Maheshwari RC. Fluoride in drinking water and its removal. Journal of Hazardous Materials. 2006;**137**(1):456-463. DOI: 10.1016/j.jhazmat.2006.02.024

[13] Boyle DR, Chagnon M. An incidence of skeletal fluorosis associated with groundwaters of the Maritime Carboniferous Basin, Gaspe Region, Quebec, Canada. Environmental Geochemistry and Health. 1995;**17**:5-12. DOI: 10.1007/BF00188625

[14] Nirgude AS, Saiprasad GS, Naik PR, Mohanty S. An epidemiological study on fluorosis in an urban slum area of Nalgonda, Andhra Pradesh, India. Indian Journal of Public Health. 2010;**54**:194-196. DOI: 10.4103/0019-557X.77259

[15] Apambire WB, Boyle DR, Michel FA. Geochemistry, genesis, and health implications of fluoriferous groundwaters in the upper Regions of Ghana. Environmental Geology.

1997;**33**:13-24. DOI: 10.1007/s002540050221

[16] Gupta SK, Deshpande RD, Agarwal M, Raval BR. Origin of high fluoride in groundwater in the North Gujarat-Cambay region, India. Journal of Hydrology. 2005;**13**(4):596-605. DOI: 10.1007/s10040-004-0389-2

[17] Brindha K, Rajesh R, Murugan R, Elango L. Fluoride contamination in groundwater in parts of Naglonda, Andhra Pradesh, India. Environmental Monitoring and Assessment. 2011;**17**(1-4):481-492. DOI: 10.1007/s10661-010-1348-0

[18] Rafique T, Rafique T, Naseem S, Bhanger MI, Usmani TH. Fluoride Ion contamination in the groundwater of Mithi Sub-District, the Thar Desert, Pakistan. Environmental Geology. 2008;**56**:317-326. DOI: 10.1007/s00254-007-1167-y

[19] Carrillo-Rivera JJ, Cardona A, Edmunds WM. Use of abstraction regime and knowledge of hydrogeological conditions to control high fluoride concentration in abstracted groundwater: San Luis Potosy Basin, Mexico. Journal of Hydrology. 2002;**261**(1-4):24-47. DOI: 10.1016/S0022-1694(01)00566-2

[20] Liu F, Song X, Yang L, Zhang Y, Han D, Ma Y, et al. Identifying the origin and geochemical evolution of groundwater using hydrochemistry and stable isotopes in the Subei Lake basin, Ordos energy base, Northwestern China. Hydrology and Earth System Sciences. 2015;**19**:551-565. DOI: 10.5194/hessd-11-5709-2014

[21] Misi A, Iyer SS, Coelho CES, Tassinari CC, Franca-Rocha WJ, Gomes ASR, et al. A metalogenic evolution model for the lead-zinc deposits of the Meso and Neoproterozoic sedimentary basins of the São Francisco Cráton, Bahia and Minas Gerais, Brazil. Revista Brasileira de Geociencias. 2000;**30**:302-305. DOI: 10.25249/0375-7536.2000302302305

[22] Instituto Brasileiro de Geografia e Estatística (IBGE). SEI - superintendência de estudos econômicos e sociais de bahia 2008. Cartas Plani-Altimétricas do Estado da Bahia, escala 1:100.000. Rio de Janeiro: IBGE [cited 2019 Mar 18]. Available from: https://ww2.ibge.gov.br/home/geociencias/download/arquivos/index1.shtm

[23] Gonçalves MVP, Cruz MJM, Santos RA, Ramos Junior ABS, Coutinho CAM. Flúor na água do Aquífero Bambuí no Oeste da Bahia (Brasil). Brazilian Journal of Aquatic Sciences and Technology. 2018;**22**(1):10-21. DOI: 10.14210/bjast.v22n1.9654

[24] Santos RA. Hidrogeoquímica dos Domínios Cársticos de Irecê, Bahia-Brasil [thesis]. Salvador: Federal University of Bahia; 2017

[25] Ghesquière O, Walter J, Chesnaux R, Rouleau A. Scenarios of groundwater chemical evolution in a region of the Canadian Shield based on multivariate statistical analysis. Journal of Hydrology: Regional Studies. 2015;**4**:246-266. DOI: 10.1016/j.ejrh.2015.06.004

[26] Cruz MJM, Coutinho CAM, Gonçalves MVP. The Dental fluorosis on Santana karst region, Bahia State, Brazil. Journal of Geography. 2015;**3**(2):51-67. DOI: 10.15640/jges.v3n2a3

[27] Instituto Brasileiro de Geografia e Estatística (IBGE). Dados do Censo demográfico 2010 publicados no Diário Oficial da União: Brasília; November 11, 2010. Rio de Janeiro: IBGE [cited 2019 Mar 18]. Available from: https://cidades.ibge.gov.br/brasil/ba/santana/panorama

[28] Atlas Brasil. Atlas do Desenvolvimento Humano no Brasil. 2013. Disponível em: www.atlasbrasil.org.br/2013 [Acesso em: March 5, 2015]

[29] Instituto Nacional de Meteorologia (INMET). Balanço Hídrico e Dados Climatológicos. Mapa Climatológico de Precipitação Pluviométrica Acumulada Anual (1931-1990), 2010. 2011-2012. Disponível em: www.inmet.gov.br [Acesso em: March 10, 2016]

[30] Misi A, Kaufman AJ, Azmy K, Dardenne MA, Sial AN, de Oliveira TF. Neoproterozoic successions of the Sao Francisco Craton, Brazil: The Bambui, Una, Vazante and Vaza Barris/Miaba groups and their glaciogenic deposits. Geological Society. Memoirs (London). 2011;**36**(1):509-522. DOI: 10.1144/M36.48

[31] Negrão FI. Hidrogeologia do Estado da Bahia: Qualidade, Potencialidade, Disponibilidade, Vulnerabilidade e Grau de Poluição [thesis]. Espanha: Universidade da Coruña, Espanha; 2007

[32] Coutinho CAM. A fluorose dentária na região cárstica do município de Santana-BA: Definição de áreas de risco para consumo humano das águas subterrâneas com base nos dados hidroquímicos e epidemiológicos [Dissertation]. Salvador: Federal University of Bahia; 2014

[33] Gonçalves MVP. Flúor no Aquífero Bambuí no Sudoeste da Bahia (Brasil) [thesis]. Salvador: Federal University of Bahia; 2014

[34] APHA. Standard Methods for Examination of Water and Wastewater. 19th ed. Washington, DC: American Public Health Association; 1998

[35] Parkhurst D L, Appelo C A J. Description of input and examples for PHREEQC version 3-A computer program for speciation, batch-reaction, one-dimensional transport, and inverse geochemical calculations: U.S. Geological Survey Techniques and Methods, Book 6, Chap. A43, 2013. 497p. Available from: http://pubs.usgs.gov/tm/06/a43. Accessed July 25 2013

[36] Merkel BJ, Planer-Friedrich B. Geoquímica de Águas Subterrâneas: Um Guia Prática de Modelagem de Sistemas Aquáticos Naturais e Contaminandos. Campinas, SP: Ed. Unicamp; 2012. 244p

[37] Landim PMB. Análise Estatística de Dados Geológicos Multivariados. São Paulo: Editora Oficina de Textos; 2011. 208p

[38] Fejerskov O, Manji F, Bælum V, Møller IJ. Fluorose Dentária: Um Manual Para Profissionais da Saúde. São Paulo: Editora Santos; 1994. 122p

[39] Ministério da Saúde-Brasil, Conselho Nacional de Saúde (CNS). Resolução n. 196, de 10 de Outubro de 1996. Aprova as Diretrizes e Normas Regulamentadoras de Pesquisas Envolvendo Seres Humanos. Brasília: Diário Oficial da União; 1996

[40] World Health Organization (W.H.O.). Oral Health Surveys: Basic Methods. 4th ed. Geneva: Word Health Organization: ORH/EPID; 1997

[41] Dean HT. Classification of mottled enamel diagnosis. The Journal of the American Dental Association. 1934;**21**(8):1421-1426. DOI: 10.14219/jada.archive.1934.0220

[42] Ministério da Saúde-Brasil. Secretaria de Atenção à Saúde. Departamento de Atenção Básica. Coordenação Nacional de Saúde Bucal. Projeto SB Brasil 2010 – Condições de Saúde Bucal da População Brasileira 2010: Resultados Principais. Brasília: MS-CNSB; 2010

[43] World Health Organization (W.H.O.). Calibration of Examiners for Oral Health Epidemiological Surveys. Geneva: ORH/EIS/EPID; 1993

[44] Velásquez LNM, Fantinel LM, Ferreira EF, Castilho LS, Uhlein A, Vargas AMD, et al. Fluorose dentária e anomalias de flúor na água subterrânea

no município de São Francisco, Minas Gerais. In: da Silva CR et al., editors. Geologia Médica no Brasil: Efeitos dos Materiais e Fatores Geológicos na Saúde Humana e Meio Ambiente. Rio de Janeiro: CPRM - Serviço Geológico do Brasil; 2006. pp. 10-117

[45] Piper AM. A graphic procedure in the geochemical interpretation of water-analyses. Eos, Transactions American Geophysical Union. 1944;**25**(6): 914-928. DOI: 10.1029/ TR025i006p00914

[46] Logan J. Interpretação de Análises Químicas da Água. Vol. 165. Recife: U.S. Agency for International Development; 1965. 75p

[47] World Health Organization (W.H.O.). Guidelines for Drinking-Water Quality. Geneva: Word Health Organization; 2006

[48] Moral F, Cruz-Sanjulián JJ, Olías M. Geochemical evolution of groundwater in the carbonate aquifers of Sierra de Segura (Betic Cordillera, Southern Spain). Journal of Hydrology. 2008;**360**:281-296. DOI: 10.1016/j.jhydrol.2008.07.012

[49] Roisenberg C, Viero AP, Roisenberg A, Schwarzbach MS, Morante IC. Caracterização geoquímica e gênese dos principais íons das águas Subterrâneas de Porto Alegre, RS. Revista Brasileira de Recursos Hídricos. 2003;**8**:137-147. DOI: 10.21168/ rbrh.v8n4.p137-147

[50] Fairchild IJ, Borsato A, Tooth AF, Frisia S, Hawkesworth CJ, Huang Y, et al. Controls on trace element Sr–Mg compositions of carbonate cave waters: Implications for speleothem climatic records. Chemical Geology. 2000;**166**(3-4):255-269. DOI: 10.1016/ S0009-2541(99)00216-8

[51] Rao SN. High-fluoride groundwater. Environmental Monitoring and Assessment. 2011;**176**(1-4):637-645. DOI: 10.1007/s10661-010-1609-y

[52] Handa BK. Geochemistry and genesis of fluoride-containing ground waters in India. Ground Water. 1975;**13**(3):275-280. DOI: 10.1111/j.1745-6584.1975.tb03086.x

[53] Costa DA. Controle lito-estrutural e estratigráfico na hidrogeoquímica e nas concentrações de fluoreto no Sistema Aquífero Cárstico - Fissural do Grupo Bambuí, Norte de Minas Gerais [Dissertation]. Belo Horizonte: Federal University of Minas Gerais; 2011

[54] Gibbs RJ. Mechanisms controlling world water chemistry. Science. 1970;**17**(3962):108801090. DOI: 10.1126/science.170.3962.1088

[55] Miranda LLL et al. Projeto Fluorita da Serra do Ramalho. Salvador-Ba, SME: CBPM, Convênio SME/CBPM; 1976. 92p

[56] Filho C et al. Projeto Bacia do São Francisco. Salvador: SICM, CBPM; 2001. 44p

[57] Filho C et al. Bacia do São Francisco entre Santa Maria da Vitória e Iuiú, Bahia: Geologia e Potencialidade Econômica. Salvador: CBPM; 2003. 76p

[58] Maron JEP, Brito PCR. Projeto Geoquímica do Bambuí. Levantamento Regional. Etapa II. Bahia. Relatório Final. Salvador: CPRM; Convênio DNPM-CPRM; 1980. 300p. Available from: http://rigeo.cprm.gov.br/jspui/ handle/doc/8141 [Accessed: January 19, 2019]

[59] Mendes B, Oliveira JFS. Qualidade da Água Para o Consumo Humano. Lisboa: Lidel, Edições Técnicas; 2004. 640p

[60] Galagan DJ, Vermilion JR. Determining optimum fluoride concentrations. Public Health Reports. 1957;**72**(6):491-493. DOI: 10.2307/4589807

[61] Ministério da Saúde-Brasil. Portaria 2914 de 12 de dezembro de 2011. Dispõe Sobre os Procedimentos de Controle

e de Vigilância da Qualidade da Água Para Consumo Humano e Seu Padrão de Potabilidade. Diário Oficial da União: Brasília; 14 de Dezembro de 2011. p.31

[62] Gonçalves MVP, Cruz MJM, Alencar CMM, Santos RA, Ramos Junior ABS. Geoquímica e qualidade da água subterrânea no município de Serra do Ramalho, Bahia (BR). Engenharia Sanitária e Ambiental. 2018;**23**:159-172. DOI: 10.1590/ S1413-41522018167893

[63] Frazão P, Ely HC, Noro LRA, Pinheiro HHC, Cury JA. The surveillance framework of water and the reporting of fluoride concentration indicators. Saúde em Debate. 2018;**42**(116):274-286. DOI: 10.1590/0103-1104201811622

[64] Rouquayrol MZ, Almeida Filho N. Epidemiologia & Saúde. 6th ed. Rio de Janeiro: Medsi; 2003. 724p

[65] Pereira JCR, Paes AT, Okano V. Espaço aberto: Questões comuns sobre epidemiologia, estatística e informática. Revista do IPC - São Paulo. 2000;**7**:12-17

[66] Naseem S, Rafique T, Bashir E, Bhanger MI, Laghari A, Usmani TH. Lithological influences on occurrence of high-fluoride groundwater in Nagar Parkar Area, Thar Desert, Pakistan. Chemosphere. 2010;**78**(11):1313-1321. DOI: 10.1016/j. chemosphere.2010.01.010

[67] Edmunds M, Smedley P. Fluoride in natural waters. In: Selinus O, Alloway B, Centeno JA, Finkelman RB, Fuge R, Lindh U, Singh H, Smedley P, editors. Essentials of Medical Geology: Impact of the Natural Environment Public Health. Amsterdã: Elsevier Academic Press; 2005. pp. 301-328

[68] Singh J, Singh P, Singh A. Fluoride ions vs removal technologies: A study. Arabian Journal of Chemistry.

2016;**9**(6):815-824. DOI: 10.1016/j. arabjc.2014.06.005

[69] Castel C, Schweizer M, Simonnot MO, Sardin M. Selective removal of fluoride ions by two-way ion-exchange cyclic process. Chemical Engineering Science. 2000;**55**(17):3341-3352. DOI: 10.1016/S0009-2509(00)00009-9

[70] Amor Z, Bariou B, Mameri N, Taky M, Nicolas S, Elmidaoui A. Fluoride removal from brackish water by electrodialysis. Desalination. 2001;**133**:215-223. DOI: 10.1016/ S0011-9164(01)00102-3

[71] Kamble SP, Deshpande G, Barve PP, Rayalu S, Labhsetwar NK, Malyshew A, et al. Adsorption of fluoride from aqueous solution by alumina of alkoxide nature: Batch and continuous operation. Desalination. 2010;**264**(1-2):15-23. DOI: 10.1016/j.desal.2010.07.001

[72] Tchomgui-Kamga E, Ngameni E, Darchen A. Evaluation of removal efficiency of fluoride from aqueous solution using new charcoals that contain calcium compounds. Journal of Colloid and Interface Science. 2010;**346**(2):494-499. DOI: 10.1016/j. jcis.2010.01.088

[73] Ansari M, KazemipouR M, Dehghani M, Kazemipour M. The defluoridation for drinking water using multi-walled carbon nanotubes. Journal of Fluorine Chemistry. 2011;**132**(8):516-520. DOI: 10.1016/j. jfluchem.2011.05.008

[74] Da Costa AB, Lobo EA, Soares J, Kirst A. Desfluoretação de águas subterrâneas utilizando filtros de carvão ativado de osso. Águas Subterrâneas. 2013;**27**(3):60-70. DOI: 10.14295/ras. v27i3.27382

[75] Costa SM, Abreu MHNG, Vargas AMD, Vasconcelos M, Ferreira EF, Castilho LS. Cárie dentária e

fluorose endêmica em distritos rurais de Minas Gerais, Brazil. Revista Brasileira de Epidemiologia. 2013;**16**(4):1021-1028. DOI: 10.1590/S1415-790X2013000400022

[76] Loyola-Rodríguez JP, Pozos-Guillén AJ, Hernández-Guerrero JC, Hernández-Sierra JF. Fluorosis en dentición temporal en un área con hidrofluorosis endêmica. Salud Pública de México. 2000;**42**:194-200

[77] Dozal SR, Herrera MA, Cifuentes E, Barraza A, Rodrìguez JL, Sanin LH. Dental fluorosis in rural communities of Chihuahua, Mexico. Fluoride. 2005;**38**(2):143-150

[78] Yadav JP, Lata S, Kataria SK, Kumar S. Fluoride distribution in groundwater and survey of dental fluorosis among school children in the villages of the Jhajjar District of Haryana, India. Environmental Geochemistry and Health. 2009;**31**(4):431-438. DOI: 10.1007/s10653-008-9196-3

[79] Vazquez-Alvarado P, Prieto-García F, Coronel-Olivares C, Gordillo-Martinez AJ, Ortiz-Espinosa RM. Fluorides and dental fluorosis in students from Tula de Allende Hidalgo, Mexico. Journal of Toxicology and Environmental Health Sciences. 2010;**2**(3):24-31

[80] Ding Y, Sun H, Han H, Wang W, Ji X, Liu X, et al. The relationships between low levels of urine fluoride on children's intelligence, dental fluorosis in endemic fluorosis areas in Hulunbuir, Inner Mongolia, China. Journal of Hazardous Materials. 2011;**186**(2-3):1942-1946. DOI: 10.1016/j.jhazmat.2010.12.097

[81] Jarquín-Yañez L, Mejía-Saavedra JJ, Molina-Frechero N, Gaona E, Rocha-Amador DO, López-Guzmán OD, et al. Association between urine fluoride and dental fluorosis as a toxicity factor in a rural community in the State of San Luis Potosi. The Scientific World Journal. 2015;**15**:1-5. DOI: 10.1155/2015/647184

[82] Larquin NL, Álvarez ML, Coca AMD, Vale LG, Betancourt JC. Fluorosis dental en escolares de una zona rural de Camagüey. Revista Electrónica Dr. Zoilo E. Marinello Vidaurreta. 2015;**40**(1):1-6

[83] Haritash AK, Aggarwal A, Soni J, Sharma K, Sapra M, Singh B. Assessment of fluoride in groundwater and urine, and prevalence of fluorosis among school children in Haryana, India. Applied Water Science. 2018;**8**(2):51-58. DOI: 10.1007/s13201-018-0691-0

[84] Chaudhry M, Prabhakar I, Gupta B, Anand R, Sehrawat P, Thakar SS. Prevalence of dental fluorosis among adolescents in schools of Greater Noida, Uttar Pradesh. Journal of Indian Association of Public Health Dentistry. 2017;**15**(1):36-36. DOI: 10.4103/jiaphd.jiaphd_144_16

[85] Churchill HV. Occurrence of fluorides in some waters of the United States. Journal of Industrial and Engineering Chemistry. 1931;**23**(9):996-998. DOI: 10.1021/ie50261a007

[86] Dean HT, Jay P, Arnold FA Jr, Elvove E. Domestic water and dental caries. II. A study of 2,832 white children, aged 12 to 14 years, of 8 suburban Chicago communities, including Lactobacillus acidophilus studies of 1,761 children. Public Health Reports. 1941;**56**(15):761-792. DOI: 10.2307/4583693

[87] Cangussu MCT, Narvai PC, Fernandez RC, Djehizian V. A fluorose no Brasil: Uma revisão crítica. Cadernos de Saúde Pública. 2002;**1**:7-15. DOI: 10.1590/S0102-311X2002000100002

[88] Funtowicz S, Ravetz JR. Emergent complex systems. Futures. 1994;**26**(6):568-582. DOI: 10.1016/0016-3287(94)90029-9

[89] Porto MF, Martinez-Alier J. Ecologia política, economia ecológica

e saúde coletiva: Interfaces para a sustentabilidade do desenvolvimento e para a promoção da saúde. Cadernos de Saúde Pública. 2007;**23**:S503-S512. DOI: 10.1590/S0102-311X2007001600011

[90] Selinus O. Geologia Médica. In: Da Silva CR et al., editors. Geologia Médica no Brasil: Efeitos dos Materiais e Fatores Geológicos na Saúde Humana, Animal e Meio Ambiente. Rio de Janeiro: CPRM - Serviço Geológico do Brasil; 2006. 220p

Evaluation of Analytical Methods to Study Aquifer Properties with Pumping Test in Deccan Basalt Region of the Morna River Basin in Akola District of Maharashtra in India

Kanak N. Moharir, Chaitanya B. Pande,
Sudhir Kumar Singh and Rodrigo Abarca Del Rio

Abstract

Fifteen pumping tests were performed in the Deccan basalt region of the Morna river basin in Akola district of Maharashtra in India. It is an artesian well as it is in the discharge zone of this coastal aquifer. Transmissivity (T) and storage coefficient (S) must be considered as aquifer parameters and used in groundwater recharge analysis. During the analysis of time-drawdown, the graphs were developed using pumping test methods and most of the pumps' water initially comes from the well storage. Analysis of the well in tapping aquifer in Deccan basalt shows the existing relationship between porosity and specific yield. All of the aquifer testing methods have suggested ground recharge structures such as open well, bore well, and reservoir in hard rock terrains. The data and information are very helpful for hydraulic conditions, aquifer zones, and open wells development and management. The aquifer's parameters are identified as important factors for groundwater resources evaluation, numerical simulation, development and protection as well as scientific management. The results are optimized, hence these aquifer parameters are important for scientific planning and engineering practices.

Keywords: pumping test, aquifer, Hantush method, Theis with Jocob method

1. Introduction

The basaltic hard rock has limited fresh water resources. Groundwater planning and management is a difficult issue for the current scenario [1, 2]. The observation wells have been storage and pumps and drawdown stages in the aquifer parameters. The aquifer characteristics were estimated using scientific methods.

The study area data like geological, hydrological, and geochemical data and laboratory results were combined to study water sustainability in the basaltic hard rocks [3]. The aquifer parameters were estimated through various pumping tests, while

groundwater has withdrawn and discharged from the open wells and bore wells, whose result is inserted into the well-flow equation and the hydraulic features [4]. The different curves matching and numerical methods are widely used to estimate aquifer parameters and plot graphs through pumping test data. In this study, two types of methods namely analytical and numerical were used for interpretation of pumping data in the aquifer software and mathematical equation [5]. Hence the present investigation has used numerical methods to achieve accurate results for aquifer characteristics conditions in the regions of Maharashtra [6].

2. Study area

The study area is located in the Akola district. The Morna river basin area covers 941 km^2 and is located between 76°47′54″ and 76°6′44″ E longitude and 20°53′26″ and 20°22′22″ N latitude (**Figure 1**). The major crops are pigeon pea, cotton, and soybean.
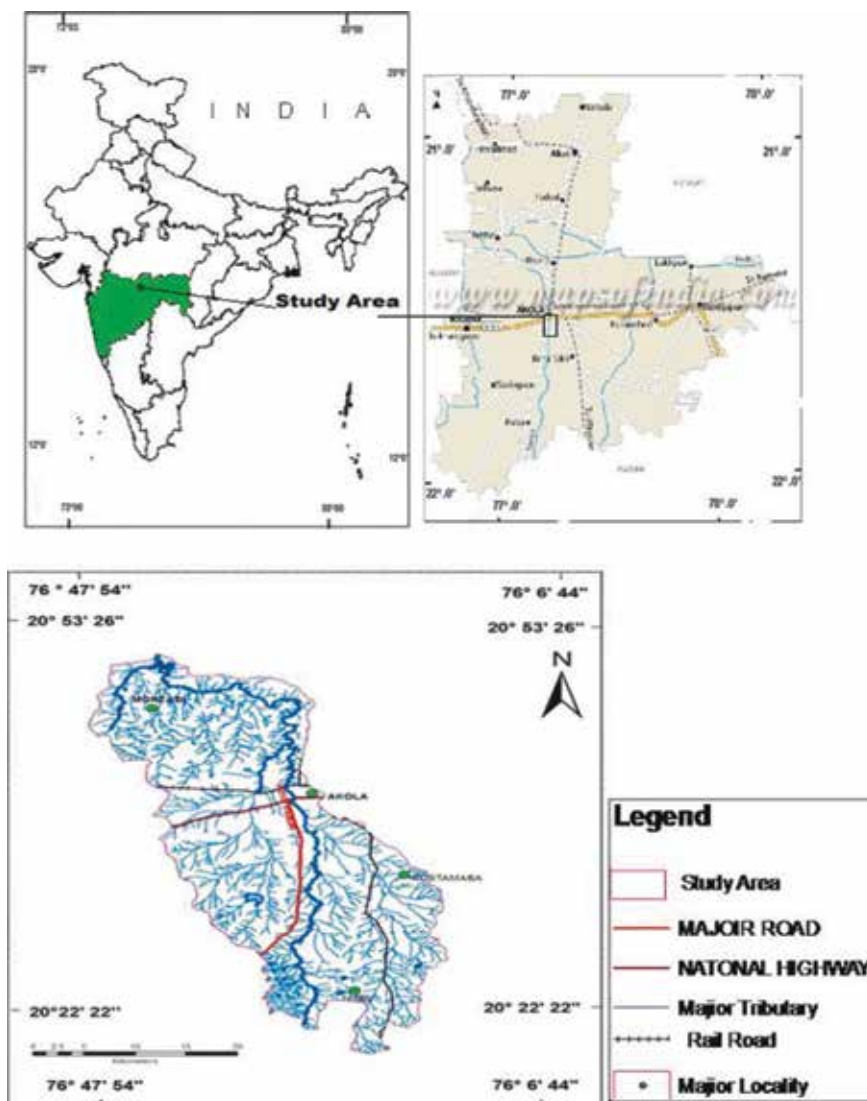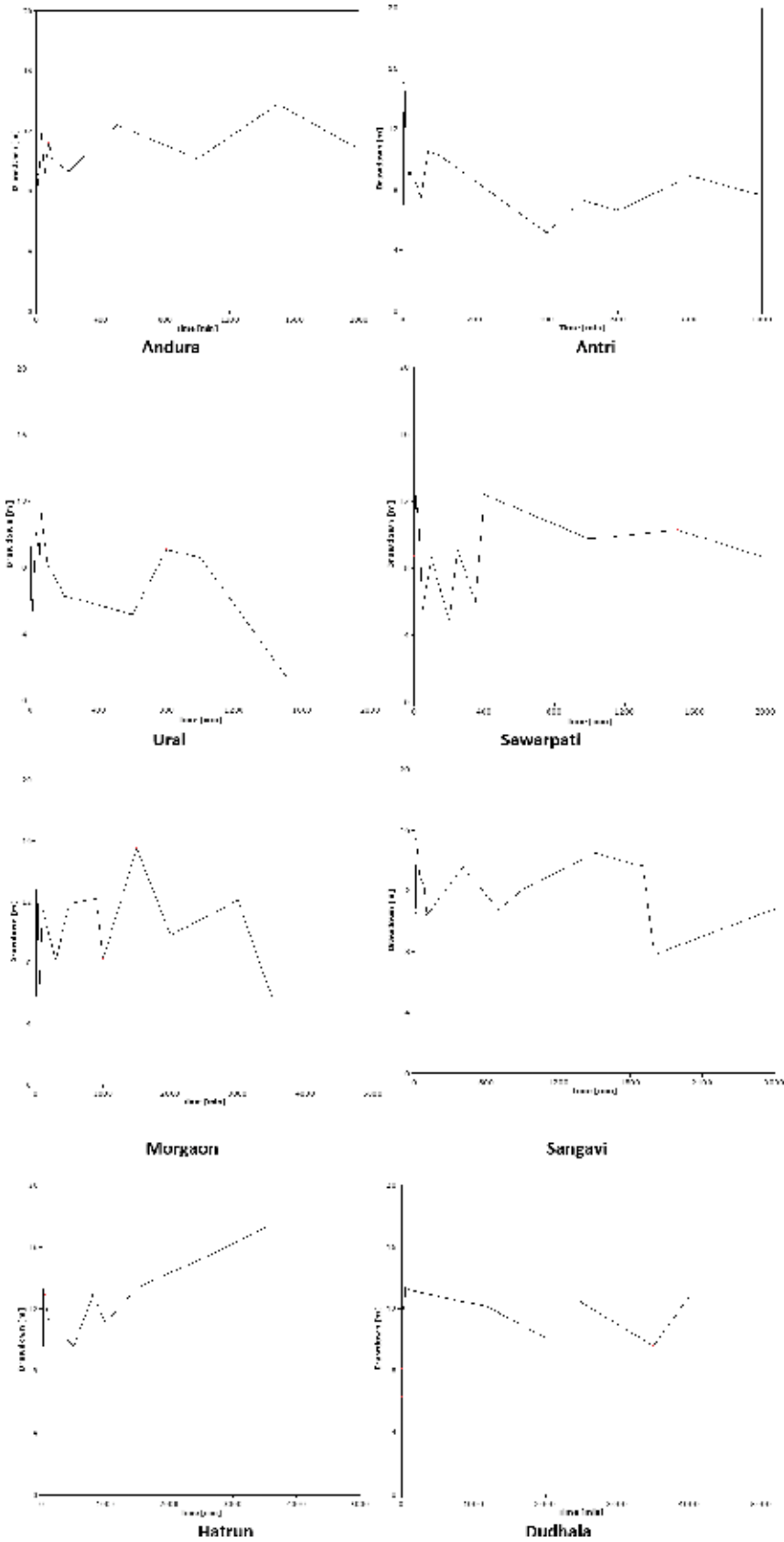

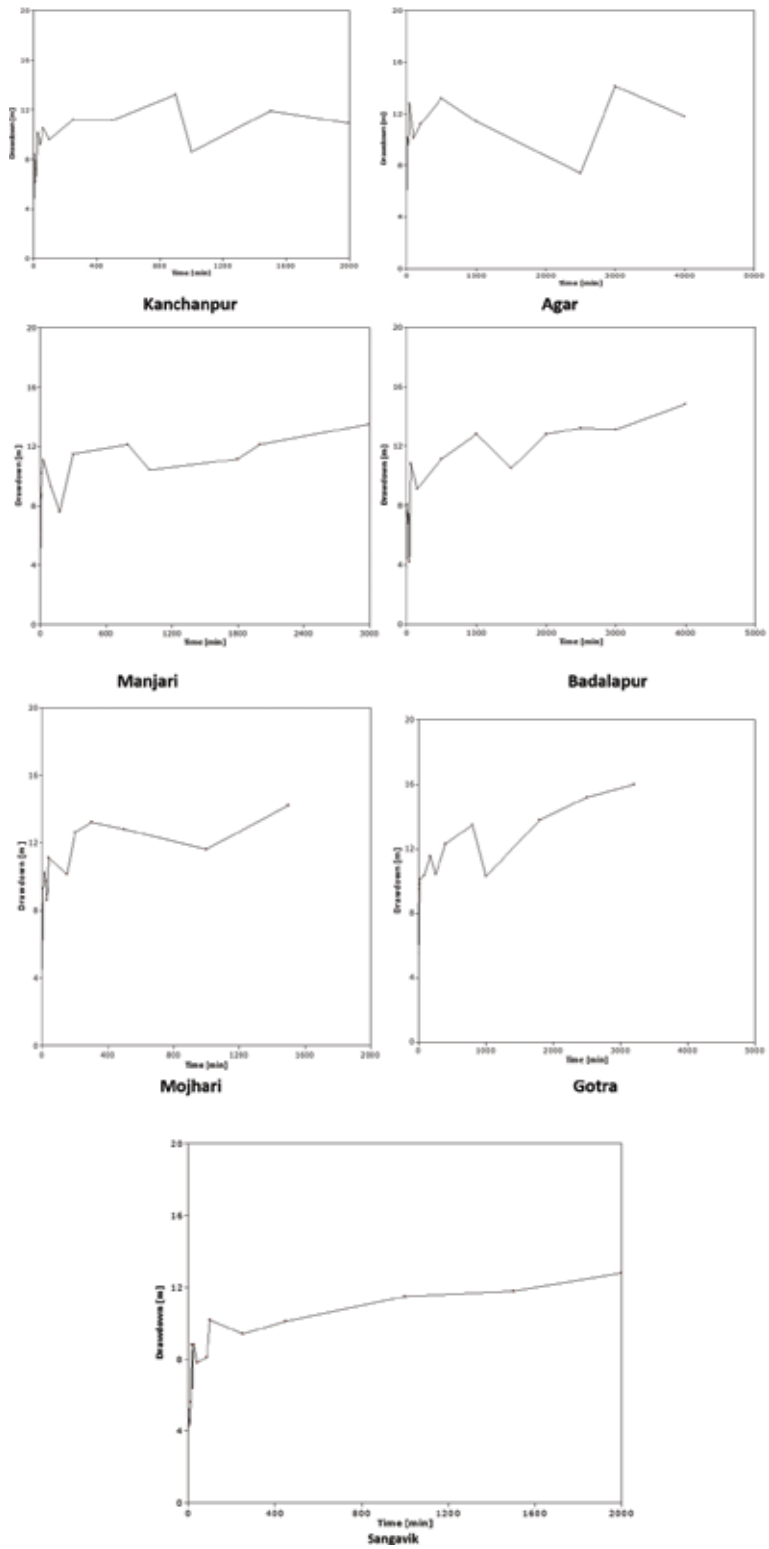**Figure 1.**
Location map of the Morna river basin.

Figure 2.
Time and drawdown graph of (i) Andura, (ii) Antri, (iii) Ural, (iv) Phal, (v) Sawarpati, (vi) Morgaon, (vii) Sangavi, (vii) Dhudhala, (viii) Hatrun, (ix) Kanchanpur, (x) Agar, (xi) Manjari, (xii) Badalapur, (xiii) Morjhadi, (xiv) Gotra, and (xv) Sangavi pumping test.

The large area is under basaltic rock and alluvium patches with reference to geological map. The average annual rainfall of the Akola district is 750–950 mm. The river originates from the southwest part of the Patur tahsil, Washim district. The Morna river basin is 90 km long; however, there are no main tributaries of this basin, with few small tributaries pouring into the river [7, 9].

3. Methodology

Fifteen observation wells were established for the analysis of pumping test data using GPS and field verification of the Morna river basin. The 15 observation wells' data were collected from study area after the time drawn graphs of these wells were prepared with the help of Aquifer software. They are particularly calculated for the graphical presentation and for obtaining detailed information about pumping test data. Therefore, two methods such as a pumping test and slug test are included in the aquifer software. These results were calculated and plotted in graphs using different aquifer parameters with five techniques, namely Papadopulos and Cooper method, Theis method, Theis with Jocob correlation, Hantush, and z time drawn method (**Figure 2**).

4. Result and discussion

Pumping tests were performed on large-diameter observation wells in basaltic rock in the Washim and Akola districts of Maharashtra, India. All observation wells were in the basaltic rock and alluvium zones. The alluvium groundwater has high salt content in the wells. The normal value of transmissivity in the Deccan trap is 30–100 sq.mt/day [10]. The analysis of the effect of the 15 pumping test wells was carried out using five aquifer methods to categorize the wells as excellent, moderate, and low productivity wells. The results show that observation wells in the basaltic hard rock regions display excellent prospective for sustainable groundwater exploration with increase of protected yields. Some observation wells in the alluvium zone displays moderate due to groundwater's high range of pH with medium safe yield to very low protected yield and poor recovery. The outcome of pumping test data is the understanding of the transmissivity and permeability values. These values can be calculated based on the pumping test data and aquifer graphs [11]. All of this analysis of aquifer properties may also be used for further groundwater development and planning of the basin area. The result of study area shows an inadequate groundwater during pumping test data and graphs (**Table 1**).

5. Geology

The study of classification of basalt rocks deciphers as main group of rock formation and lava flows. The basaltic rock is deposited around the southern part of Deccan rocks belonging to the Cretaceous age. These basalt rocks are divided into primary and secondary openings with regard to fractures and joints [12].

6. Pumping test

The groundwater was monitored and water level variations of wells were recorded with help of aquifer graphs and convention methods of pumping test analysis [13]. In past years, many different methods were proposed on the aquifer mapping by few

Manjari village		Badalapur village		Morjhadi village		Gotra village		Sangavik village		Andura village		Antri village		Ural village		Saarpati village		Morgaon village		Sangavi village		Dhudhala village		Hatrun village		Kanchanpur village		Agar village	
Time	Water level	Time	Water level	Time	Water level	Time	Water level	Time	Water level	Time	Water level	Time	Water level	Time	Water level	Time	Water level	Time	Water level	Time	Water level	Time	Water level	Time	Water level	Time	Water level	Time	Water level
1	4.1	1	3.8	1	4.5	1	5.5	1	4.2	1	4.5	1	5.8	1	6	1	8.7	1	11.38	1	5.3	1	4.8	1	5.2	1	4.8	1	5.6
5	6.1	4	5.11	2	8.4	4	6.8	3	5.2	3	6.1	3	13	2	8.7	2	8.9	3	7.2	2	7.8	3	8.4	2	8.9	5	8.4	2	6.12
6	8.8	9	8.11	3	6.2	6	8.10	5	4.38	5	7.10	4	15	3	9.2	3	9.4	5	12.8	4	10.5	4	7.2	3	7.8	8	7.6	3	8.4
8	8.5	18	6.8	5	9.3	12	9.5	10	5.6	8	8.4	6	15.15	5	7.1	7	11.14	10	5.8	8	13.6	6	5.11	5	6.3	10	6.12	4	7.2
15	10.2	28	7.4	8	9.3	15	9.8	15	8.4	15	9.12	10	8.8	10	5.4	11	12.3	30	12	10	15.4	8	6.8	10	8.12	15	7.2	8	9.2
25	10.5	40	4.2	15	10.2	20	10.12	18	6.4	25	10.1	20	9.10	30	10.2	30	10.4	50	6.1	40	13.1	15	11.2	15	9.6	25	10.11	15	10.5
30	11.1	60	10.8	25	9.7	80	10.32	25	8.8	30	11.8	40	8.18	50	8.74	50	5.6	100	11.5	80	12.2	20	13.2	20	12.4	40	8.14	25	9.6
100	9.3	150	9.12	30	8.6	170	11.55	40	7.8	50	9.20	50	7.4	60	11.24	100	8.63	300	8.18	100	10.4	50	12.9	45	11.8	60	10.11	40	12.8
180	7.6	500	11.14	40	11.12	250	10.4	85	8.12	80	11.2	70	10.5	80	9.5	200	4.9	500	11.88	400	13.55	100	11.3	60	13.4	100	9.2	100	10.11
300	11.5	1000	12.8	150	10.11	400	12.3	100	10.18	100	10.12	100	10.3	100	8.2	250	9.12	900	12.2	700	10.75	500	9.6	100	13.2	250	10.5	200	11.2
800	12.12	1500	10.5	200	12.6	800	13.5	250	9.4	200	9.30	400	5.14	200	6.3	350	5.9	1000	8.15	900	12.1	800	12.9	1200	12.12	300	9.4	500	13.2
1000	10.4	2000	12.8	300	13.2	1000	10.30	500	10.11	500	12.4	500	7.3	600	5.2	400	12.4	1500	15.5	1500	14.48	1000	11.10	2000	10.11	900	11.2	1000	11.4
1800	11.15	2500	13.2	500	12.8	1800	13.8	1000	11.5	1000	10.15	600	6.6	800	9.1	1000	9.75	2000	9.8	1900	13.6	1500	13.4	2500	12.4	1000	11.14	2500	7.2
2000	12.12	3000	13.11	1000	11.6	2500	15.20	1500	12.5	1500	13.8	800	8.9	1000	8.6	1500	10.3	3000	12.10	2000	7.8	2500	15.20	3500	9.6	1500	13.2	3000	9.8
3000	13.5	4000	14.8	1500	14.2	3200	16.0	2000	12.8	2000	10.8	1000	7.6	1500	15	2000	8.63	3500	5.8	3000	10.80	3500	17.21	4000	12.8	2000	8.6	4000	14.14

Note: Time (min) and water level (ft).

Table 1.
Details pumping test data of Morna river basin.

researchers to study the pumping test data and aquifer parameters. The output of the study area may be utilized for the analysis of groundwater flow in unconfined and confined aquifer of the Deccan trap rock especially in Maharashtra, India [14].

7. Theis with Jocob correlation method

Aquifer parameters are determined by easy methods; for example Cooper and Jacob [15] modified the Theis method and suggested it for better understanding of groundwater flow in the basalt rocks [15, 16]. The method does not require curve matching. The semi-log papers can be used for plotting time-drawdown data (time on log axis and drawdown on linear axis). The wells values should be less than 0.01 because the test should be conducted. From 15 observation wells, data have been correlated in Theis with Jacob equations of aquifer method using Aquifer software. The maximum wells' recharge time is very low due to the availability of groundwater flow in the region and remaining wells is good but the recharge is so much large show in the Theis with Jacob correlated graph (**Figure 3**). Theis type curve is one of the presented type curves, which has the plotted values of W (u) and 1/u on a log-log sheet. On a similar log-log sheet, field values of drawdown and time are plotted. In the matched position, a match point is selected. The values of W (u) and l/u for this match point is read from the type curve (Eq. (1) and (2)).

The Theis (log-log) graph shows the maximum observation wells of water level ranges in between 4 and 12 m and the recharge time is very less as compared to other wells of the study area (**Figure 4**).

The aquifer parameters are calculated by the following formulas:

$$T = 2.3 \frac{Q}{(4\pi\Delta s)}, \tag{1}$$
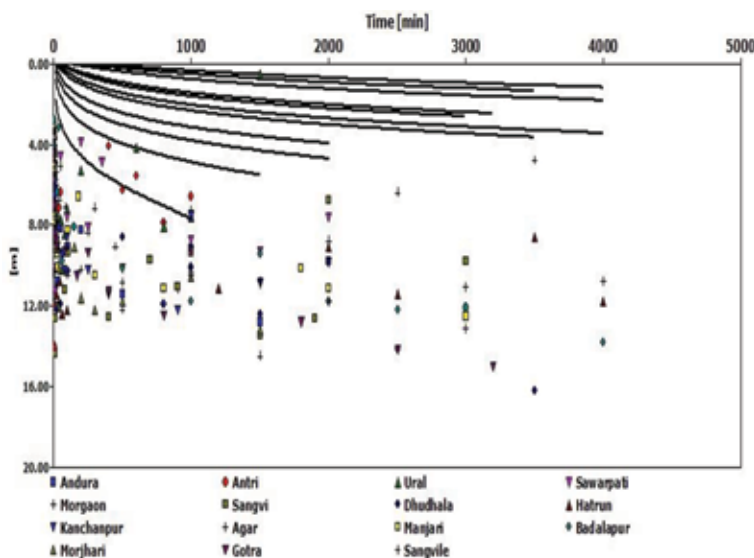
$$S = 2.25 \frac{Tt_0}{r.r} \tag{2}$$

Figure 3.
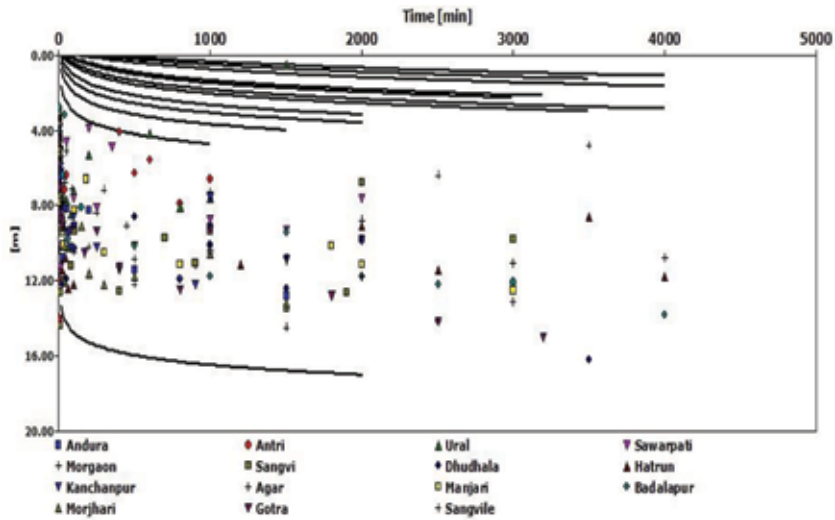*Drawdown versus time plot using Theis with Jacob correlation.*

Figure 4.
Drawdown versus time plot using the Theis log-log method.

8. Hantush's method

The groundwater flow of observation wells under the leaky aquifer which is a horizontal plane may be analyzed with the aquifer technique. The Hantush method is used for confined aquifers on the straight flat surface. From the pumping test, data have been analyzed using the Hantush log-log method by the aquifer software (Eq. (3)) (**Figure 5**). There is a single additional unidentified parameter mixed up, the leakage feature L, which is specified [17–19]
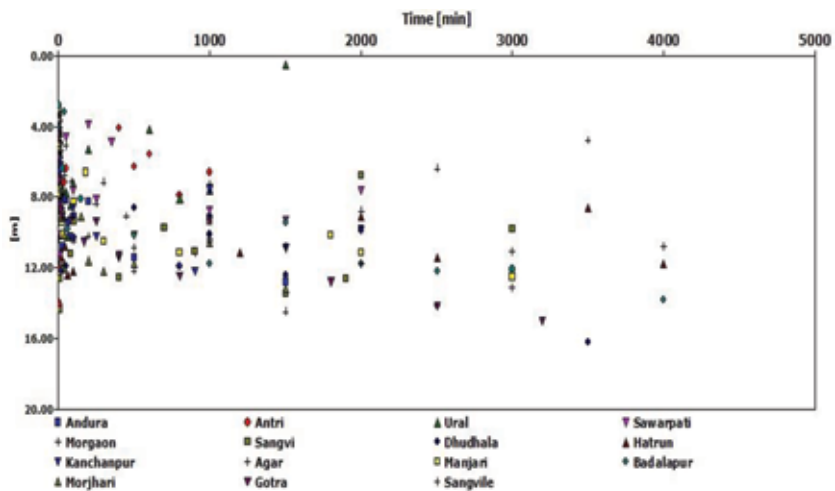
$$Ln = \sqrt{(KD)}_n{}^c \tag{3}$$

Figure 5.
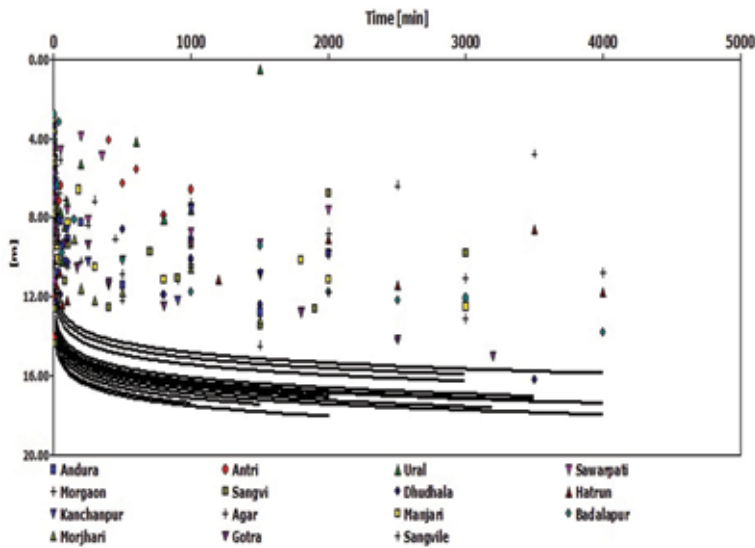*Drawdown versus time plot using the Hantush method (log-log).*

Figure 6.
Drawdown versus time plot using Papadopulos and Cooper log-log method.

9. The Papadopulos and Cooper method

Papadopulos and Cooper [20] have given a theoretical solution for analyzing the pumping test data from large diameter wells taking into account the storage capacity of the wells. Papadopulos and Cooper equation is totally dependent on the assumption that the aquifer is confined, isotropic, and extensive; the entire thickness of the aquifer is penetrated by the well, unstudied state of flow at constant discharge date and negligible well losses [21]. The general flow equation is given by Papadopulos and Cooper for a well of large diameter as follows (Eq. (4) and (5)):

$$T = Q.F (Uw)/4 \tag{4}$$

$$SS = (4Tt)/(1/Uw\ rw2) \tag{5}$$

The field data are plotted on a transparent bio logarithmic paper (of modules equivalent to that of type curve) with "s," the drawdown on Y-axis, and "t," the time since pumping started on Y-axis. In this method, the groundwater flow is shown using log-log methods using Aquifer software (Cooper and Jacob) (**Figure 6**).

10. Discussion and conclusion

Many aquifer mapping project implementers have observed problems and knowledge gaps that require to be focused or would be cooperative to know at different stages in a setup to handle aquifer or groundwater recharge projects. The issue of study area, every graph and pumping data, as discussed above, makes an input to the area of information that helps block these breaks, as shown in results. These tables of pumping data can be used as guidelines to help discover information on problems most essential to developers and supervisors of future and current projects.
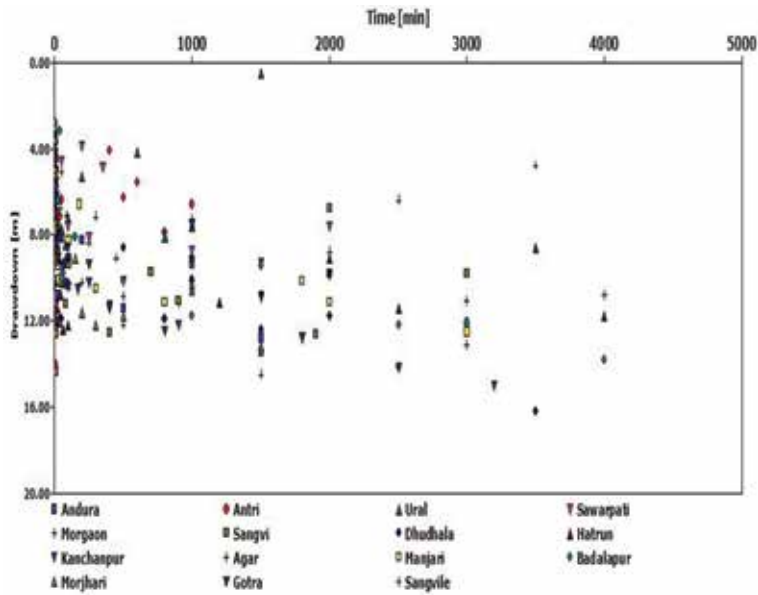
Figure 7.
Time drawn method using aquifer software 2014; Jacob's semi-log (slope) method.

The area is very high runoff found on the surface and this since all area is need water conservation structures in the ground of confined and unconfined layers. The analysis of Theis with Jacob correlation, Jacob's semi-log, Hantush, and Papadopulos and Cooper methods systematically shows groundwater recharge and their level in the basaltic rock area. The results can be used by local village society and government agency to approach the sustainable use of groundwater (**Figure 7**).

Author details

Kanak N. Moharir[1*], Chaitanya B. Pande[1], Sudhir Kumar Singh[2]
and Rodrigo Abarca Del Rio[3]

1 Department of Geology, Sant Gadge Baba Amravati University, Amravati, India

2 K. Banerjee Centre of Atmospheric and Ocean Studies, IIDS, Nehru Science Centre, University of Allahabad, Allahabad, India

3 Departamento de Geofísica, University of Concepción, Concepción, Chile

*Address all correspondence to: kanak.moharir1@gmail.com

IntechOpen

References

[1] Detay M, Poyet P, Emsellem Y, Bernardi A, Aubrac G. Development of the saprolite reservoir and its state of saturation: Influence on the hydrodynamic characteristics of drillings in crystalline basement. Comptes Rendus Geosciences. 1989;**309**: 429-436

[2] Taylor R, Howard K. A tectono-geomorphic model of the hydrogeology of deeply weathered crystalline rock: Evidence from Uganda. Hydrogeology Journal. 2000;**8**(3):279-294

[3] Moharir K, Pande C, Patil S. Inverse modeling of Aquifer parameters in basaltic rock with the help of pumping test method using MODFLOW software. Geoscience Frontiers. 2017;**8** (I6):1187-1494

[4] Khadri SFR, Pande C. Ground water flow modeling for calibrating steady state using MODFLOW software—A case study of Mahesh river basin, India. Modeling Earth Systems and Environment. 2016;**2**(1):2 of 17

[5] Khadri SFR, Moharir K. Characterization of aquifer parameter in basaltic hard rock region through pumping test methods: A case study of Man river basin in Akola and Buldhana Districts Maharashtra India. Modeling Earth Systems and Environment. 2016; **2**:33

[6] Pande CB, Moharir K. GIS-based quantitative morphometric analysis and its consequences: A case study from Shanur river basin, Maharashtra India. Applied Water Science. 2015; **7**(2):861-871

[7] Pande CB, Moharir KN, Pande R. Assessment of morphometric and hypsometric study for watershed development using spatial technology—A case study of Wardha river basin in the Maharashtra, India. International

Journal of River Basin Management. 2018. DOI: 10.1080/15715124.2018. 1505737. Published Date 25/11/2018. pp. 1-11

[8] Pande CB, Moharir KN, Khadri SFR, Patil S. Study of land use classification in the arid region using multispectral satellite images. Applied Water Science. 2018;**8**(5):1-11

[9] Pande CB, Khadri SFR, Moharir KN, Patode RS. Assessment of groundwater potential zonation of Mahesh river basin Akola and Buldhana districts, Maharashtra, India using remote sensing and GIS techniques. Sustainable Water Resources Management. 2017;**4** (4):965-979. DOI: 10.1007/s40899-017-0193-5

[10] Javandel I, Witherspoon PA. Analytical solution for partially penetrating in two-layer aquifer. Water Resources Research. 1983;**19**:567-578

[11] Chow VT. On the determination of transmissibility and storage coefficients from pumping test data. Transactions of the American Geophysical Union. 1952; **33**:397-404

[12] Khadri SFR, Pande C, Moharir K. Geo-morphological investigation of WRV-watershed management in Wardha district of Maharashtra India; using remote sensing and geographic information system techniques. International Journal of Pure and Applied Research. 2013;**1**(10):IJPRET-76

[13] Singhal BBS, Gupta RP. Applied Hydrology of Fractured Rocks. London: Kluwer Academic Publishers; 1999

[14] Theim G. Hydrologische Motheodem. Leipzig: Gebhardt; 1906

[15] Cooper HH, Jacob JF. A generalized graphical method for evaluating formation constants and summarizing

well field history. Transactions of the American Geophysical Union. 1946; **24**(4):526-534

[16] Theis CS. The relation between the lowering of piezometric surface and the data and duration of discharge of a well using groundwater storage. In: American Geophysical Union Transactions, 16th Annual Meeting, Part 2; 1935. pp. 519-524

[17] Hantush MS. Modification of the theory of leaky aquifers. Journal of Geophysical Research. 1960;**65**: 3713-3725

[18] Hantush MS. Analysis of data from pumping tests in anisotropic aquifers. Journal of Geophysical Research. 1966; **71**:421-426

[19] Hantush MS, Jacob CE. Non-steady radial flow in an infinite leaky aquifer. American Geophysical Union Transcripts. 1955;**36**:95-100

[20] Papadopulos IS, Cooper HH Jr. Drawdown in a well of large diameter. Water Resources Research. 1967;**3**: 241-244

[21] Raj P. Trend analysis of groundwater fluctuations in a typical groundwater year in weathered and fractured rock aquifers in parts of Andhra Pradesh. Journal of the Geological Society of India. 2001;**58**:5-13

Edited by Muhammad Salik Javaid

The two fields of knowledge "geology" and "hydrology" always go hand in hand, often giving rise to the terms "geohydrology" and "hydrogeology." The importance of the science of water, commonly called "hydrologic science," is always complemented by the "science of the interior of the earth." Whereas hydrology is concerned with the quality and quantity of underground water, its movement, extraction, and recharge, geology talks of the rock matrix and the structure in which this water is contained, stored, and moved around.In recent times, the knowledge of geohydrology or the hydrology of groundwater has gained an impetus many times its original scale; and with that, acquisition, expansion, research, advancement, and dissemination of this knowledge have become more significant. With so many dimensions of geohydrology available for exploration, research, and technological advancement, any work contributing to any dimension of geohydrology and groundwater will find its right place. This compilation of chapters is going to play a very important part in furthering the knowledge of geohydrology and may prove an interesting and useful read for various cross-sections of academia, researchers, engineers, hydrologists, and all categories of water consumers.

IntechOpen